

**COMPOSITE POLY(DIMETHOXYANILINE)
ELECTROCHEMICAL NANOBIOSENSOR FOR GLUFOSINATE
AND GLYPHOSATE HERBICIDES**

EVERLYNE APIYO SONGA



**A thesis submitted in partial fulfilment of the requirements for the
degree of Doctor Philosophiae in the Department of Chemistry,
University of the Western Cape.**

WESTERN CAPE

Supervisors: Prof. Emmanuel I. Iwuoha

Prof. Priscilla G. L. Baker

November 2008

**COMPOSITE POLY(DIMETHOXYANILINE) ELECTROCHEMICAL
NANOBIOSENSOR FOR GLUFOSINATE AND GLYPHOSATE
HERBICIDES**

Everlyne Apiyo Songa

KEYWORDS

Poly(2,5-dimethoxyaniline)

Poly(4-styrenesulfonic acid)

Nanostructured Polymers

Horseradish Peroxidase

Electrochemical Nanobiosensor

Glufosinate

Glyphosate

Herbicides

Aminomethylphosphonic acid

Inhibition

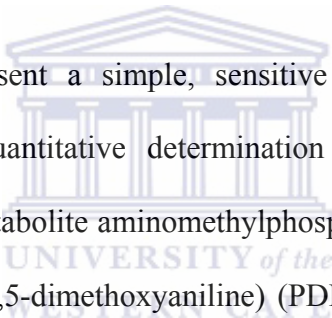


ABSTRACT

COMPOSITE POLY(DIMETHOXYANILINE) ELECTROCHEMICAL NANOBIOSENSOR FOR GLUFOSINATE AND GLYPHOSATE HERBICIDES

E. A. Songa

PhD Thesis, Department of Chemistry, University of the Western Cape



In this thesis, I present a simple, sensitive and low cost electrochemical nanobiosensor for quantitative determination of the herbicides glufosinate, glyphosate and its metabolite aminomethylphosphonic acid (AMPA). Firstly, the nanostructured poly(2,5-dimethoxyaniline) (PDMA) materials were synthesized on gold electrode by the electrochemical “soft template” method using poly(4-styrenesulfonic acid) (PSS) as the dopant and structure-directing molecule. Fourier transform infrared (FTIR) spectroscopy, UV-Vis Spectroscopy, Transmission electron microscopy (TEM) and Scanning electron microscopy (SEM) studies inferred successful doping of the nanostructured PDMA film by PSS and that the template PSS directed the synthesis of both nanotubes and nanoparticles of PDMA with diameters less than 100 nm.

The nanobiosensor was then constructed by electrostatic attachment of the model enzyme, horseradish peroxidase (HRP) onto the surface of PDMA-PSS modified electrode. Voltammetric results inferred that HRP immobilized on the nanostructured PDMA-PSS film retained its bioelectrocatalytic activity towards the reduction of H₂O₂ and was not denatured during its immobilization. The nanostructured PDMA-PSS materials provided a suitable micro-environment for immobilization of HRP and were thus applied as a mediator to enhance the direct electron transfer of HRP on gold. The HRP/PDMA-PSS nanobiosensor was finally applied for the detection of glufosinate, glyphosate and AMPA. The biosensing principle was based on determination of the sensor response to the herbicides by amperometric and voltammetric methods. The voltammetric method involved the determination of cathodic responses of the immobilized HRP to H₂O₂, before and after incubation in glyphosate standard solutions. Glyphosate inhibited the activity of HRP causing a decrease in its response to H₂O₂. The limit of detection for glyphosate by the voltammetric method was 1.7 µg L⁻¹ within a concentration range of 0.25-15.0 µg L⁻¹. The limit of detection for AMPA by amperometric method was determined to be 1.0 µg L⁻¹ within a concentration range of 1.5-80.0 µg L⁻¹. Glyphosate and glufosinate analyses were realized on spiked corn samples by amperometric method, within a concentration range of 2.0-78.0 µg kg⁻¹ corroborating that the nanobiosensor is sensitive enough to detect the herbicides in these matrices. Based on a 20 µL sample injection volume, the limits of detection by amperometric method were 0.1 µg kg⁻¹ for both glyphosate and glufosinate without sample clean-up or pre-

concentration. This study demonstrates that the developed nanobiosensor is sensitive enough and could be a useful tool in screening of these herbicides at low concentrations.

The interactions involving HRP and glyphosate were further investigated and the results indicated that glyphosate inhibited the HRP electrocatalytic activity for the reduction of H_2O_2 by coordinating with the oxygen atoms of the carbonyl groups in the peptide chain of HRP to form a complex which led to the obstruction of the electron transfer of Fe (III) in the porphyrin cycle of its heme group, and thus a reduction in HRP/PDMA-PSS nanobiosensor response. The apparent Michaelis-Menten constant (K_m^{app}) calculated for the HRP/PDMA-PSS nanobiosensor in the presence and absence of glyphosate were found to be 2.67 μM and 2.71 μM respectively. The low K_m^{app} values obtained for the HRP/PDMA-PSS biosensor indicates strong binding to HRP by the substrates.

November 2008

DECLARATION

I declare that *Composite Poly(dimethoxyaniline) Electrochemical Nanobiosensor For Glufosinate And Glyphosate Herbicides* is my own work, that it has not been submitted before for any degree or examination in any other university, and that all the sources I have used or quoted have been indicated and acknowledged as complete references.

Everlyne Apiyo Songa



November 2008

Signature -----

Supervisors: Prof. Emmanuel I. Iwuoha

Prof. Priscilla G.L. Baker

ACKNOWLEDGEMENTS

I would like to acknowledge the University of the Western Cape, South Africa, for giving me the opportunity to pursue my Doctoral degree at this University. Special thanks to the Department of Chemistry and SensorLab, University of the Western Cape for providing all the apparatus and instrumentation required for my research.

I would also like to acknowledge my Supervisors, Professor Emmanuel I. Iwuoha and Professor Priscilla G.L. Baker for their excellent supervision, support and encouragement during this period.

I gratefully acknowledge my Sponsors, Third World Organization for Women in Science (TWOWS), Italy, for their Funding and Support. Financial support from National Research Foundation (NRF), South Africa is also acknowledged.

Many thanks to all my family members and special friends for their patience, love, support and encouragement during the period I have been away from home.

The support of all my colleagues in SensorLab, University of the Western Cape is gratefully acknowledged. I also would like to extend my acknowledgement to the Physics department at University of the Western Cape for their assistance with TEM and SEM experiments. Special thanks to Mr. Adrian of physics department.

TABLE OF CONTENTS

Title page	i
Keywords	ii
Abstract	iii
Declaration	vi
Acknowledgements	vii
Table of contents	viii
List of figures and tables	xiii
List of publications	xvii
Abbreviations	xviii
CHAPTER 1	1
General Introduction	1
1.1 Background information	1
1.2 Problem statement	11
1.3 Objectives of the research work	12
1.3.1 General objectives	12
1.3.2 Specific objectives	12
1.4 Thesis statement	14
1.5 Thesis layout	15
CHAPTER 2	17
Literature Review	17
2.1 Introduction	17
2.2 Herbicides	18
2.2.1 Glyphosate	19
2.2.1.1 Health effects of glyphosate	20
2.2.1.2 Residues of glyphosate in food and water	22
2.2.2 Glufosinate	23
2.2.2.1 Health effects of glufosinate	24

2.2.2.2	Residues of glufosinate in food and water	25
2.2.3	Detection of herbicides	26
2.3	Biosensors	32
2.3.1	Enzyme biosensors	40
2.3.1.1	Enzyme kinetics	40
2.3.1.2	Enzyme inhibition	43
2.3.1.3	Horseradish peroxidase biosensors	47
2.3.1.4	Horseradish peroxidase inhibition	53
2.4	Conducting polymers (CPs)	57
2.4.1	Historical background of conducting polymers	59
2.4.2	Synthesis of conducting polymers	62
2.4.3	Polyaniline and its derivatives	64
2.4.3.1	Conductivity and doping of polyaniline	68
2.4.3.2	pH sensitivity and switching properties of polyaniline	69
2.4.3.3	Spectroscopic determination of the redox states of polyaniline	72
2.4.4	Nanostructured conducting polymers	75
2.4.5	Synthesis of nanostructured polyaniline	79
2.4.5.1	Hard template synthesis	80
2.4.5.2	Soft template synthesis	83
2.4.5.3	Electrochemical no-template synthesis	88
2.4.6	Properties of nanostructured polyaniline and its derivatives	89
2.4.7	Conclusions and future trends	89
CHAPTER 3		92
Experimental Section		92
3.1	Reagents and materials	92
3.2	Sample preparation	94
3.3	Measurement and instrumentation	94
3.3.1	Electrochemical techniques	95
3.3.1.1	Instrumentation	95
3.3.1.2	Principles of cyclic voltammetry	99
3.3.1.3	Principles of amperometry	103
3.3.1.4	Principles of the rotating disk electrode (RDE)	104

3.3.1.5	Electrochemical enzyme biosensors _____	106
3.3.1.5.1	Principles of operation _____	107
3.3.1.5.2	Practical aspects _____	109
3.3.1.5.2.1	Response time _____	110
3.3.1.5.2.2	Biosensor calibration _____	111
3.3.2	Other techniques _____	114
3.3.2.1	Fourier transform infrared (FTIR) spectroscopy _____	114
3.3.2.2	Ultra violet-visible (UV-Vis) spectroscopy _____	115
3.3.2.3	Transmission electron microscopy (TEM) _____	115
3.3.2.4	Scanning electron microscopy (SEM) _____	116
3.4	<i>Electrochemical procedures</i> _____	116
3.4.1	Electrochemical synthesis and characterization of poly(2,5-dimethoxyaniline) doped with poly(4-styrenesulfonic acid) (PDMA-PSS) _____	116
3.4.2	Preparation and characterization of the enzyme biosensor _____	119
3.4.3	Detection of herbicides _____	120
3.4.3.1	Detection of glyphosate by cyclic voltammetry (incubation method) _____	120
3.4.3.2	Amperometric detection of glyphosate, glufosinate and aminomethylphosphonic acid _____	121
3.5	<i>Graphing and data analysis</i> _____	123
3.6	<i>Determination of the limit of detection (LOD)</i> _____	123
CHAPTER 4 _____		124
Synthesis and Characterization of Poly(2,5-dimethoxyaniline) Doped with Poly(4-styrenesulfonic acid) _____		124
4.1	<i>Introduction</i> _____	124
4.2	<i>Electrochemical synthesis and characterization of PDMA-PSS</i> _____	126
4.3	<i>Spectroscopic characterization of PDMA-PSS films</i> _____	130
4.3.1	Fourier transform infrared (FTIR) spectroscopy _____	130
4.3.2	UV-Vis spectroscopy _____	132
4.4	Characterization of PDMA-PSS by scanning electron microscopy (SEM) and transmission electron microscopy (TEM) _____	134
4.5	<i>Conclusions</i> _____	137

CHAPTER 5	139
HRP/PDMA-PSS Biosensor Characterization and Optimization	139
5.1 Introduction	139
5.2 Spectroscopic analysis of PDMA-PSS and HRP/PDMA-PSS films	141
5.2.1 Fourier transform infrared (FTIR) spectroscopy	141
5.2.2 UV-Vis spectroscopy	143
5.3 Direct electrochemistry of HRP and electrochemical characterization of the HRP/PDMA-PSS biosensor	145
5.4 Investigation of the electrocatalytic activity of the HRP/PDMA-PSS biosensor	149
5.5 Response time of the HRP/PDMA-PSS biosensor	155
5.6 Reproducibility and stability of the HRP/PDMA-PSS biosensor	155
5.7 Conclusions	156
CHAPTER 6	157
Application of HRP/PDMA-PSS Biosensor for the Detection of Herbicides	157
6.1 Introduction	157
6.2 Detection of glyphosate by the incubation method	158
6.3 Detection of herbicides by steady-state amperometry (direct method)	166
6.3.1 Glyphosate and aminomethylphosphonic acid standard solutions	167
6.3.2 Detection of glyphosate and glufosinate by the rotating disk electrode	171
6.3.2.1 Glyphosate and glufosinate standard solutions	171
6.3.2.2 Glyphosate and glufosinate in samples	176
6.4 Evaluation of the interaction of horseradish peroxidase with the herbicides	182

CHAPTER 7	188
Conclusions and Recommendations	188
7.1 Conclusions	188
7.2 Recommendations	191
References	193
Appendices	223



LIST OF FIGURES AND TABLES

<i>Figure 1.1. Structures of glyphosate, aminomethylphosphonic acid and glufosinate.</i> -----	2
<i>Figure 1.2. Structures of horseradish peroxidase.</i> -----	6
<i>Figure 2.1. Schematic representation of biosensors.</i> -----	33
<i>Figure 2.2. Schematic representation of an electrochemical enzyme biosensor.</i> -----	39
<i>Figure 2.3. (a) Variation of the reaction velocity v, with the substrate concentration and (b) Lineweaver-Burk plots for different types of reversible enzyme inhibitors.</i> -----	42
<i>Scheme 2.1. Kinetic schemes for reversible enzyme inhibition.</i> -----	46
<i>Table 2.1 Structures and conductivities of some conducting polymers commonly used in biosensors</i> -----	61
<i>Figure 2.4. Electrochemical polymerization of aniline in presence of a dopant anion A^-.</i> -----	63
<i>Figure 2.5. (A) The general polymeric structure of polyaniline (B) Oxidation of aniline to polyaniline showing its redox states.</i> -----	65
<i>Figure 2.6. The structure of poly(2,5-dimethoxyaniline) (PDMA).</i> -----	67
<i>Table 2.2. Assignments for FTIR absorption bands for polyaniline</i> -----	75
<i>Figure 3.1. Schematic representation of an electrochemical cell consisting of three electrodes.</i> -----	97
<i>Figure 3.2. Schematic representation of the major components of the electroanalytical system used for the electrochemical measurements.</i> -----	99
<i>Figure 3.3. A typical cyclic voltammogram.</i> -----	101
<i>Table 3.1. Diagnostic tests for the electrochemical reversibility of a redox couple, carried out by cyclic voltammetry</i> -----	102
<i>Figure 3.4. Convective flow resulting from the rotation of a rotating gold disk electrode.</i> -----	106
<i>Figure 3.5. Schematic representation of the diffusion of the substrate S and the product P in the enzymatic layer on a transducer.</i> -----	109
<i>Figure 3.6. Calibration of an amperometric enzyme electrode for H_2O_2.</i> -----	112

<i>Figure 3.7. Electrochemical synthesis of nanostructured poly(2,5-dimethoxyaniline) in the presence of a dopant anion, A⁻ (PSS).</i> -----	118
<i>Figure 4.1. Cyclic voltammograms for electrochemical synthesis of (a) PDMA-PSS and (b) PDMA films in 1.0 M HCl at a scan rate of 40 mV s⁻¹.</i> -----	127
<i>Figure 4.2. Cyclic voltammograms of electrodeposited PDMA-PSS film in (a) 1.0 M HCl solution at scan rates 20-600 mV s⁻¹ and (b) 0.1 M PBS (pH 6.10), scan rate of 5 mV s⁻¹.</i> -----	129
<i>Figure 4.3. FTIR spectra of undoped PDMA and doped PDMA (PDMA-PSS) films.</i> -----	132
<i>Figure 4.4. UV-Vis spectra of PDMA and PDMA-PSS films.</i> -----	134
<i>Figure 4.5. (a) SEM image of PDMA microfibers (b) SEM image of PDMA-PSS nanoparticles and (c) TEM image of PDMA-PSS nanotubes (magnification of 100 000 x).</i> -----	136
<i>Figure 5.1. FTIR spectra of (a) PDMA-PSS film, (b) HRP/PDMA-PSS film and (c) free HRP.</i> -----	143
<i>Figure 5.2. UV-Vis spectra for HRP in PBS pH 6.10, HRP/PDMA-PSS and PDMA-PSS films in PBS-DMF solution.</i> -----	144
<i>Figure 5.3. (a) Cyclic voltammograms of HRP/PDMA-PSS biosensor in PBS (pH 6.10) at scan rates 2, 3, 5, 7, 10 mV s⁻¹ and (b) the plot of cathodic and anodic peak currents versus scan rates.</i> -----	146
<i>Figure 5.4. The dependency of the formal potential (E^{0'}) on the pH of PBS.</i> -----	148
<i>Figure 5.5. Cyclic voltammograms of HRP/PDMA-PSS biosensor in PBS (pH 6.10) in response to various concentrations of H₂O₂ at a scan rate of 5 mV s⁻¹.</i> -----	151
<i>Figure 5.6. The proposed mechanism for the nanostructured PDMA-PSS/HRP biosensor in anaerobic medium. PDMA^{0/+} are the nanostructured PDMA-PSS-bound redox sites.</i> -----	151
<i>Figure 5.7. Biosensor responses to successive injections of H₂O₂ in stirring PBS (applied potential of -0.28 V). Insets are the calibration curves for the responses. In (a) 60 μL of 2.0 mg/mL and (b) 60 μL of 4.0 mg/ mL buffer solution of HRP was used.</i> -----	154
<i>Figure 6.1. The effect of incubation time on the biosensor response and decay of enzyme activity.</i> -----	160
<i>Figure 6.2. (A) Cyclic voltammograms of HRP/PDMA-PSS biosensor in PBS (pH 6.10) in response to various concentrations of H₂O₂ and (B) Cyclic voltammograms for the HRP/PDMA-PSS/Au electrode in PBS (pH 6.10) in presence of 0.7 μM H₂O₂ after</i>	

<i>incubation in 0.25, 6.0, 12.0, 13.0 and 14.0 $\mu\text{g L}^{-1}$ glyphosate solutions (a-e). Scan rate of 5 mV s^{-1}.</i>	162
Figure 6.3. (a) The effect of inhibitor concentration on the activity of HRP and (b) Inhibition plot for the HRP/PDMA-PSS biosensor, data given as mean \pm S.D.	163
Figure 6.4. Biosensor responses to successive injections of H_2O_2 in absence and presence of 9.6 $\mu\text{g L}^{-1}$ glyphosate, at applied potential of -0.28 V, in stirring PBS.	165
Figure 6.5. Lineweaver-Burk plot for HRP response to H_2O_2 in absence and presence of 9.6 $\mu\text{g L}^{-1}$ glyphosate.	166
Figure 6.6. Biosensor responses to successive additions of (A) H_2O_2 (a-b) and glyphosate standard solutions (b-c) (B) H_2O_2 (a-b) and AMPA standard solutions (b-c) into PBS while stirring at 400 rotations per minute (rpm).	168
Figure 6.7. Inhibition plots showing the effects of glyphosate and AMPA on the activity of the immobilized HRP.	170
Figure 6.8. Biosensor responses to successive injections of (A) H_2O_2 (a-b) and glyphosate standard solutions (b-c) (B) H_2O_2 (a-b, d), blank solutions (b-c) and glufosinate standard solutions (c-d) into PBS under RDE rotation of 400 rpm.	173
Figure 6.9. Calibration curves for biosensor response to (a) glyphosate and (b) glufosinate standards.	176
Figure 6.10. (a) Biosensor responses to successive injections of corn samples spiked with glyphosate (b) response of the biosensor to injections of corn samples spiked with glufosinate (c) extrapolated linear curve for glufosinate in samples.	179
Table 6. 1. Comparison of the analytical parameters of the HRP/PDMA-PSS biosensor with other analytical techniques	181
Figure 6.11 Structures of glyphosate, AMPA and glufosinate in their ionic forms dominant in aqueous solution at pH 6.3.	182
Figure 6.12. FTIR spectra illustrating the interaction of glyphosate with horseradish peroxidase.	184
Figure 6.13. SEM images of (a) PDMA-PSS film, (b) HRP/PDMA-PSS film, (c) HRP/PDMA-PSS film (mag. 2500 x), (d) HRP/PDMA-PSS-Glyphosate, (e) HRP/PDMA-PSS-Glufosinate and (f) HRP/PDMA-PSS-AMPA (magnifications of 2500 and 1000x).	187

<i>Appendix A1. EDX spectra for undoped poly(2,5-dimethoxyaniline)(PDMA).</i>	-----223
<i>Appendix A2. EDX spectra for doped poly(2,5-dimethoxyaniline)(PDMA-PSS).</i>	-----224
<i>Appendix A3. Calibration curves for biosensor response to (a) glyphosate and (b) AMPA standard solutions.</i>	-----225



LIST OF PUBLICATIONS

Everlyne A. Songa, Vernon S. Somerset, Tesfaye Waryo, Priscilla G. L. Baker & Emmanuel I. Iwuoha (2009). Amperometric Nanobiosensor for Quantitative Determination of Glyphosate and Glufosinate Residues in Corn Samples. *Pure and Applied Chemistry*, 81, 123-139.

Everlyne A. Songa, Tesfaye Waryo, Nazeem Jahed, Priscilla G. L. Baker, Boitumelo V. Kgarebe & Emmanuel I. Iwuoha (2009). Electrochemical Nanobiosensor for Glyphosate Herbicide and its Metabolite. *Electroanalysis*, DOI: 10.1002/elan.200804452 [In Press].

Everlyne A. Songa, Omotayo A. Arotiba, Joseph H. O. Owino, Nazeem Jahed, Priscilla G. L. Baker, & Emmanuel I. Iwuoha (2009). Electrochemical Detection of Glyphosate Herbicide Using Horseradish Peroxidase Immobilized on Sulfonated Polymer Matrix. *Bioelectrochemistry*, [In Press].

Tesfaye T. Waryo, **Everlyne A. Songa**, Mangaka C. Matoetoe, Rachel F. Ngece, Peter M. Ndangili, Amir Al-Ahmed, Nazeem M. Jahed, Priscilla G. L. Baker & Emmanuel I. Iwuoha (2009). Functionalization of Polyaniline nanomaterials for amperometric biosensing, *Book chapter: Nanostructured Materials for Electrochemical Biosensors*, [In Press].

ABBREVIATIONS

EU	European Union
UK	United Kingdom
EPA	Environmental Protection Agency
MRL	Maximum residue limit
USA	United States of America
FAO	Food and Agricultural Organization
AMPA	Aminomethylphosphonic acid
PDMA	Poly(2,5-dimethoxyaniline)
PSS	Poly(4-styrenesulfonic acid)
CP	Conducting polymer
HRP	Horseradish peroxidase
PBS	Phosphate buffer solution
PPy	Polypyrrole
PTh	Polythiophene
PANI	Polyaniline
PPh	Polyphenylene
SEM	Scanning electron microscopy
TEM	Transmission electron microscopy
FTIR	Fourier transform infrared
UV-Vis	Ultra violet-visible
RDE	Roating disk electrode
rpm	Rotations per minute
CV	Cyclic voltammetry
POEA	Polyoxyethyleneamine
WHO	World Health Organization
MPAA	2-Methylphosphonicoacetic acid
MPPA	3-Methylphosphonicopropionic acid
GC	Gas chromatography
CE	Capillary electrophoresis
LC	Liquid chromatography
MS	Mass spectrometry
HPLC	High performance liquid chromatography

CHAPTER 1

General Introduction

1.1 Background information

Glyphosate [*N*-(phosphonomethyl)glycine] and glufosinate [DL-homoalanine-4-yl-(methyl)phosphonic acid] (Fig.1.1) are phosphorus-containing, broad-spectrum, non-selective herbicides for control of long grasses and broad-leaved weeds. The phosphorus-containing herbicides interfere with the formation of amino acids and other chemicals in plants (Kataoka, et al., 1996; Cikalo et al., 1996). Degradation of glyphosate in plants, water and soil mainly occurs under biological conditions yielding aminomethylphosphonic acid (AMPA) (Fig.1.1) as the major metabolite.

The introduction of transgenic plants that are resistant to glyphosate and glufosinate herbicides has tremendously increased their use in the agricultural fields. However, because their effects on non-target organisms and overall environmental impact have not been fully investigated, questions regarding the environmental safety with their increasing use have to be addressed. The presence of pesticide (herbicides, fungicides, insecticides etc.) residues in the environment and the public concern on their possible toxic effects has forced the official international institutions to establish maximum allowable concentration levels of these chemicals. In the European Union (EU) as well as in the United States of America, lists of compounds are established

through the National Pesticide Survey, based on the effects of the compounds on human health and the environment (Stalikas and Konidari, 2001; US EPA, 1990; US EPA, 1992). For instance, the Environmental Protection Agency (EPA) has set a maximum residue limit (MRL) of glyphosate in fruits and vegetables in the range of 0.2–5.0 mg kg⁻¹, in soybean at 20 mg kg⁻¹, and in drinking water at 0.7 mg L⁻¹ (EPA, 2006). The Food and Agricultural Organization (FAO) of the United Nations has set a MRL of glyphosate in the range of 0.1–5.0 mg kg⁻¹ for fruits and grains and MRL of glufosinate at 0.05 mg kg⁻¹ for grains (FAO, 2006). The European Union (EU) limit of any pesticide in drinking water has been set at 0.1 µg L⁻¹ irrespective of their toxicological effects (Stalikas and Konidari, 2001). Therefore, the monitoring of residue or trace levels of these compounds in environmental and biological samples has gained increasing importance and attracted considerable attention (Stalikas and Konidari, 2001).

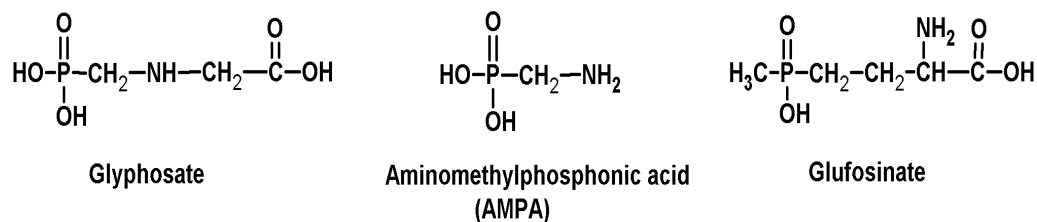


Figure 1.1. Structures of glyphosate, aminomethylphosphonic acid and glufosinate.

A simple analytical method for the determination of glyphosate, glufosinate and AMPA at residue or the sub µg L⁻¹ level has however proven to be very difficult to obtain, mainly due to their ionic character, high solubility in water, low volatility,

insolubility in organic solvents, high polarity and low mass and favoured complexing behaviour (Songa et al., 2009). Additionally, the absence of chromophore or fluorophore groups in their structures disables the photometric and fluorometric detection of these substances by liquid chromatography (LC) techniques. Majority of the methods reported for the determination of glyphosate, glufosinate and AMPA involves the employment of gas chromatography (GC), liquid chromatography (LC) and capillary electrophoresis (CE) techniques which require pre- or post-column derivatization procedures to lower the polarity and enhance volatility of the compounds (Stalikas and Konidari, 2001; García de Llasera et al., 2005; Ibáñez et al., 2005; Songa et al., 2009). However, the procedure of derivatization is always tedious, time-consuming and sometimes generates unstable products. Glyphosate, glufosinate and AMPA exist in the environment at very low concentrations, from parts per trillion (ng L^{-1}) to parts per million (mg L^{-1}) (Piriyaipittaya et al., 2008) therefore, the development of new methods for rapid, sensitive and inexpensive detection of these compounds at such low concentrations is desirable.

Biosensors are the most suitable to complement the standard analytical methods for the detection and quantification of these herbicides due to their low cost of analysis, ease of operation, high sensitivity and minimization of sample pre-treatment. They are defined as analytical devices incorporating a biological recognition element which is integrated within a physicochemical signal transducer or transducing micro-system. Enzymes were historically the first biological recognition elements included in biosensors and continue to be the basis for a significant number of publications

reported for biosensors in general as well as biosensors for environmental applications. The several advantages of enzyme biosensors include a stable source of material (primarily through biorenewable sources), the ability to modify the catalytic properties of substrate specificity by means of genetic engineering, and catalytic amplification of the biosensor response by modulation of the enzyme activity with respect to the target analyte.

Horseshoe peroxidase (HRP) enzyme, in particular has served a unique role in the understanding of enzyme reactions in general and in the development of spectroscopic approaches to elucidate molecular or electronic structural properties and relevant functions (Chen et al., 2000). It is a member of a large class of heme peroxidases which catalyze the oxidation of organic and inorganic substrates by H_2O_2 or organic peroxides. Most heme peroxidases contain iron (III) protoporphyrin IX (ferriprotoporphyrin IX) as the prosthetic group. HRP is the most commonly used enzyme for practical analytical applications, mainly because it retains its activity over a broad range of pH and temperature (Freire et al., 2003). From analytical point of view, the interesting feature of HRP immobilized electrode is its low operating potential (close to 0 V versus Ag/AgCl) which offers low background currents and minimizes the risk of surface fouling and interference by electroactive species (Petit et al., 1998). The three-dimensional and crystal structures of HRP (1H5A) are shown in Fig.1.2. Facilitation of the direct electron transfer between HRP and the bare electrode surface has however been very challenging due to the insulation of their redox centres by a thick shell of proteins. Thus, numerous efforts have been devoted

to improving its electrochemical reaction by modifying the electrode surface using surfactant matrix, membranes, nanoparticles, hydrogel polymers, microcapsule, conducting polymers etc. (Collings and Caruso, 1997; Shan et al., 2007). Studies have shown that the incorporation of HRP onto conducting polymer film leads, in principle, to the enhancement of charge transport and its physical (and often chemical) stability (Ernst et al., 2007). Conducting polymers are capable of penetration of the insulating shell of the enzyme enabling a means of direct electrical communication between its redox centre and the electrode surface (Grennan et al., 2006). Due to their excellent conductivity and electroactivity, conducting polymers act as self-contained electron transfer mediators for enzyme electrodes, where they undergo redox cycling and can couple electrons directly from the enzyme active site to the electrode surface. In this case, no additional diffusional mediators are required in the sensing system for electron transfer to take place. This phenomenon is referred to as “electrical wiring” of the enzyme to the electrode (Grennan et al., 2006). The confinement of the mediator to the electrode surface prevents it from leaching into solution thus increases the stability of the biosensor. Studies have revealed that further incorporation of polyelectrolytes such as poly(styrenesulfonic acid) or dopants during polymerization enhances stability and maintains the conductivity of the polymer film at neutral pH (Bartlett and Wallace, 2000).

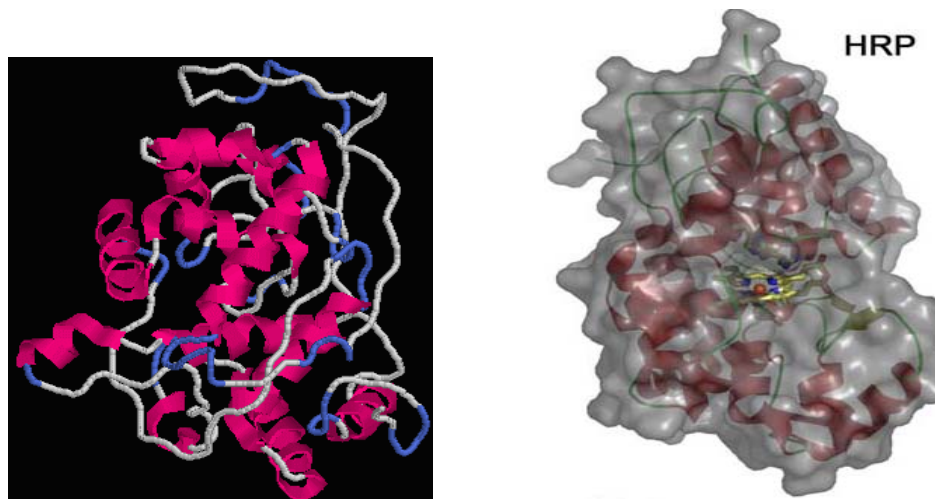


Figure 1.2. Structures of horseradish peroxidase.

Over the past two decades, tremendous advances have been made in understanding of the chemical, electrochemical, structural, electrical and optical phenomena of inherently conducting polymers, such as polypyrrole (PPy), polythiophene (PTh), polyaniline (PANI), polyphenylene (PPh) and their derivatives. The peculiarity of these polymers is that they are characterized by alternating single and double bonds and therefore can be reversibly oxidized or reduced (Iwuoha et al., 1996). The great interest in these polymers arises from their relative ease of synthesis by chemical or electrochemical oxidative polymerization of the monomers, their considerable importance as candidates for new materials that would lead to the next generation of electronic and optical devices and as promising transducers for chemical or biosensors. Different approaches to the synthesis and application of conducting polymers in chemical sensors and biosensors have been extensively studied (Janata and Josowicz, 2003; Iwuoha et al., 1997; Gerard et al., 2002, Morrin et al., 2005; Luo et

al., 2007; Somerset et al., 2007; Michira et al., 2007; Akinyeye et al., 2007; Songa et al., 2009). Conducting polymers have gained increasing applications in the development of biosensors in particular, especially those incorporating enzymes either as a recognition element such as enzyme biosensors or as a redox active label such as the antibody-based biosensors. Modification of electrodes with multi-layered polymeric materials is a popular procedure towards the fabrication of high performance reagentless sensors. The use of conducting polymers for electrode modification allows for the tailoring of the electrode surface towards the detection of a specific analyte besides overcoming overpotential problems related to the analyte detection. Conducting polymers are well known for their ability to provide a suitable micro-environment for immobilization of biomolecules. They also localize the biomolecules close to the electrochemical interface thus minimizing interferences which may lead to undesired side reactions for large background currents. The fact that the 2000 Nobel Prize in Chemistry went to Alan J. Heeger, Alan G. MacDiarmid and Hideki Shirakawa “*for the discovery and development of conductive polymers*” (*Nobel Citation*) also reflects both research and practical importance of conducting polymers and their applications in modern science and daily life (<http://nobelprize.org/chemistry/laureates/2000>).

Of these polymers, PANI has elicited the most interest since its electric conductivity was discovered by MacDiarmid et al. in 1985 (MacDiarmid et al., 1985). This is due to its wide range of conductivity from insulating to metallic regime, unique redox tunability, good environmental stability, low cost, ease of synthesis, and promising

applications in various fields, such as metallic corrosion protection (Plesu et al., 2006), electrochromic devices (Yang and Heeger, 1994), light-weight batteries (Oyama et al., 1995), sensors (Shinohara et al., 1988; Iwuoha et al., 1997; Morrin et al., 2005), etc. Despite the great potential use of PANI, its processability has remained a difficult problem due to its insolubility in common organic solvents. As a result, alkyl- and alkoxy-substituted PANIs such as poly(2-methoxyaniline), poly-*o*-methoxyaniline, poly(2,5-dimethoxyaniline) (PDMA), etc., synthesized by the chemical or electrochemical oxidation of the substituted aniline monomer have become a suitable alternative to increasing its solubility. Such substitution imparts solubility in organic solvents that is markedly improved over the parent (unsubstituted) salts upon their emeraldine salt products. It has been reported that aniline substituted with two methoxy groups, 2,5-dimethoxyaniline (DMA) produces soluble polymer, poly(2,5-dimethoxyaniline), PDMA with a conductivity similar to PANI (Storrier et al., 1994; Chen et al., 2003). It is also reported that preparation of PANI in aqueous solution of poly(4-styrenesulfonic acid), polyacrylic acid, or dodecyl benzene sulfonic acid results in self-doped soluble PANI (Bisak et al., 2005).

With recent development in nanoscience and nanotechnology, micro-/nanostructured PANI have received considerable attention because of the unique properties of PANI which has lead to their wide applications in micro/nano-materials (Athawale and Kulkarni, 2000; Huang, et al., 2002) and in the fabrication of macromolecular electronic devices such as microelectronics, photonics (Holdcroft, 2001), sensors in

chemical (Virji et al., 2004), electrochemical (Janata and Josowicz, 2003) and biological applications (Liu et al., 2005). Nanostructured PANIs are known to exhibit properties superior to those of their corresponding macroscopic materials. (Huang and Kaner, 2004; Virji et al., 2004; Nandi et al., 2008). When used as sensors, they have shown enhanced performance, greater sensitivity and faster response time in contrast to their conventional bulk counterpart due to higher effective surface area and shorter penetration depth for target molecules (Huang and Kaner, 2004; Virji et al., 2004; Nandi et al., 2008). In general, “template synthesis” method is the most common and effective method for synthesizing nanostructured PANI. It is further subdivided into hard template (physical template) synthesis and soft template (chemical template) synthesis approach according to the solubility of the templates in the reacting media. The hard template synthesis involves polymerization of monomeric species within the nanoscopic void spaces of templates such as anodic alumina, polycarbonate track-etched membranes and mesoporous aluminosilicate (Wei et al., 2002). The soft template method, also known as the “template-free” method entails the use of structure-directing molecules such as surfactants, polyelectrolytes, etc. In comparison with PANI nanoparticles, which are mainly synthesized by dispersion technique and electrochemical methods, one-dimensional nanostructured PANI, including nanofibers, nanowires, nanorods, nanotubes, nanofibrils, nanobelts and nanoribbons, synthesized by the “template” method presents several advantages in fabricating nanodevices and in preparing nanoscale electrical connections in highly conducting polymer composites, etc. (Zhang and Wang, 2006).

This research work focuses on advances, directions and strategies in the development of a simple, cheap and sensitive electrochemical nanobiosensor for inhibitor determination of the herbicides glufosinate, glyphosate and its metabolite AMPA. It entails the use of electrochemical methods such as cyclic voltammetry (CV) and amperometry; spectroscopic methods such as Fourier transform infrared (FTIR) and ultra violet-visible (UV-Vis) spectroscopy as well as the morphological techniques such as scanning electron microscopy (SEM) and transmission electron microscopy (TEM). The electrochemical techniques are important for the characterization of the electroactive species, the study of the electrochemical reactions and direct electron transfer of enzymes at the electrode surfaces as well as in the detection of analytes by incorporation of biological recognition elements such as enzymes. Spectroscopic techniques are highly valuable for the determination of the conducting states of the polymers as well as in the investigation of the changes that occur in the secondary structures of proteins by monitoring the changes in their absorption bands. The morphological techniques are highly applicable for the characterization of materials and for the estimation of their sizes. Special attention has been given to the synthesis of nanostructured poly(2,5-dimethoxyaniline) (PDMA) by the electrochemical “soft template” method (using poly(4-styrenesulfonic acid) as the dopant and structure-directing molecule) to be used as mediators in the horseradish peroxidase (HRP) biosensor; the development of HRP biosensor and its application for inhibitor determination of the herbicides. HRP was the desirable model molecule for this study because of its commercial availability, moderate cost, its known documented

structure and its direct electron transfer when immobilized on electrode surfaces. The detection principle used was based on the inhibition of the activity of the enzyme HRP by the herbicides.

1.2 Problem statement

The presence of glyphosate, glufosinate and AMPA residues in the environment and the public concern on their possible toxic effects calls for precise and accurate methods for quantifying their residues at levels encompassing and above their maximum residue limits. However, these herbicides and their metabolites often present an analytical challenge mainly due to their chemical and physical properties. Majority of the methods reported for their determination involve the use of GC, LC and CE techniques which require pre- or post-column derivatization procedures to lower the polarity and enhance volatility of the compounds. These conventional methods allow high accuracy of quantification and low detection limits, but they require the use of sophisticated instruments and chemical manipulation of samples before measurement which is time consuming and inconvenient. In view of these analytical challenges, it is hoped that the electrochemical HRP/PDMA-PSS inhibition based biosensor developed in this study will provide an alternative to quantification of these herbicides at residue levels.

1.3 Objectives of the research work

1.3.1 General objectives

The main aim of this research was to develop an electrochemical nanobiosensor for sensitive and rapid determination of the herbicides glufosinate, glyphosate and its metabolite AMPA.

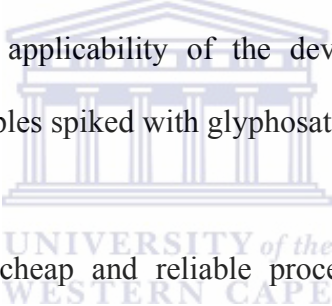
1.3.2 Specific objectives

The specific objectives include:

- i. To synthesize nanostructured poly(2,5-dimethoxyaniline) (PDMA) by the electrochemical “soft template” method employing the dopant and structure-directing molecule poly(4-styrenesulfonic acid) (PSS);
- ii. To characterize the synthesized nanostructured PDMA-PSS films by cyclic voltammetry (CV), transmission electron microscopy (TEM), scanning electron microscopy (SEM), Fourier transform infrared (FTIR) and UV-Vis Spectroscopy;
- iii. To develop an electrochemical nanobiosensor by electrostatic attachment of the enzyme HRP onto the surface of gold disk/rotating gold disk electrode modified with nanostructured PDMA-PSS film;



- iv. To characterize the developed HRP/PDMA-PSS biosensor by CV, FTIR and UV-Vis spectroscopy and to optimize the biosensor parameters such as sensitivity, stability and limit of detection;
- v. To investigate the effects of glyphosate, glufosinate and AMPA on the HRP electrocatalytic activity towards the reduction of H_2O_2 and to study the interaction between the immobilized HRP and the herbicides by FTIR and SEM;
- vi. To apply the developed biosensor for the detection of glyphosate, glufosinate and AMPA in standard solutions;
- vii. To determine the applicability of the developed biosensor by analyzing extracted corn samples spiked with glyphosate and glufosinate.

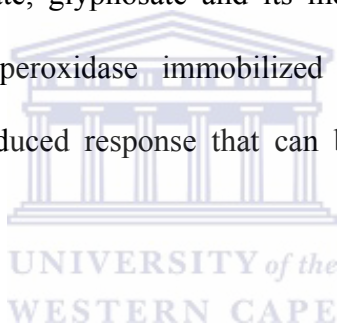


In this study, a simple, cheap and reliable procedure for preparing HRP-based nanobiosensor for novel detection of glyphosate, glufosinate and AMPA is described. Firstly, the nanostructured PDMA films were polymerized on a gold electrode surface by the electrochemical “soft template” method using PSS as the dopant and structure-directing molecule. The use of PSS is important due to the fact that it is known to shift the redox activity of PANI films to a neutral pH environment required during measurements involving the use of enzymes. The heme-protein HRP was then incorporated onto the electrosynthesized PDMA-PSS film and its direct electrochemistry monitored on a gold disk electrode. Nanostructured PDMA-PSS film was used to provide a suitable micro-environment for HRP immobilization in order to enhance the direct electron transfer between HRP and the electrode surface.

The resulting nanobiosensor (HRP/PDMA-PSS/Au) was applied for the detection of glyphosate, glufosinate and AMPA. Hydrogen peroxide was used as the substrate to study the electrocatalytic activity of the immobilized HRP before and after its contact with the herbicide solutions.

1.4 Thesis statement

In light of the problem statement and the research objectives, the thesis of this work is “The herbicides glufosinate, glyphosate and its metabolite AMPA can inhibit the activity of horseradish peroxidase immobilized on the PDMA-PSS modified electrode leading to a reduced response that can be measured and used for their quantification.”



Glyphosate and glufosinate have three chemical groups (amine, carboxylate and phosphonate) that can bind strongly to ions resulting in the formation of complexes. AMPA has the amine and phosphonate chemical groups. HRP is capable of binding to the chemical groups present in these herbicides resulting in inhibition of its activity. The inhibition effect can be as a result of the formation of a complex due to the herbicide chemical groups binding to the peptide backbone chain $\{-(C=O)-NH-\}$ present in HRP. The formation of the complex may change the HRP secondary conformation. The changes in the conformation of HRP would obstruct the electron transfer of Fe (III) in the porphyrin ring of the heme group, thus inhibiting its electrocatalytic activity for the reduction of H_2O_2 . The biosensing principle was

therefore based on measuring the electrocatalytic response of the immobilized HRP before and after its contact with the herbicide solutions.

1.5 Thesis layout

Chapter 2 presents reviews on the health effects and environmental occurrence of glyphosate and glufosinate herbicides as well as the analytical techniques used for their detection; the recent developments in the use of conducting polymers and nanostructured conducting polymers as materials for biosensor construction, as well as the features and applications of biosensors. Various synthetic routes for nanostructured polyaniline materials and their improved features over the conventional polyaniline are discussed. The chapter also highlights the enzyme kinetics in relation to their inhibition principles.

Chapter 3 describes the various analytical techniques employed, detailed research methodology and general experimental procedures for the electrochemical synthesis of nanostructured conducting polymer, biosensor construction, characterization and application of the developed biosensor for the determination of herbicides.

Chapter 4 presents the results for the characterization of the poly(2,5-dimethoxyaniline) (PDMA) electrochemically synthesized by the “soft template” method employing the structure-directing molecule poly(4-styrenesulfonic acid) (PSS). The results for the electrochemical characterization of the PDMA-PSS film are

presented. The doping properties of PDMA-PSS films were investigated by Fourier transform infrared (FTIR) and UV-Vis spectroscopy and the results are presented in this chapter. In addition, the results obtained from the morphological characterization of PDMA-PSS by transmission electron microscopy (TEM) and scanning electron microscopy (SEM) to estimate their sizes are presented. The features of the nanostructured materials were investigated in relation to their application as biosensor materials.

Chapter 5 presents the results for the characterization of the HRP/PDMA-PSS biosensor as well as those for its optimization for the detection of H_2O_2 . The direct electron transfer of HRP immobilized on nanostructured PDMA-PSS film as well as the biosensor parameters were characterized by cyclic voltammetry (CV) and spectroscopic techniques such as FTIR and UV-Vis spectroscopy and the results discussed in this chapter.

Chapter 6 presents the results of inhibition analysis of glyphosate, glufosinate and Aminomethylphosphonic acid (AMPA) by HRP/PDMA-PSS biosensor employing voltammetric and amperometric techniques as well as the results obtained from monitoring the interaction of HRP and the herbicides by SEM and FTIR techniques.

Chapter 7 summarizes the major findings of this study and the conclusions drawn from the results of the research. The conclusions drawn have been used to formulate the recommendations for further studies.

CHAPTER 2**Literature Review****2.1 Introduction**

In recent years, biosensors have been increasingly used for continuous monitoring of biological and synthetic processes and to aid our understanding of these processes. Biosensors can meet the need for continuous, real-time in vivo monitoring to replace or complement the intermittent analytical techniques used in industrial and clinical chemistry (Fraser, 1997). Typical applications of biosensors include environmental monitoring and chemical measurements in the agriculture, food and drug industries. The systematic description of a biosensor should include features such as the detected or measured parameter; the working principle of the transducer; the physical and chemical or biochemical model; the application for analyte detection and; the technology and materials for sensor fabrication (Göpel and Schierbaum, 1991). Rapid growth in biomaterials, especially the availability and application of a vast range of conducting polymers and copolymers associated with new sensing techniques have led to remarkable innovation in the design and construction of biosensors, significant improvements in sensor function and the emergence of new types of biosensors. This chapter presents reviews on the health effects and environmental occurrence of glyphosate and glufosinate herbicides as well as the analytical techniques used for their detection; the recent developments in the use of conducting polymers and

nanostructured conducting polymers as materials for biosensor construction; and the features and applications of biosensors. Various synthetic routes for nanostructured PANI materials and their improved features over the conventional PANI are discussed. The chapter also highlights the enzyme kinetics in relation to their inhibition principles.

2.2 Herbicides

Herbicides are a heterogeneous group of chemicals used to kill or inhibit the growth of undesirable plants that might cause damage, present fire hazards, or impede work crews. They are known to suppress the photosynthetic reactions in plants as well as the activity of tyrosinase and peroxidase enzymes (Evtugyn et al., 1998). They have largely replaced mechanical methods of weed control in countries where intensive and highly mechanized agriculture is practiced. Among the herbicides used, phosphonic and amino acid group-containing herbicides including the predominantly employed glyphosate [*N*-(phosphonomethyl)glycine] and glufosinate [DL-homoalanine-4-yl-(methyl)phosphonic acid] herbicides constitute an important category of herbicides requiring continuous monitoring in the environment. The present research therefore focuses on their detection. The general description of these herbicides, their environmental occurrence as well as their health effects follow.

2.2.1 Glyphosate

Glyphosate [*N*-(phosphonomethyl)glycine] is a broad-spectrum, non-selective, post-emergent herbicide which is used extensively worldwide to kill a wide range of weeds. It is the active ingredient in the commercial herbicide Roundup[®], a product widely applied in agricultural practice. Glyphosate itself is an acid, but it is usually formulated in salt form, most commonly the isopropylamine or trimethylsulfonium salt. A surfactant (wetting agent) known as polyoxyethyleneamine (POEA), which helps the active ingredient penetrate the plant surface, is usually added to glyphosate formulations. Glyphosate has three chemical groups (amine, carboxylate and phosphonate) that can bind strongly to metal ions, especially to transition metals (Morillo et al., 1994; Daniele et al., 1997). It has been reported to possess a high affinity and chelating capacity for iron and other metals, resulting in the formation of poorly soluble glyphosate-metal complexes or insoluble precipitates in soil or hard water (Barja et al., 2001). Aminomethylphosphonic acid (AMPA) is the major degradation product of glyphosate found in plants, water and soil. Glyphosate and AMPA are very polar compounds ($\log P_{\text{oct}} = -3.2$ and -2.36 , respectively) and present high solubility in water (12 g L^{-1} for glyphosate) and insolubility in organic solvents. They are also amphoteric compounds (Stalikas and Konidari, 2001). Owing to their physicochemical properties, it is not easy to establish simple and cheap methodologies to extract and determine residues of these compounds in the environment.

Dramatic increases in the agricultural use of glyphosate occurred in 1997 corresponding to the introduction of crops (e.g. corn, soybeans, rice, cotton, and canola) that have been genetically engineered to be tolerant to glyphosate (Kolpin et al., 2006). The chemicals and biotechnology company Monsanto, which produces glyphosate (Roundup[®]), also produces the genetically engineered crops that are now on the market, usually labelled as "Roundup Ready" (Buffin and Jewell, 2001). To genetically engineer a plant, a gene from a soil bacterium (*Agrobacterium* sp.) is added into the plant enabling crops to be sprayed with glyphosate without being affected. Monsanto claims that the introduction of the genetically modified crops is of benefit because of the low toxicity and environmental safety of glyphosate, while independent research indicates that glyphosate may not be as safe as previously thought and may pose a threat to human health and the environment (Buffin and Jewell, 2001). The environmental occurrence of glyphosate and AMPA has been associated with their high use on crops, forests and railway tracks (Giesy, et al., 2000; Kolpin et al., 2006). New extraction procedures as well as detection techniques are slowly but increasingly being developed for monitoring of the environmental occurrence of glyphosate. The possible health effects of glyphosate and its environmental occurrence are documented below.

2.2.1.1 Health effects of glyphosate

The chemical and toxicological properties of glyphosate are well documented (WHO, 1994; Giesy, et al., 2000), with multiple studies finding that glyphosate-based

formulations are more toxic to aquatic organisms than glyphosate itself due to surfactants present in the technical formulations. The surfactant POEA used as a wetting agent in glyphosate formulations is the major cause of some of the acute and chronic toxic effects observed (Tsui and Chu, 2003; Tsui and Chu, 2004). Some studies have found that the combination of glyphosate and POEA is more toxic than POEA alone. More recently it was discovered that POEA is likely to be a cause of human death through suicide and also have adverse impacts on other organisms (Buffin and Jewell, 2001). AMPA is thought to be equal or less toxic than glyphosate (Giesy, et al., 2000).

Low levels of glyphosate have frequently been detected in the urine of farm workers shortly after a glyphosate application (Acquavella et al., 2004). As a result, studies have been conducted to monitor the exposure of workers to glyphosate products. In the USA, a study to monitor the exposure of workers to glyphosate was conducted and the results indicated that the dilution and use of Roundup[®] with hand applicators or tractor sprayers resulted in a range of exposure to glyphosate despite the use of special protective clothing (Buffin and Jewell, 2001). Occupational or accidental exposure to smaller amounts of glyphosate products has been shown to cause a variety of symptoms including eye and skin irritation, contact dermatitis, eczema, cardiac and respiratory problems and allergic reactions (Buffin and Jewell, 2001). In-vitro studies have shown glyphosate to have an effect on progesterone production in mammalian cells and can affect mortality of placental cells in-vitro. Some studies

suggest that glyphosate can cause chronic health effects in laboratory animals (Buffin and Jewell, 2001).

2.2.1.2 Residues of glyphosate in food and water

The use of glyphosate may result in its residues being found in crops, animal tissues or drinking water destined for human consumption. The WHO found that pre-harvest use of glyphosate (for late season weed control or as a pre-harvest desiccant) results in significant residues in the grain and plant material. The WHO also found that the presence of glyphosate residues in animal feeds arising from pre-harvest treatment of cereals with glyphosate may result in its low residues in meat, milk and eggs. In storage, residues of glyphosate are reported to be stable for one year in plant material and for two years in animal products. Glyphosate residues were found in some food items when they were planted a year after glyphosate was applied (Buffin and Jewell, 2001). However, the residues of glyphosate have not been adequately monitored despite their presence in food because the methods of analysis are complex and costly. In 1994, the WHO recommended that “a market-basket survey” be carried out to determine the possible exposure of the general population to glyphosate through diet (WHO, 1994). The MRLs for glyphosate have been set by the FAO/WHO Joint Meeting on Pesticide Residues, and varies for different crops. The acceptable daily intake has been set by the FAO/WHO’s Codex Alimentarius Commission at $0.3 \text{ mg kg}^{-1} \text{ day}^{-1}$ for an average 60 kg man (FAO/WHO, 1996).

Generally, glyphosate residues in water are not adequately monitored because they are extremely difficult to isolate. There are occasional reports of water contamination by glyphosate. In the US, glyphosate was found in seven US wells (US EPA, 1992). It was also reported that the urban use of glyphosate contributes to glyphosate and AMPA concentrations in streams in the United States with AMPA being detected much more frequently (67.5%) compared to glyphosate (17.5%) (Kolpin et al., 2006).

2.2.2 Glufosinate

Glufosinate [DL-homoalanine-4-yl-(methyl)phosphonic acid] is a short name for the ammonium salt, glufosinate ammonium. It is majorly marketed under the name Basta® and is widely used in various applications for weed and vegetation control. It is a broad-spectrum, non-selective, post-emergence herbicide and it is also used to desiccate (dry out) crops before harvest. The anionic surfactant, sodium polyoxyethylene alkylether sulphate, is usually added to glufosinate formulations to enhance the plant's absorption of glufosinate. Glufosinate and its main metabolites, 3-methylphosphonicopropionic acid (MPPA) and 2-methylphosphonicoacetic acid (MPAA) are readily soluble in water (for example, 1370 and 794 g L⁻¹, for glufosinate and MPPA, respectively) and can form strong complexes. Such complexes cause problems during the quantitative determination of glufosinate residues.

Agricultural use of glufosinate ammonium is expected to rise since genetically modified organisms (like corn, soybeans, canola, cotton and sugar beets) resistant to this herbicide are being introduced on a commercial scale. Indeed, such a resistance allows farmers to use glufosinate herbicides in order to improve their crop yield by eliminating undesirable weeds with doses tolerated by glufosinate resistant crops. Aventis, the biotechnology company producing these crops, claims that their introduction will be of benefit because of the low toxicity and environmental safety of glufosinate ammonium (Jewell and Buffin, 2001). However, there are many gaps in the evidence for this claim and independent research indicates that glufosinate ammonium may pose a threat to human health and the environment (Jewell and Buffin, 2001). It is thus essential that questions on the safety of glufosinate owing to its increase in use be answered and more research be carried out to investigate its health and environmental impacts. The health effects of glufosinate and its environmental occurrence are documented below.

2.2.2.1 Health effects of glufosinate

Glufosinate ammonium can be environmentally friendly and less toxic than other herbicides if used as recommended and a detrimental effect on the health of both users and consumers would be extremely unlikely. Glufosinate ammonium structurally resembles glutamate, a typical excitatory amino acid in the central nervous system. It is recognized that excess release of glutamate results in the death of nerve cells in the brain. Clinical studies report that acute glufosinate ingestion

induces convulsions and memory impairment in humans (Calas et al, 2008). Chronic exposure to glufosinate ammonium is also reported to induce spatial memory impairments, hippocampal MRI modifications and GS activation in mice (Calas et al., 2008). Glufosinate has been found to cause a number of neurological symptoms in laboratory animals following both oral and dermal exposure. The incidence of poisoning in humans caused by the ingestion of high quantities of glufosinate ammonium was reported in Japan. All the patients developed various neurological symptoms such as seizures, loss of memory, unconsciousness, convulsions, irregular breathing and salivation which appeared after an asymptomatic interval of several hours (Hori et al., 2003; Cox, 1996). Death was due to circulatory failure, which may mainly come from the surfactant. The metabolite, MPPA like glufosinate, is reported to be a neurotoxin though the mechanisms of these neurotoxicities of glufosinate ammonium have not been established. The administration of glufosinate ammonium to the rat induces behavioural changes such as aggressiveness, 'wet-dog shakes' induced by administering kainic acid. Kainic acid stimulates glutamate receptors in the brain. It is also reported that glufosinate ammonium induces apoptosis in the neuroepithelium of mouse embryos in culture ((Jewell and Buffin, 2001).

2.2.2.2 Residues of glufosinate in food and water

Residues in food are an area of concern, especially when glufosinate is used as a pre-harvest desiccant. It is reported that consumers are most likely to be exposed to residues of glufosinate in potatoes and dried (or processed) peas, dried cereals,

oilseed rape, linseed and in liver and kidney from animals fed on contaminated cereal straw (Jewell and Buffin, 2001). It was also reported that when wheat grain containing residues was turned into flour, 10-100% of the residue was retained. Another report indicated that the use of glufosinate herbicide in glufosinate-tolerant oilseed rape crops may result in the formation of a metabolite (N-acetyl-L-phosphinothricin) whose physiological activity corresponds to that of glufosinate (Jewell and Buffin, 2001). This finding has implications for consumers, as oil extracted from the crop is used in cooking oil, margarine, mayonnaise, dressings and cocoa butter substitutes. The WHO/FAO recommended the acceptable daily intake for glufosinate to be 0.02 mg kg^{-1} body weight (WHO/FAO, 2006).

Glufosinate ammonium has not been reported as a major groundwater contaminant in any of the developed countries where it is registered for use (WHO, 1996). The relatively short half-life (3-70 days) in soil suggests that there is a low potential for glufosinate transport to groundwater if used as recommended. However, the increase in its use with the commercialization of glufosinate tolerant crops could increase the likelihood of its water contamination. Only monitoring over time will establish if glufosinate is a threat to drinking water or not.

2.2.3 Detection of herbicides

The difficulties in establishing simple methodologies for the extraction and determination of glyphosate, glufosinate and AMPA at residue levels are mainly due

to their chemical and physical properties (Stalikas and Konidari, 2001; Songa et al., 2009). Additionally, they have no ultraviolet (UV) chromophore or fluorophore making simple UV detection impossible. The analytical methods reported for the determination of these compounds are mainly based on gas chromatography (GC), liquid chromatography (LC), and capillary electrophoresis (CE). Most of these conventional analytical methods employ pre- or post-column derivatization procedures to confer volatility, fluorescence or UV absorption properties to the analytes, thus increasing the time of analysis, cost and analytical uncertainty to the assay. The analytical methods employed for their analysis, as well as the sample pre-treatment methods have been comprehensively reviewed by Stalikas and Konidari (2001). Normally, HPLC has been used in combination with fluorescence and UV-Vis detection after derivatization, although in a few cases glyphosate has been determined directly by ion chromatography (IC) with UV detection or suppressed conductivity detection, but with limited sensitivity. The detection of glyphosate derivatives in LC and GC exhibited high sensitivity and selectivity; however, these derivatization procedures are quite complicated and require special equipment. Capillary electrophoresis methods for glyphosate provided high resolutions and efficiency, but some of them suffered low sensitivity owing to the limited sample injection volume (Songa et al., 2009). Detection methods for glyphosate and glufosinate without derivatization, such as electrogenerated chemiluminescence detection, conductivity detection, ion chromatography coupled with inductively-coupled plasma–mass spectrometry (ICP–MS), and integrated pulsed amperometric detection (IPAD) at gold electrode, have also been reported though they are

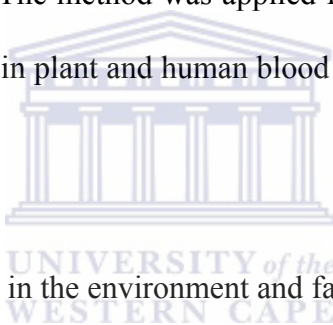
complicated and expensive (Songa et al., 2009). Moreover, the use of conductivity detection may preclude its application for complex matrices.

The requirements, both in terms of time and costs, of the conventional analytical methods (e.g. chromatographic methods) often constitute an important impediment for their application on regular basis. In this context, biosensors and electrochemical methods appear as suitable alternative or complementary analytical tools for a number of environmental monitoring applications due to their low cost of analysis, ease of operation, high sensitivity and minimization of sample pre-treatment. Biosensor application to environmental monitoring has been continuously growing in the last few years. Majority of the biosensor methods reported for the detection of herbicides are based on enzyme-linked immunosorbent assay (ELISA) in which the herbicides are detected by competitive reactions with labelled antibodies. Since ELISA was discovered, it has been recognized as a valuable tool in residue analysis and complements or even surpasses conventional analytical methods providing rapid sample testing, accurate results with little or no matrix interferences (Stalikas and Konidari, 2001). The potential of a competitive indirect ELISA for application in the detection and quantification of glyphosate in water has been reported (Clegg et al., 1999). Contrary to the expensive and time-consuming conventional methods, ELISA provided a sensitive, rapid, cost-effective and efficient method for analysis of environmental samples containing glyphosate and as many as 40 samples could be analyzed simultaneously in a few hours. Nevertheless, the limited solubility of glyphosate in organic solvents required for synthesizing the immunogens and coating

conjugates, the tedious glyphosate polyclonal antisera production and the cross-reactivity to AMPA and glyphosphine, a structurally related herbicide are still the limiting factors to its widespread use. The high limit of detection of $7.6 \mu\text{g mL}^{-1}$ is another limiting factor to the routine use of ELISA for glyphosate analysis although a simple pre-concentration step can lower the limit of detection to $0.1 \mu\text{g mL}^{-1}$ (Stalikas and Konidari, 2001). In other ELISA related applications, Dzantiev et al. (2004) combined the essential properties of anti-chlorsulfuron antibodies and the enzyme HRP attached to a screen-printed electrode to construct an electrochemical immunoassay technique for the detection of chlorsulfuron herbicide. Yulaev et al. (2001) presented an immunosensor for simazine herbicide detection. It was based on the potentiometric detection of the peroxidase label after a competitive immune reaction on the electrode surface. Gold planar electrodes were found to be the most effective supports for the immunosensors. Although the immunoassay techniques permit one to detect herbicides with high sensitivity and selectivity, the procedure is complicated, expensive and currently the commercial availability of the test kit is highly unlikely. The other limitation is the problems encountered during the regeneration of the immuno-surface.

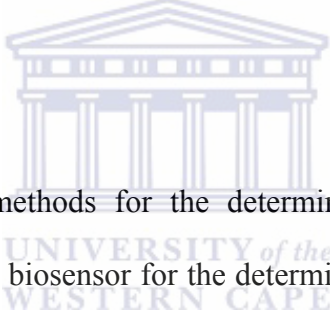
In a preliminary study, Redshaw et al. (2007) investigated the use of biosensors to screen stomach contents for organic and inorganic poisons such as herbicides (e.g. glyphosate, 2,4-dichlorophenoxyacetic acid, 2,4,5-trichlorophenoxyacetic acid and pentachlorophenol), arsenic and mercury. They studied the bioluminescence response of two genetically modified (*lux*-marked) bacteria *Escherichia coli* HB101 and

Salmonella typhimurium to these poisons. Both biosensors were sensitive to all the herbicides, arsenic and mercury at a concentration range likely to be found in stomach content samples submitted for toxicological analysis. The study demonstrated that biosensor bioassays could be a useful preliminary screening tool in forensic toxicology. In another study, Kintzios et al. (2001) developed bioelectric recognition assay (BERA) biosensors for the determination of various chemical and biological molecules by assessing their electrophysiological interactions with a group of cells and cell components immobilized in a gel matrix that preserves their 'physiological' functions. The method was applied for the detection of glyphosate in aqueous solutions, viruses in plant and human blood samples at a concentration lower than 100 pg mL⁻¹.



In order to detect pollution in the environment and farm products, a few sensors based on inhibition of photosystem II (PSII) of chloroplast thylakoid by the photosynthesis-inhibiting herbicides were developed (Nakamura et al., 2003; Li, et al., 2005). These sensors are suitable to detect all possible herbicides that inhibit photosystem II due to the receptor properties of the thylakoid membrane. However, the devices and procedures are complicated, since highly intense irradiation is needed. Li et al. (2005) reported the development of a novel herbicide biosensor based on inhibition of activity of the enzymes in thylakoid modified membrane electrode in which thylakoid was entrapped in a membrane of poly(vinylalcohol) with the styrylpyridinium group (PVA-SbQ) fixed on the surface of a platinum electrode and the modified electrode applied for indirect detection of the herbicides paraquat, diuron, prometryn, atrazine

and ametryn. The detection of the herbicides was achieved by applying differential pulse voltammetry method to measure the oxidative current of hydrogen peroxide in the presence and absence of the herbicides. The sensor provided sensitive determination of the herbicides at trace levels though the application of thylakoid membrane is expensive and complicated due to the fact that thylakoid contains a mixture of proteins. A few potentiometric sensors (ion selective electrodes) were also reported (Karube et al., 1995) although it was only possible to detect positively charged herbicides by this kind of sensor. Saad et al. (1998) reported the use of a flow injection potentiometric method for rapid determination of paraquat herbicide in biological samples.



Several electrochemical methods for the determination of herbicides have been reported although a simple biosensor for the determination of glyphosate, glufosinate and AMPA has not been reported. In view of the analytical challenges presented by these herbicides in general, it is hoped that the HRP/PDMA-PSS inhibitor-based biosensor developed in this study will provide an alternative to quantification of these compounds in environmental samples at residue levels. The developed biosensor technique was based on the fact that herbicides suppress the activity of peroxidase enzymes (Evtugyn et al., 1998). The detection principle was therefore based on the inhibition of the activity of the enzyme HRP by the herbicides being monitored. It is well known that when inhibitors are present in the analyte solution, some of the active centres of the enzymes are blocked, the electroactive product diminishes and

the signal decreases. The decreased signal is frequently related to the concentration of the inhibitor in the test solution and is often used for their quantification.

2.3 Biosensors

The recognition abilities of biological organisms for foreign substances are unparalleled. Scientists have developed new chemical analysis tools known as biosensors. They are defined as analytical devices incorporating a biological recognition element (enzyme, antibody, whole-cell, DNA, receptor or microorganisms) (Sadik and Wallace, 1993), which is integrated within a physicochemical signal transducer or transducing micro system (Fig. 2.1). The signal transducing element (electrode, optical detector, piezo crystal etc.) converts the biochemical response into electric and optic signals which are amplified, measured and decoded by an appropriate electronic unit. A biosensor can produce either individual or successive digital electronic signals that are equivalent to the concentration of a single analyte or a group of analytes being monitored. Many parameters have been used to characterize a biosensor. Some are commonly used to evaluate the functional properties and quality of the sensor, such as sensitivity, stability and response time; while other parameters are related to the application rather than to the sensor functional properties.

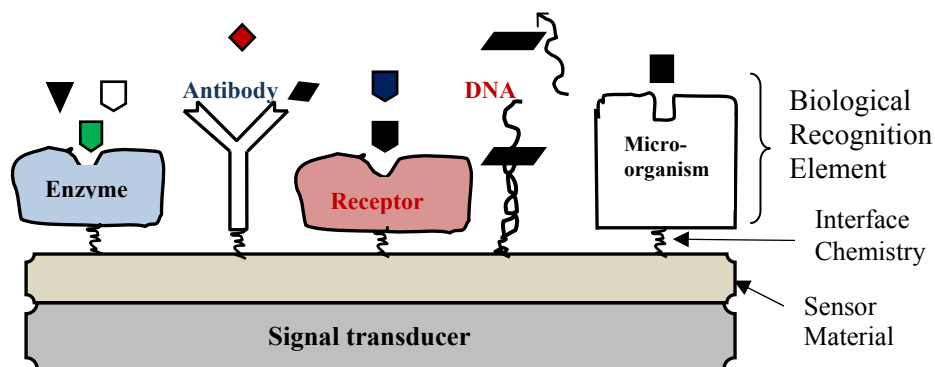


Figure 2.1. Schematic representation of biosensors.

The first blood pO_2 electrode was introduced by Clark et al. (Clark et al., 1953) and the first biosensor was constructed by applying an enzyme membrane onto this electrode by Clark and Lyons (Clark and Lyons, 1962). Since then, many biosensors have been developed for numerous decentralized analytical applications and they are quickly becoming useful tools in medicine, biotechnology, genetic engineering, food quality control, military, agriculture, environmental monitoring and other practical fields (Rodriguez-Mozaz et al., 2004). Biosensors have many favourable analytical characteristics, such as selectivity, sensitivity, portability, low cost and potential for miniaturization. They present advantages over conventional analytical methods (such as gas chromatography, liquid chromatography, atomic absorption spectrometry, mass spectrometry, etc.) in that there is a possibility of working on-site and the measurement of pollutants in complex matrices can be achieved with minimal sample preparation. In principle, biosensors can be tailored to match individual analytical demands for almost any target molecule or compound that can interact with the

biological system. For environmental control and monitoring, biosensors can provide fast and specific data of contaminated sites.

Biosensors can be classified into various groups according to the signal transduction and to the biorecognition principles. On the basis of the transducing element, they are categorized as electrochemical, optical, piezoelectric, and thermal sensors. According to the biorecognition principle, they can be classified as immunochemical, enzymatic, non-enzymatic receptor, whole-cell, and DNA biosensors. Electrochemical electrodes have been used for pH monitoring for over 100 years and the principle established in this technique provides the basis for the most widely used electrochemical biosensors (Kohrausch, 1885). The electrochemical principle is now well established and both chemical and mathematical models have been developed, including two and three dimensions (Zhang et al., 2000). In the simplest applications, the electrochemical reactions occur directly on the electrode surface, or in the space between the electrodes, by the restoration of redox balance between the target molecule, or ion, and the electrolyte (Clark et al., 1953). However, modern electrochemical biosensors incorporate enzymes, sometimes combined with mediators. Electrochemical biosensors often employing amperometric or potentiometric techniques are today at the forefront of a multidisciplinary science combining the fields of electrochemistry and biology. In potentiometric techniques, the analytical information is obtained by converting the biorecognition process into a potential signal, whereas the amperometric techniques are based on measuring the current produced during the oxidation or reduction of a product or reactant usually at a constant applied potential.

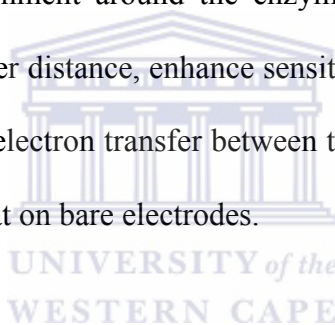
Enzymes were historically the first molecular recognition elements included in biosensors and continue to be the basis for a significant number of publications reported for biosensors in general as well as biosensors for environmental monitoring. They are suitable to act as recognition elements because of their specificity and availability. Amperometric enzymatic electrodes hold a leading position among the presently available biosensor systems and are more attractive due to their fast response time and high sensitivity (Freire et al., 2003). These devices combine the specificity of the enzyme for the recognition of a given target analyte with the direct transduction of the rate of the biocatalytic reaction into a current signal, allowing a rapid, simple and direct determination of various compounds.

Depending on the level of integration, biosensors can be divided into three generations. The first generation biosensors are based on the electroactivity of the enzyme substrate or product whereby the substrate or product of the reaction diffuses to the transducer and causes the electrical response. The second generation biosensors involve utilization of specific soluble mediators (e.g. ferrocene derivatives, ferrocyanide etc.) in order to generate improved response. The drawbacks with the first generation biosensors, such as too high applied potentials, led to the use of mediators, which are redox active molecules that could react with the active site of the enzyme and with the electrode surface, shuttling the electrons between the enzyme and the electrode. The use of soluble mediators made it possible to decrease the applied potential for many redox enzyme-based biosensors. Unfortunately, the uses of soluble redox mediators together with the redox enzymes facilitate not only

the electron transfer between the electrode and the enzyme but also various interfering reactions (Freire et al., 2003). The third generation biosensors, also known as reagentless biosensors are based on direct electron transfer between the redox-active biomolecule and the electrode surface. In these biosensors, the electron transfer is associated with, or occurs during the catalytic transformation of the substrate to the product.

Third generation biosensors usually offer better selectivity, because they are able to operate in a potential range closer to the redox potential of the enzyme itself, becoming less exposed to interfering reactions. Although they present favourable characteristics, only a few groups of enzymes or proteins were found to be capable of interacting directly with an electrode while catalyzing the corresponding enzymatic reaction. This is because the distance between the prosthetic group and the bare electrode surface is often rather too long for direct electron transfer, due to shielding by the protein shell (Freire et al., 2003). Over the past few decades, the design of optimized electrochemical enzyme-based biosensors have drawn increasing attention and enzymes have been immobilized on electrodes to give measurable responses by interacting with the target molecules (Liu and Ju, 2002; Tang et al., 2003). A lot of studies have therefore been carried out on the development and optimization of materials to be used as electron transfer interfaces between the redox enzymes and electrodes. The aim in the design of enzymatic biosensors is to provide fast electron transfer processes. In this way, an optimally designed electrode configuration has to ensure that the electron transfer distance between an immobilized redox enzyme and

a suitable electrode surface is made as short as possible (Freire et al., 2003). An ideal material should be compatible with the enzyme and should provide a suitable interface between the enzyme and the electrode to partly or completely eliminate the denaturation of the enzyme on the electrode surface. Recently, major improvements have been accomplished by modifying the electrode surfaces with matrices such as membranes, surfactant matrix, organic conducting polymers, nanoparticles, silk fibroin film, microcapsule, gels, lipids, hydrogel polymers, carbon, graphite, silica etc. before immobilization of enzymes. All these matrices have been characterized to improve the micro-environment around the enzymes, provide suitable orientation, shorten the electron transfer distance, enhance sensitivity and stability of the enzyme, and to enhance the direct electron transfer between the immobilized enzymes and the electrodes compared to that on bare electrodes.



Among the matrices used for the incorporation of enzymes, organic conducting polymers present greater advantages due to their good interaction with metallic and carbon conductors. Furthermore, the unique electronic properties of conducting polymers allow direct, efficient and interactive electrical communication between the enzyme redox centre and the electrode surface thus producing a range of analytical signals. The polymers also localize the enzymes close to the electrochemical interface thus minimizing interferences which may lead to undesired side reactions for large background currents. Among the conducting polymers used in fabricating enzyme-based biosensors, PANI is considered as the most fascinating and has gained particular popularity due to its electroactivity; favourable storage stability and ease of

preparation thus tremendous works have been undertaken in this field. Nevertheless, it has been observed that applications of the conventional PANI and the composite films remain limited by poor sensitivity resulting from the poor diffusion of analyte molecules (Collins & Buckley, 1996; Huang et al., 2004). However, with recent development in nanoscience and nanotechnology, nanostructured PANI/PANI derivatives exhibiting unique properties have extensively been investigated as sensor materials raising hopes that the problems related to interactions between foreign surfaces and biomolecules may soon be solved. One-dimensional nanostructured PANI has been reported to enhance significantly the diffusion of target molecules due to their greater surface area and shorter penetration depth for target molecules than the conventional PANI, and have therefore become alternative materials to improving the sensitivity and response time of biosensors (Zhang and Wang, 2006). The conducting polymer materials can be deposited electrolytically from the solution onto a conducting support to provide a three-dimensional matrix for immobilized enzymes where reactants are converted to products (Zhang et al., 2000). The attractive feature of the direct electron transfer systems is presumably their simplicity of construction. Figure 2.2 illustrates the design of an electrochemical enzyme biosensor incorporating mediators (e.g. conducting polymers).

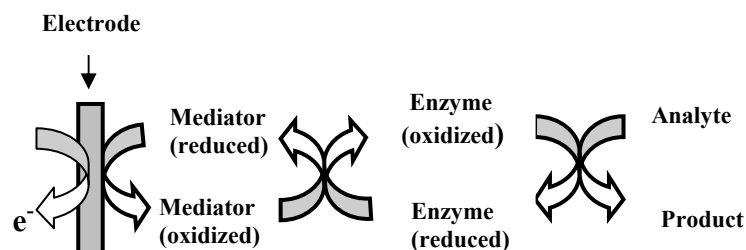


Figure 2.2. Schematic representation of an electrochemical enzyme biosensor.

A number of techniques such as physical adsorption, entrapment, cross-linking between molecules and covalent binding have been used for immobilization of enzymes onto the electrode surfaces. In addition to these conventional methods, sol-gel entrapment, Langmuir-Blodgett (LB) depositions, electropolymerization, self-assembled biomembranes and bulk modification have recently been used (Rodriguez-Mozaz et al., 2004). The activity, stability and performance of immobilized enzymes depend upon the surface area, porosity, hydrophilic character of immobilizing matrix, reaction conditions and the immobilization procedure. A common approach for the immobilization of enzymes onto the electrode surfaces is the electrostatic attachment to a previously electropolymerized polymer film on the electrode surface (Grennan et al., 2006). This immobilization procedure offers numerous advantages over conventional procedures for the design of biosensors in that there is complete coverage of the active surface area; greater control over film thickness and reproducibility and the distribution of the immobilized enzyme can be spatially controlled irrespective of geometry, shape and dimension of the electrode. A series of biosensors have been produced in this way and a variety of enzymes, including

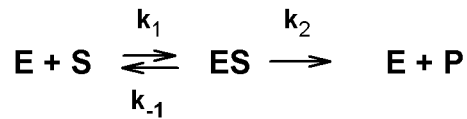
galactose oxidase, HRP, glucose oxidase (GOD), sarcosine oxidase, cholesterol oxidase, cytochrome P450, AChE and ascorbate oxidase have been immobilized to a PANI backbone (Iwuoha et al., 1997; Mathebe et al., 2004; Morrin et al., 2005; Grennan et al., 2006; Somerset et al., 2007; Songa et al., 2009). The present work focuses on a similar electrostatic approach for the immobilization of the enzyme HRP onto the nanostructured PDMA-PSS-coated gold electrodes.

2.3.1 Enzyme biosensors

An enzyme biosensor is derived from a combination of a transducer with a thin enzymatic layer, which normally measures the concentration of a substrate. The enzymatic reaction transforms the substrate into a reaction product that is detectable by the electrode. The concentration of any substance can be measured provided that its presence affects the rate of an enzymatic reaction which is especially true for enzyme inhibitors. The signal (current or potential) measured is proportional to the rate-limiting step in the overall reaction.

2.3.1.1 Enzyme kinetics

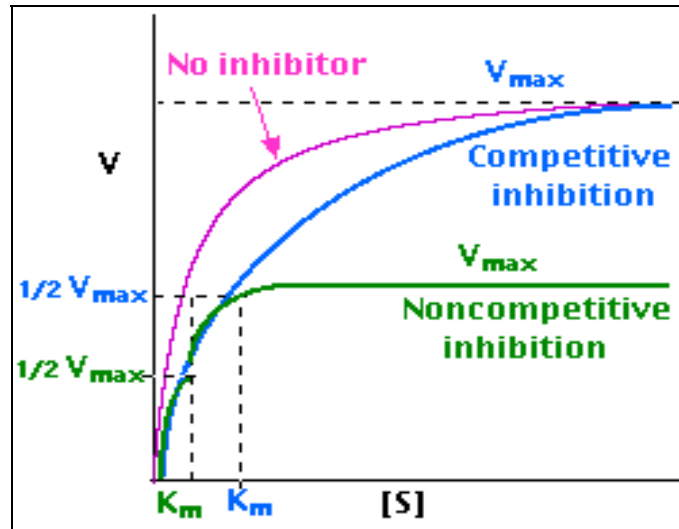
The presence of the enzyme ensures the transformation of the substrate into the reaction product according to the following reaction:



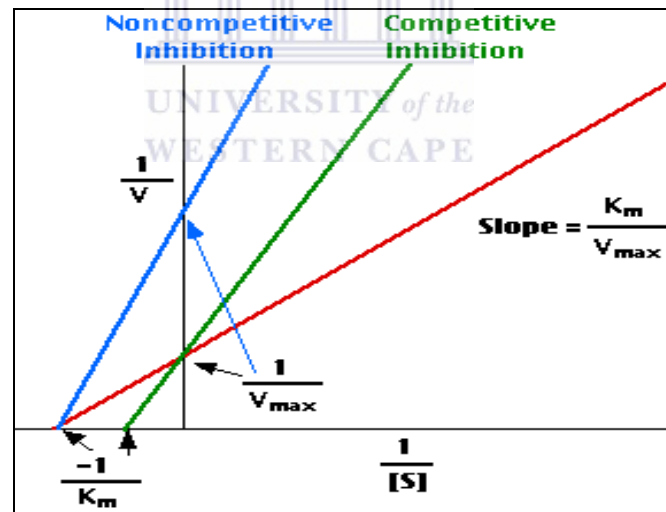
where E represents the enzyme, S the substrate and P the reaction product; k_1 , k_{-1} and k_2 are the rate constants of the reactions (Tran-Minh, 1993). The Michaelis-Menten kinetics model postulates that enzymatic reactions proceeds through the formation of a transition complex intermediate ES. Once formed, the ES complex either converts to a product or decomposes to the free enzyme and substrate. The Michaelis-Menten model assumes that only a negligible amount of ES complex reverts back to the reactants. According to this model, the hyperbolic relations governing the rate of catalysis and the substrate concentrations are expressed by the equation:

$$v = \frac{V_{max}[S]}{K_m + [S]} \quad (2.1)$$

where v is the initial rate (moles/time), V_{max} is the maximum rate of catalysis, K_m is the apparent Michaelis-Menten constant and $[S]$ is the substrate concentration. The Michaelis-Menten constant refers to the substrate concentration at which the enzymatic reaction occurs at half the maximum velocity ($V_{max}/2$). The relationship between v and $[S]$ in the absence and presence of inhibitors is illustrated in Fig. 2.3a.



(a)



(b)

Figure 2.3. (a) Variation of the reaction velocity v , with the substrate concentration and (b) Lineweaver-Burk plots for different types of reversible enzyme inhibitors.

When $[S] \gg K_m$, a maximum value of the rate constant, V_{max} , is reached, so that $V_{max} = k_2 [E_0]$, and when $[S] = K_m$, $v = V_{max}/2$. It is experimentally more convenient to plot the data in a straight line form, and inverting the Michaelis-Menten equation can achieve the equation:

$$\frac{1}{v} = \frac{K_m}{V_{max}} + \frac{[S]}{V_{max} [S]} = \frac{K_m}{V_{max}} + \frac{1}{V_{max}} \quad (2.2)$$

When $1/v$ is plotted against $1/[S]$, a straight line is obtained with a slope of K_m/V_{max} and a y-intercept of $1/V_{max}$; hence both K_m and V_{max} can be obtained. The double reciprocal plot obtained is referred to as a Lineweaver-Burk plot (Fig. 2.3b).

2.3.1.2 Enzyme inhibition

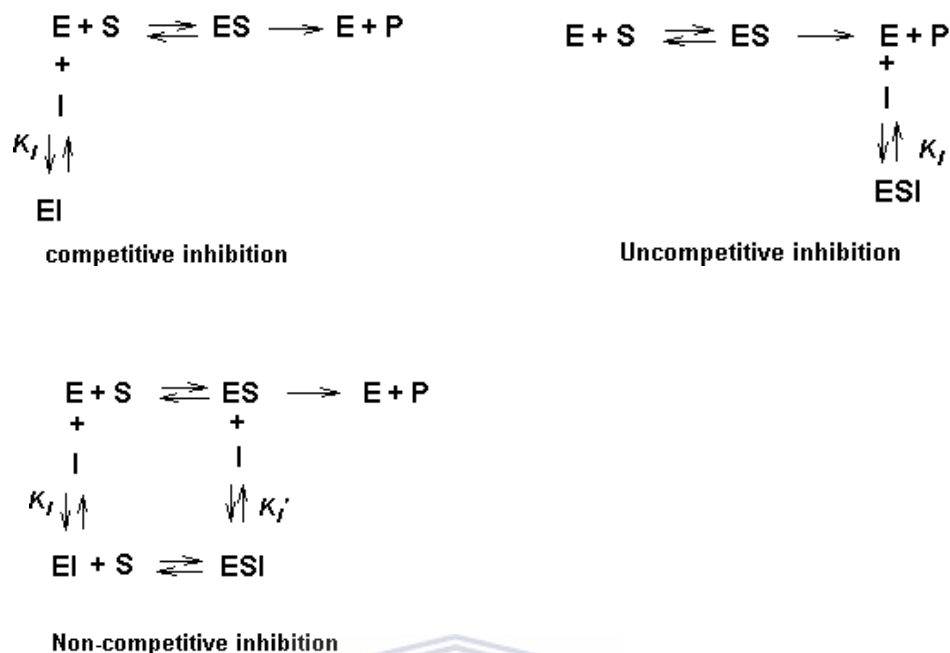
Enzyme inhibitors are molecules that bind to enzymes thus decreasing their activity. The binding to the immobilized enzyme or the enzyme in solution results in a decrease in biosensor signal. The mode of enzymatic inhibition is variable from one inhibitor to another, and may be reversible or irreversible. The response of the enzyme sensor provides a continuous measure of the activity of the immobilized enzyme, whether or not its inhibitor is present. Enzyme biosensors thus allow convenient and rapid study of the inhibition of enzymes and their subsequent reactivation. The reduction of the enzyme activity by inhibitors leads to a decrease in signal production that is directly proportional to the concentration of the inhibitor in

the test solution. Typically, the percentage of inhibited enzyme ($I\%$) that results after exposure to the inhibitor is quantitatively related to the inhibitor (i.e. analyte) concentration and the incubation time (Amine et al., 2006).

Reversible inhibition is characterized by equilibrium between the enzyme and the inhibitor, defined by an equilibrium constant, K_i , which represents the affinity of the inhibitor for its enzyme (Tran-Minh, 1993). Reversible inhibitors are classified into three groups according to their effect on the enzymatic sites. The inhibition is “competitive” when the inhibitor and the substrate are in competition for the same site, and the degree of inhibition decreases as the substrate concentration increases. When the degree of inhibition increases with the substrate concentration, the inhibition is called “uncompetitive.” In this case, the inhibitors only interact with ES complexes and bind only when the ES is formed. If the degree of inhibition is independent on the substrate concentration, then the inhibition is said to be “non-competitive.” Non-competitive inhibition is a form of inhibition where the binding of the inhibitor to the enzyme reduces its activity but does not affect the binding of the substrate. As a result, the extent of inhibition depends only on the concentration of the inhibitor. The kinetic schemes for different kinds of reversible inhibition are presented in Scheme 2.1.

To study the type and kinetics of inhibition, Lineweaver-Burk plots for the enzymatic reaction in the presence and absence of inhibitors at their 50 % rate reduction (IC_{50}) are plotted using a double reciprocal plot and the values of K_m and V_{max} obtained from

the plots (Sariri et al., 2006). Figure 2.3b illustrates an example of Lineweaver-Burk plots in the absence and presence of inhibitors. It is known that non-competitive inhibitors bind equally well to both E and the complex ES (i.e., they have identical affinities for E and ES). This results in the formation of three complexes ES, EI and ESI, of which only ES can yield the product of enzymatic reaction. The inhibitor is represented by I while K_I and $K_{I'}$ are the dissociation constants for the non-competitive inhibition. Obviously, the inhibitor is not binding to the same site as S, and this kind of inhibition cannot be overcome by increasing the concentration of the substrate. It also suggests that the inhibitor may be interacting with a site on the enzyme which is not its active site. Non-competitive inhibition occurs if $K_I = K_{I'}$. In the Lineweaver-Burk plot for non-competitive inhibition (Fig. 2.3b), the x-intercept remains the same with or without I. Non-competitive inhibition does not change K_m (i.e., it does not affect the substrate binding) but decreases V_{max} (i.e., the inhibitor binding hampers catalysis). On the contrary, a competitive inhibitor does not change V_{max} but increases the K_m value (Sariri et al., 2006; Amine et al., 2006). The plot for competitive inhibition shows a change in the x-intercept but the y-intercept remains unchanged.

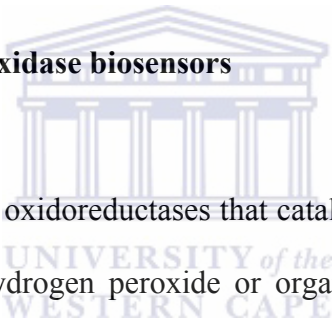


Scheme 2.1. Kinetic schemes for reversible enzyme inhibition.

All the kinetic equations mentioned above are based on the assumption of homogeneous kinetics of the enzyme-substrate and enzyme-inhibitor(s) interactions. The appropriate parameters of inhibition (i.e. K_I and K_I' etc.) indicate the potentialities of an enzyme which could be extended or reduced through the immobilization and incorporation of the enzyme into the membrane material. The immobilization of an enzyme is an indispensable part of the development of biosensors and the multiplicity of application of the enzyme due to immobilization reduces the cost of measurement. The immobilized enzyme is more stable towards extreme working conditions, e.g. high temperature, and can be easily combined with an appropriate sensor in the biosensor assembly (Evtugyn et al., 1998). When an enzyme is immobilized, the reaction occurs in the heterogeneous phase because the

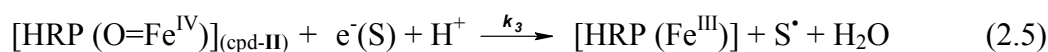
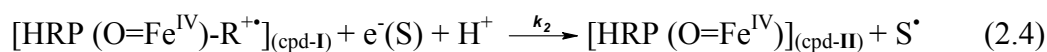
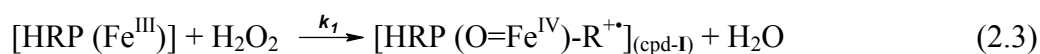
active sites are in the solid phase and the substrate is in the aqueous phase. The concentration of the substrate varies from one point in the solid support to another, and so the rate of the enzymatic reaction is not the same as that occurring at the solid surface. During the reaction, a profile of the substrate and product concentrations is established across the support such that the substrate concentration in the active layer is always lower than that in solution. The saturation of the immobilized enzyme therefore requires higher substrate concentrations in the bulk solution than those normally obtained for the enzyme in solution (Tran-Minh, 1993).

2.3.1.3 Horseradish peroxidase biosensors



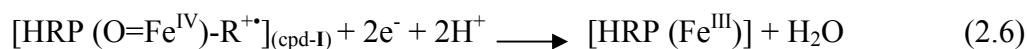
Peroxidases are defined as oxidoreductases that catalyze the oxidation of organic and inorganic substrates by hydrogen peroxide or organic peroxides. They are usually isolated from plants (e.g. horseradish roots, soybean and tobacco), fungi, and bacteria but also increasingly from mammalian sources. All heme peroxidases (E.C. 1.11.1.7) contain iron (III) protoporphyrin IX (ferriprotoporphyrin IX) prosthetic group located at the active site (Dunford, 1999). The iron in the heme is capable of undergoing oxidation and reduction usually to +2 and +3, though stabilized ferryl (Fe^{IV}) compounds are well known in the peroxidases. The heme group is essential for the enzyme activity and undergoes spectroscopic changes during the oxidation reaction indicating that the iron atom participates in the reaction mechanism.

Although there are a great variety of peroxidases, horseradish peroxidase (HRP) is undoubtedly the most employed in various biotechnological processes. HRP belongs to the family of the heme-containing plant peroxidases and it is the most commonly used enzyme for practical analytical applications, mainly because it retains its activity over a broad range of pH and temperature. HRP catalyzes the oxidation of a substrate (SH) by H₂O₂ via a reaction cycle that involves two intermediates, compounds **I** and **II**. An early step in the catalytic cycle following the binding of H₂O₂ to the heme in the Fe (III) state is the heterolytic cleavage of the oxygen-oxygen bond of H₂O₂. A water molecule is released during this reaction with the concomitant two-electron oxidation of the heme to form an unstable intermediate, compound **I** (cpd-I) that contains an oxyferryl centre with the iron in the ferryl state (Fe^{IV} = O), and a porphyrin π cation radical. Two successive one-electron reductions return the enzyme to its resting state (Fe^{III}) via a second intermediate, compound **II** (cpd-II) (Veitch, 2004). The reaction can be represented as follows:



When immobilized on the electrode surface, HRP can display unique bioelectrocatalytical properties in the reduction reaction of H₂O₂, by direct electron transfer from the electron-donating electrode through the active site of the enzyme

and to the peroxide in solution (Ferapontova et al., 2002). Kinetic models of the bioelectrocatalytical reduction of H_2O_2 catalyzed by HRP are similar to the mechanism of enzymatic catalysis. HRP immobilized on the electrode surface can be oxidized by H_2O_2 to compound **I** (equation 2.3), followed by further direct (mediatorless) electro-reduction of compound **I** at the electrode surface to the initial HRP state (equation 2.6). The electrode is considered as an electron donor (Ferapontova et al., 2002; Freire et al., 2003). Mediatorless heterogeneous electron transfer from the electrode to the active site of the enzyme (equation 2.6) enables one to develop biosensing systems for the detection of H_2O_2 or organic hydroperoxidases based on direct electron transfer. However, the efficiency of direct electrochemical reduction of compound **I** of HRP on majority of investigated electrode materials is usually low (Ferapontova et al., 2002). The reasons for this are the deep burying of the electroactive groups within the protein structure resulting from the unfavourable orientations of the molecules at the electrode surface and the long electron transfer distance between the electrode surface and the active site of HRP, which are unfavourable for direct electron transfer (Zhang et al. 2007; Ferapontova et al., 2002).



To overcome the kinetically limited heterogeneous electron transfer (equation 2.6), the reduction of compound **I** to HRP (Fe^{III}) is performed in the presence of a second substrate-mediator in two successive one-electron/proton transfer steps (equation 2.4

and 2.5). When an electron donor (S) is present in a peroxidase-electrode system, the direct and mediated processes can occur simultaneously, with the electrochemical reduction of the oxidized donor S^* by the electrode (equation 2.7) (Freire et al., 2003). Reactions 2.3, 2.4, 2.5 and 2.7 are known as mediated electron transfer. In amperometric or voltammetric sensor, both approaches result in a reduction current, which is then correlated to the concentration of H_2O_2 in the solution. Thus, a simple electrode for peroxide detection can be developed with a layer of HRP immobilized onto the electrode surface.

It has been reported that when electrodes were modified with nanoparticles (Liu and Ju, 2002; Zhang et al., 2007; Liu et al., 2008), conducting polymers (Kong et al., 2003; Chen & Gu, 2008), biomolecule films (Song et al., 2006; Tang et al., 2003), redox dye (Salomi and Mitra, 2007), and ionic liquid (Yan et al., 2007), HRP showed direct electrochemical behaviour and good electrocatalytic activity towards the reduction of H_2O_2 . For instance, Chen et al. (2008) constructed an amperometric H_2O_2 biosensor based on the immobilization of HRP in PANI/bovine serum albumin, BSA film on a platinum electrode via an electrochemical approach. The authors reported that the biosensor (HRP/PANI/BSA)/Pt electrode) exhibited enhanced sensitivity and excellent stability. The results suggested that the embedded BSA might have served as an initial template for aniline polymerization and stabilized the microstructure of the PANI film significantly. Nevertheless, the electrodes constructed with or without BSA displayed the linear correlation with H_2O_2 in the range of 0.01-35.2 mM. Wu et al. (2006) incorporated HRP in silk fibroin (SF) films

and applied the biosensor for the detection of H₂O₂. The thermally stable and biocompatible SF film provided a feasible micro-environment for HRP and directed electron transfer on graphite electrodes. The HRP immobilized on SF film was characterized by increased activity and stability and it catalyzed the reduction of H₂O₂ within a linear range of 2.02×10^{-6} - 3.54×10^{-4} M. In another study, Li, et al. (2008) immobilized HRP on a composite of gemini surfactant (i.e. dodecyl- α,ω -bis (dimethylcetylammmonium bromide), C₁₆-C₁₂-C₁₆) and hydrophobic room temperature ionic liquid (i.e. 1-octyl-3-methylimidazolium hexafluorophate, OMIMPF₆). The resulting C₁₆-C₁₂-C₁₆-OMIMPF₆-HRP/GC electrode exhibited good stability, reproducibility and catalytic responses to dissolved H₂O₂. The cathodic peak current of the electrode was linear to H₂O₂ in the range of 5.82 μ M - 388 μ M. The apparent Michaelis-Menten constant was estimated to be 0.159 mM. In yet another study, Mathebe et al. (2004) constructed an amperometric biosensor for the detection of H₂O₂ by in situ deposition of HRP onto a PANI modified platinum electrode. The HRP/PANI based biosensor catalyzed the reduction of H₂O₂ within a linear range of 2.5×10^{-4} - 5.0×10^{-3} M.

The research on HRP biosensors dominates and continues to develop through many forms, from the traditional voltammetric- and amperometric-based methods of detection to nano-sized devices. Size reduction remains a pivotal area in sensor research, and the use of nanoparticles and one-dimensional nanostructured materials offers increased surface area for enzyme immobilization with a simultaneous reduction in apparatus size. Currently, HRP nanobiosensors are at the forefront of

biosensor research and amperometric HRP-modified electrodes have been developed for the detection of hydrogen peroxide, organic hydroperoxides, phenols and aromatic amines. HRP can also bind to a range of structurally related substrates or substrate analogs (Sariri et al., 2006). These molecules are substrates, activators, or inhibitors of the reactions catalyzed by peroxidases. Michira et al. (2007) developed a biosensor for the detection of H₂O₂ by immobilizing HRP onto nanofibrillar anthracene sulfonic acid (ASA) doped PANI modified platinum electrode. HRP was immobilized through drop-coating technique. The resulting biosensor catalyzed the reduction of H₂O₂ with a sensitivity of $3.3 \times 10^{-3} \text{ A cm}^{-2} \text{ mM}^{-1}$ and a detection limit of $1.2 \times 10^{-2} \text{ mM}$. The apparent Michaelis-Menten constant obtained for the peroxide biosensor was $0.18 \pm 0.01 \text{ mM}$. Elsewhere, an amperometric biosensor for H₂O₂ utilizing DBSA or PVS doped PANI nanoparticles was reported (Morris et al., 2005). According to the authors, the PANI nanoparticles allowed uniform absorption of protein with improved biosensor performances. The PANI-DBSA sensor was found to have better performance with a signal-to-noise ratio (S/N) of 61 ± 3 compared to that of PANI-PVS which was 17 ± 14 . The response times for the PANI-DBSA and PANI-PVS sensors were $0.62 \pm 0.04 \text{ s}$ and $9.46 \pm 4.12 \text{ s}$ respectively.

Although real-time quantification of hydrogen peroxide continues to be one of the main reasons for HRP sensor development, other diverse applications include the detection of glucose, ethanol (Castillo et al., 2003), HRP inhibitors (Sariri et al., 2006), etc. Biosensors, including immunochemical sensors (Penalva et al., 1999) and electrochemical sensors (Iwuoha et al., 1997; Iwuoha et al., 2007; Campanella et al.,

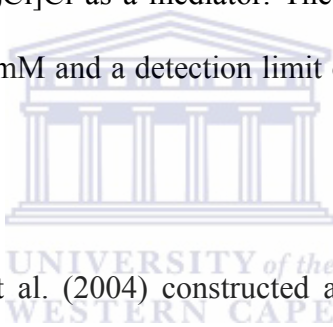
1999; Konash et al., 2005), incorporating organic solvents have been developed as a part of the expanding area of peroxidase research, primarily because of the insolubility of many analytes in aqueous solutions. Organic-solvent-compatible, bi-enzyme peroxidase sensors have also been cited in the literature (Castillo et al., 2003).

2.3.1.4 Horseradish peroxidase inhibition

The ability of certain substances to inhibit the catalytic action of enzymes can be exploited for their detection and quantification in the so-called enzyme-inhibition biosensor. Among various biosensors, recent attention has turned towards the enzyme-inhibition biosensors to determine and quantify the concentration of inhibitors in the assayed sample by measuring the inhibition degree with the lower detection limits. Biosensors for pesticides and toxic metals monitoring are mostly based on the inhibition of enzymes (Marty et al., 1992; Badihi-Mossberg et al., 2007). Several metal ions and organic molecules, such as Cd^{2+} , Co^{2+} , Cu^{2+} , Tb^{3+} , Fe^{3+} , Mn^{2+} , Ni^{2+} , Pb^{2+} , *p*-aminobenzoic acid, cyanide, L-cystine, dichromate, ethylenethiourea, hydroxylamine, vanadate, sodium azide, sulfides, diazinon, thiourea, cysteine, glutathione etc. have been reported to inhibit HRP activity (Zollner, 1993; Sariri et al., 2006; Michira, 2007; Guo et al., 2008). For instance, Michira (2007) reported the inhibition of HRP by an organophosphate pesticide, diazinon. In this study, electrochemical HRP biosensors based on the use of PANI and poly-*o*-methoxyaniline (POMA) were constructed and used for voltammetric study of the

inhibition of HRP by diazinon. Non-competitive inhibition of HRP was achieved by exposing it to diazinon in a concentration range of 0.88 - 4.0 μM . Inhibition degrees of 41% and 81% were observed for the PANI and POMA based biosensors respectively. Detection limits of 0.21 and 0.71 μM were achieved for PANI and POMA biosensors respectively.

An amperometric sol-gel-based enzyme inhibition electrode was constructed for the detection of low levels of cyanide by immobilizing HRP and an osmium redox polymer $[\text{Os}(\text{bpy})_2(\text{PVP})_{10}\text{Cl}]\text{Cl}$ as a mediator. The linear range of the biosensor to cyanide was 0.004 - 0.04 mM and a detection limit of 0.5 μM was achieved (Park et al., 1997).



In another study, Yang et al. (2004) constructed an amperometric HRP inhibition biosensor based on a thiolate self-assembled monolayer (SAM) for the determination of sulfides (HS^- , H_2S and small amount S^{2-}). Cysteamine SAM was applied to the gold electrode surface then HRP was immobilized on the electrode by cross-linking with glutaraldehyde. The measurement was performed in the presence of an electron mediator hydroquinone and 0.067 M phosphate buffer of pH 6.5 at an applied potential of -150 mV versus SCE. The determination of sulfides was achieved in the range of 0.5-12.7 μM with a detection limit of 0.3 μM . Lineweaver-Burk plots of HRP activity on H_2O_2 in the presence and absence of sulfides were plotted then K_m^{app} and I_{max} values calculated from the plots. The K_m^{app} value in absence of sulfide was found to be 6.34 mM while that in presence of sulfides was found to be 3.58 mM.

The authors therefore deduced that the type of inhibition of sulfides on HRP is anti-competitive inhibition. In another related study, Zhao et al. (1996) demonstrated the feasibility of quantitatively detecting cyanide, thiourea and sulfide through their inhibition effect on an enzyme electrode that utilized colloidal gold-immobilized horseradish peroxidase (HRP). However, this biosensor was very sensitive to cyanide and thiourea, but less sensitive to sulfide. The detection limit achieved for sulfide by this method was 8 μM which is higher than that obtained by Yang et al.

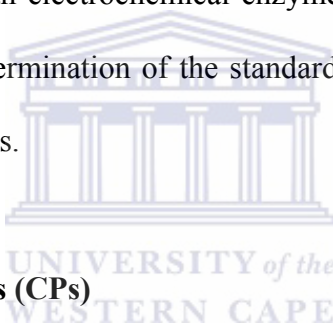
Sariri et al. (2006) studied the inhibition of HRP by cysteine and glutathione. The biological activity of HRP was measured in the presence of each inhibitor using 4-amino antipyrine as the substrate. The authors found that reduced glutathione was a more potent inhibitor on peroxidase activity than L-cysteine. They also investigated the kinetics of the peroxidase inhibition by glutathione and compared to L-cysteine inhibition. The kinetic studies revealed that the inhibition by glutathione and L-cysteine was non-competitive and mixed non-competitive. Lineweaver-Burk plots of HRP activity on 4-amino antipyrine in the presence and absence of reduced glutathione and cysteine were plotted and the values of K_m and V_{max} calculated from the plots. The K_m and V_{max} values for glutathione were calculated to be 2.06 μM and $0.45 \times 10^2 \mu\text{M s}^{-1}$ respectively, while those of L-cysteine were 4.43 μM and $1.27 \times 10^2 \mu\text{M s}^{-1}$ respectively.

In yet another study, Guo et al. (2008) investigated the spectroscopic properties of the interactions involving HRP and Tb^{3+} in simulated physiological solution by

electrochemical and spectroscopic methods, such as cyclic voltammetry (CV), circular dichroism (CD), X-ray photoelectron spectroscopy (XPS) and synchronous fluorescence (SF). The authors found that Tb^{3+} can coordinate with oxygen atoms in carbonyl groups in the peptide chain of HRP, form the complex of Tb^{3+} and HRP (Tb-HRP), and then lead to the conformation change of HRP. The authors suggested that the increase in the random coil content of HRP can disturb the microstructure of the heme active centre of HRP, in which the planarity of the porphyrin cycle in the heme group is increased and the exposure extent of the electrochemical active centre is decreased. Thus they concluded that Tb^{3+} can inhibit the electrochemical reaction of HRP and its electrocatalytic activity for the reduction of H_2O_2 at the Au/ Cys/GC electrode. They further stated that changes in the microstructure of HRP obstructed the electron transfer of Fe (III) in the porphyrin cycle of the heme group, thus HRP catalytic activity is inhibited. The inhibition effect of Tb^{3+} on HRP catalytic activity was found to be increasing with increase in Tb^{3+} concentration.

In this study, the possibility of inhibition of HRP activity by glyphosate, glufosinate and AMPA has been investigated by studying the interactions of the immobilized HRP with the herbicides by cyclic voltammetry, amperometry, SEM and FTIR spectroscopy. FTIR spectroscopy, as a sensitive technique is frequently used for investigation of the secondary structure of proteins. The profiles of the amide I and amide II infrared bands for proteins usually provide the detailed information on the secondary structure of the polypeptide backbone chain -CO-NH- in both naturally occurring and artificial proteins (Li and Hu, 2003; Liu et al., 2005). FTIR

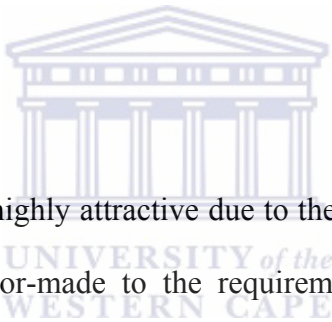
spectroscopy has therefore been used to study the changes in the polypeptide backbone chain of HRP when it interacts with glyphosate. Based on the fact that herbicides can suppress the activity of peroxidase (Evtugyn et al., 1998), and the report by Guo et al. (2008) that inhibitors such as Tb^{3+} can coordinate with oxygen atoms of carbonyl groups in the peptide chain of HRP to form Tb-HRP complex that inhibits its activity, there is a reason to believe that glyphosate can behave in a similar manner since it has three reactive functional groups (amine, carboxylate and phosphonate) that can coordinate with HRP to form complexes that can inhibit HRP activity. In view of this, an electrochemical enzyme biosensor has been constructed and used for inhibitor determination of the standard solutions of these herbicides as well as the assayed samples.



2.4 Conducting polymers (CPs)

Conducting polymers (CPs) contain π -electron backbone responsible for their unusual electronic properties such as electrical conductivity, low energy optical transitions, low ionization potential and high electron affinity. The extended π -conjugated systems of the CPs have single and double bonds alternating along the polymer chain (Gerard et al., 2002). CPs show almost no conductivity in the neutral (uncharged) state but become electrically conductive upon partial oxidation or reduction, a process commonly referred to as 'doping'. A new class of polymers known as intrinsically conducting polymers or electroactive conjugated polymers has recently emerged. Their intrinsic conductivity results from the formation of charge carriers upon

oxidizing (*p*-doping) or reducing (*n*-doping) their conjugated backbone. Such materials exhibit interesting electrical and optical properties previously found only in inorganic systems (Duke and Schein, 1980). They are readily oxidized and reduced at relatively low potentials, and the redox process is reversible and accompanied by large changes in the composition, conductivity and colour of the material. A key requirement for a polymer to become intrinsically electrically conductive is that there should be an overlap of molecular orbitals to allow the formation of delocalized molecular wave function. Besides this, molecular orbitals must be partially filled so that there is a free movement of electrons throughout the lattice (Bloor and Movaghar, 1983).



Conducting polymers are highly attractive due to their electrical conductivity and the fact that they can be tailor-made to the requirements of the application through modifications in the polymer structure and varying the functional groups in their organic moiety. Many applications of CPs including analytical chemistry and biosensing devices have been reviewed by various researchers (Wring and Hart, 1992; Schuhmann, 1995; Trojanowicz and Krawczyk, 1995; Guiseppi-Elie et al., 1997; Situmorang et al., 1998; Gerard et al., 2002; Ahuja et al., 2007; Guimard et al., 2007). The CPs have widened the possibility of modification of surfaces of conventional electrodes providing new and interesting properties. The common properties desired when CPs are used for biomolecules immobilization is their biocompatibility and redox stability. However, there is always a desire to further optimize a material when targeting a specific application. For biosensors, it is

important to tune the hydrophobicity, conductivity, stability, and reactive functionalities in order that the biomolecules can be successfully incorporated and to improve detection limits of the biosensor. In general, manipulation of CP properties such as morphology, porosity, hydrophobicity, mechanical strength, malleability, degradability, redox stability, conductivity etc., can be achieved through chemical means, such as the incorporation of molecules such as dopants or through insertion of functional groups into the CP backbone that may increase conductivity or permit degradation (Guimard et al., 2007).

The current commercial applications of CPs are in thin film transistor, batteries, antistatic coatings, electromagnetic shielding, artificial muscles, light-emitting diodes, gas- and bio-sensors (Morris et al., 2005), fuel and solar cells, fillers (Jang et al., 2005), corrosion protective coatings (Plesu et al., 2006), etc. Generally conducting polymers can be used in electrical, electronic, plastics, medical industries, etc.

2.4.1 Historical background of conducting polymers

The electrically conducting polymer PPy dates back to the 1960s, but little was understood about the polymer at this time and the discovery was essentially lost (Street, 1986). Research interest in electroactive polymers started in 1977, when Heeger, MacDiarmid, Shirakawa and their co-workers demonstrated that the conductivity of polyacetylene (PAC) can be increased by several orders of magnitude

by treatment with appropriate oxidizing or reducing agents, the so-called ‘dopants’ (Shirakawa et al., 1977). These scientists were awarded the Nobel Prize in chemistry in 2000 for the discovery and development of the so-called ‘conducting polymers’ (<http://nobelprize.org/chemistry/laureates/2000>). This has generated renewed interest of the scientific community towards the study and discovery of new conducting polymeric systems. Consequently, the development of aromatic conducting polymers for different applications has received much attention and polyheterocycles, such as polypyrrole (PPy), polythiophene (PTh), polyaniline (PANI), and poly(phenylene vinylene) (PPV) developed in the 1980s, have since then emerged as a class of aromatic conducting polymers that exhibit good stabilities, conductivities, and ease of synthesis (Hong and Marnick, 1992; Kundu and Giri, 1996). Structures of some typical conducting polymers and their conductivities are given in Table 2.1 (Guimard et al., 2007; Rahman et al., 2008).

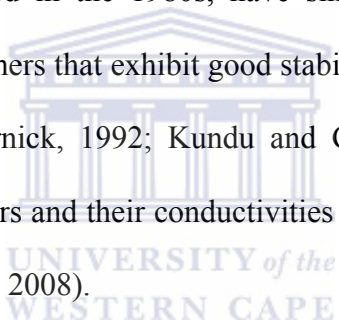
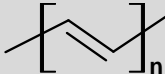
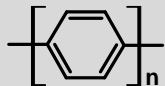
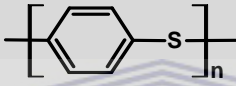
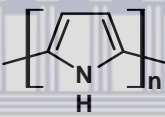
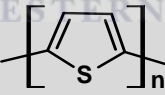
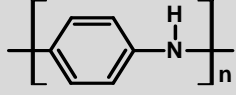
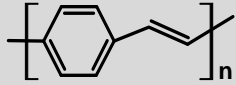


Table 2.1 Structures and conductivities of some conducting polymers commonly used in biosensors

Conducting polymer	Structure	Conductivity (S cm ⁻¹)	Type of doping
Polyacetylene (PAC)		200-1000	n, p
Poly(paraphenylene) (PPP)		100-500	n, p
Poly(paraphenylene sulfide) (PPS)		3-300	p
Polypyrrole (PPy)		40-200	p
Polythiophene (PTh)		10-100	p
Polyaniline (PANI)		1-100	n, p
Poly(paraphenylene vinylene) (PPV)		~ 3	p

2.4.2 Synthesis of conducting polymers

Conducting polymers can be synthesized either chemically or electrochemically. The most widely used technique is the oxidative coupling involving the oxidation of monomers to form a cation radical followed by coupling to form di-cations and the repetition leads to the polymer formation. Chemical synthesis is known to permit the scale-up of the polymers, which is currently not possible with electrochemical synthesis. However, electrochemical polymerization is the most preferred general method for preparing CPs because of its relatively straightforward synthetic procedure, simplicity and reproducibility. Generally, electrochemical polymerization can be carried out galvanostatically (constant current), potentiostatically (constant potential) or by potential scanning/cycling or sweeping methods. By varying either the potential or current with time, the thickness of the film can be controlled. In this procedure, the monomers at the working electrode surface undergo oxidation to form radical cations that react with other monomers or radical cations, forming insoluble polymer chains on the electrode surface. The mechanism of electrochemical polymerization of CPs, using PANI as an example is shown in Fig. 2.4. Formation of the radical cation of aniline by oxidation on the electrode surface (step 1) is considered to be the rate determining step. This is followed by coupling of radicals, mainly *N*- and *para*-forms, and elimination of two protons. The dimer (oligomer) formed then undergoes oxidation on the electrode surface along with aniline. The radical cation of the oligomer couples with an aniline radical cation, resulting in

propagation of the chain. The formed polymer is doped by the acid (HA) present in solution (step 4) (Wallace et al., 2003).

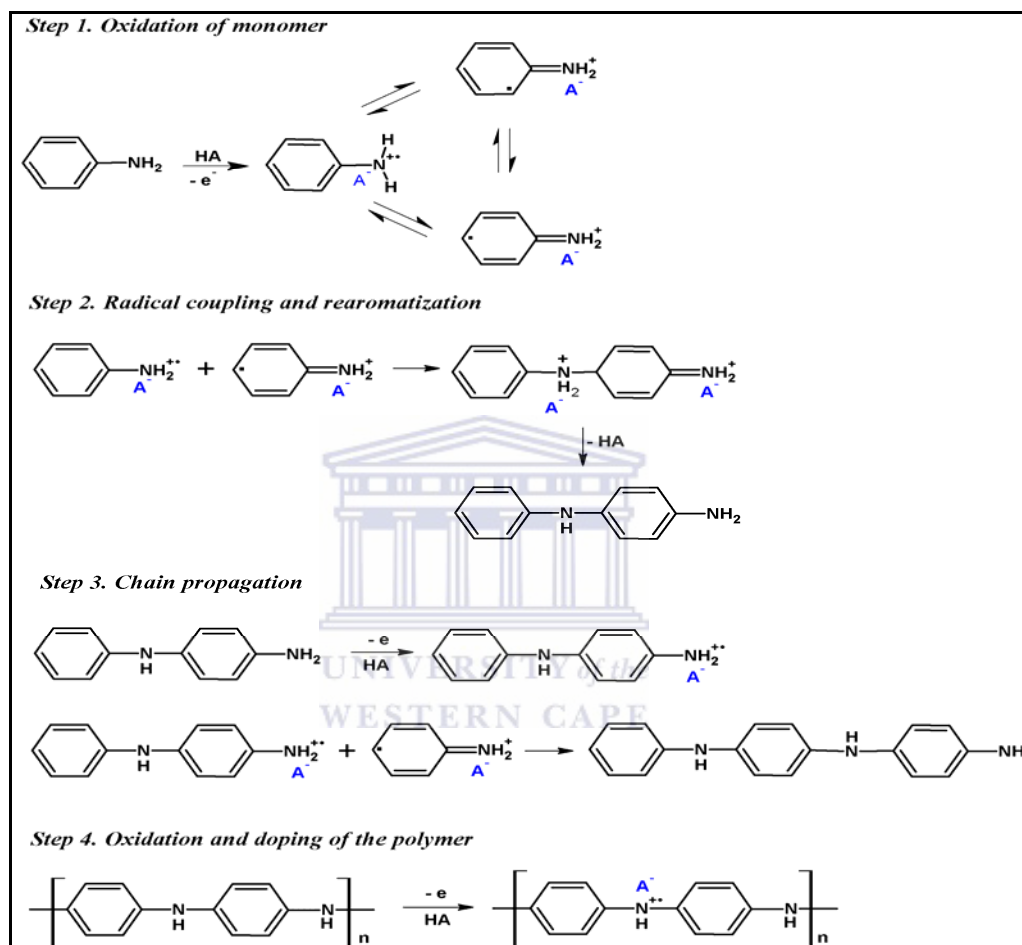


Figure 2.4. Electrochemical polymerization of aniline in presence of a dopant anion A^- .

A number of important variables including deposition time and temperature, nature of solvent, pH of solvent, electrolyte, electrode materials, and deposition charge must be considered during electrochemical polymerization. Each of these parameters has an

effect on film morphology (thickness and topography), mechanics, and conductivity, which are properties that directly impact the utility of the material for biosensor applications. All CPs can be synthesized chemically, but electrochemical synthesis is limited to those systems in which the monomer can be oxidized in the presence of a potential to form reactive radical ion intermediates for polymerization. The common CPs such as PPy, PTh and PANI can be synthesized both chemically and electrochemically. However, several novel conducting polymers with modified monomers are only amenable to chemical polymerization. Electrochemical synthesis has been used to prepare homogeneous and self doped films. Besides this, it is possible to obtain copolymers and graft copolymers (Guimard et al., 2007).

2.4.3 Polyaniline and its derivatives



Among the conducting polymers, PANIs have been of particular interest because of their low cost, ease of synthesis, unique redox tunability, good environmental stability, controllable electrical conductivity and interesting redox properties associated with the chain nitrogens. The aniline polymers also exhibit crystallinity and solution- or counterion-induced processability. Furthermore, the electrical properties of PANI can be substantially improved through secondary doping. PANI is accepted to have the general polymeric structure shown in Fig. 2.5A (Wallace et al., 2003). PANI can exist in several oxidation states ranging from the fully reduced ($y=1$) *leucoemeraldine base* (LEB) state to the fully oxidized ($y=0$) *pernigraniline base* (PNB) state. The half oxidized ($y=0.5$) *emeraldine base* (EB) state is composed

of an alternating sequence of three benzenoid units and one quinonoid unit. Fig. 2.5B shows the representation of the various intrinsic redox states of PANI. The fully oxidized and fully reduced states of PANI are insulators, although they possess other interesting physical and chemical properties. Emeraldine is the state with the highest conductivity. However, the conducting *emeraldine salt* (ES) form can be obtained through a redox-doping process in acidic conditions from its corresponding reduced LEB form or oxidized PNB form by either a chemical or an electrochemical step.

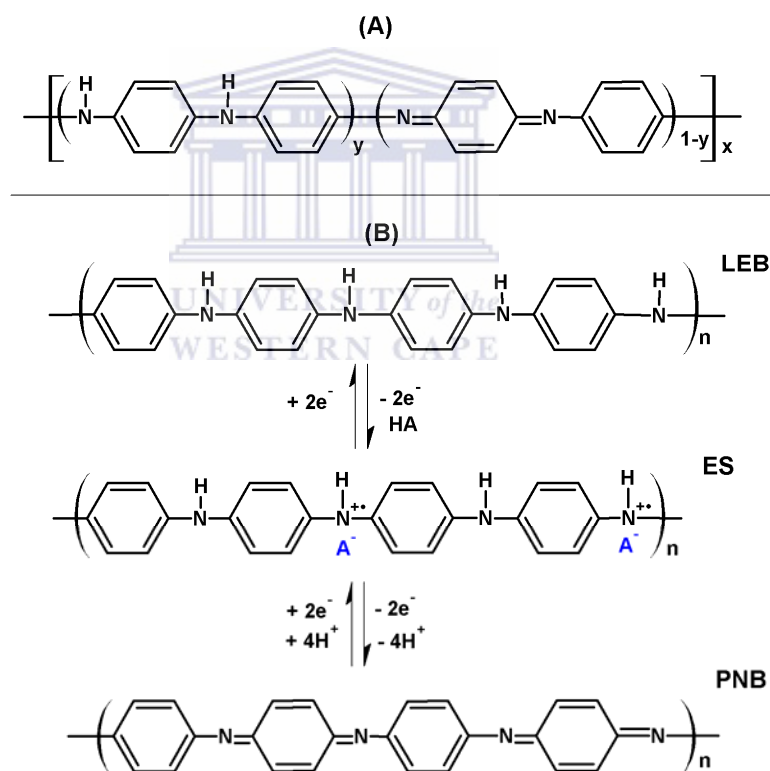


Figure 2.5. (A) The general polymeric structure of polyaniline (B) Oxidation of aniline to polyaniline showing its redox states.

Polyaniline and its derivatives are generally synthesized by chemical or electrochemical oxidative polymerization of the respective aniline monomers in acidic solution, although some other approaches such as plasma polymerization (Cruz et al., 1997; Paterno et al., 2002), electroless polymerization (Liao and Gu, 2002), solid-state polymerization (Gong et al., 2002), biocatalysis (Kim et al., 2007), enzyme-catalyzed polymerization and photochemically initiated polymerization (Wallace et al., 2003) have also been reported. It has been reported that the formation of polyaniline and its derivatives depend on the reaction conditions such as the type of supporting electrolyte, monomer concentration, applied potential, the type of solvent and pH of the electrolyte (Wallace et al., 2003; Iwuoha et al., 1997). The influence of anions on the electrodeposition of polyaniline and on polyaniline redox reactions has also been extensively described in literature (Wallace et al., 2003; Tang et al., 1996; Inzelt & Horanyi, 1990; Kalaji et al., 1991). These factors are known to determine the morphology and properties of the generated polyaniline.

The difficult encounter with PANI is its low solubility in common organic solvents with an ultimate restricted processability. Several research studies have been directed towards improving its solubility in organic solvents to enable its utilization for suitable applications (Chen et al., 2003). Substituted PANI became an alternative choice to have the desired properties. Polymerization of a typical derivative of aniline, such as 2-methoxyaniline, resulted in soluble conducting polymer. In this case, the substituent groups present in the units of the polymer chain caused decrease in the stiffness of the polymer chain to result in better solubility. Unfortunately,

substitution of groups in phenyl ring or *N*-position of polyaniline units resulted in decrease of conductivity (Chen et al., 2003). However, aniline substituted with two methoxy groups, 2,5-dimethoxyaniline (DMA), has been reported to produce soluble polymer, poly(2,5-dimethoxyaniline), PDMA (Fig. 2.6) with a conductivity similar to PANI (Storrier et al., 1994). The anion present in the electrolyte medium influences the degradation of PDMA (Palys et al., 2000). PDMA has been reported to show redox transitions for *leucoemeraldine* to more oxidized PANI forms at lower potentials in comparison with PANI. The potential for converting PDMA into its fully oxidized state was found to be much less positive than PANI (0.70 V for PANI and 0.27 V for PDMA) (Wen et al., 20001). Hence, the presence of dimethoxy- units in the backbone of conducting polymer is expected to improve its solubility and redox characteristics (Chen et al., 2003).

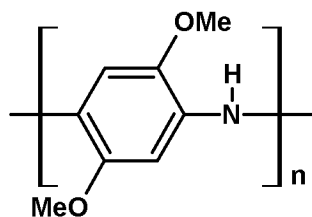


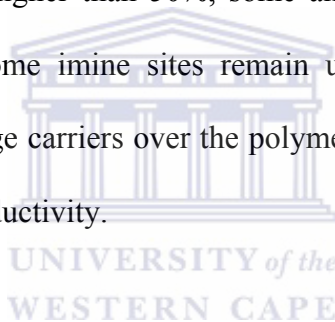
Figure 2.6. The structure of poly(2,5-dimethoxyaniline) (PDMA).

2.4.3.1 Conductivity and doping of polyaniline

Conductivity is a measure of electrical conduction and thus a measure of the ability of a material to pass current. Doping is the process of oxidizing (*p*-doping) or reducing (*n*-doping) a neutral polymer and providing a counter anion or cation (i.e., dopant), respectively (Guirmad et al., 2007). It is well known that π -conjugated polymeric films or coatings may undergo oxidation and reduction from their electrically neutral, non-conductive state, with the formation of electrochromic, highly conductive *p*- and *n*-doped states. This process introduces mobile electronic charge carriers, in the form of charged polarons (i.e., radical ions) or bipolarons (i.e., dications or dianions), into the polymer chain. The attraction of electrons in one repeat-unit to the nuclei in neighbouring units yields charge mobility along the chains and between chains, often referred to as “electron hopping”. The ordered movement of these charge carriers along the conjugated polymer backbone produces electrical conductivity. Doping of CP can be achieved chemically or electrochemically.

Polyaniline has an electronic conduction mechanism that is unique among CPs, because it is doped by both protonation and the *p*-type doping. This results in the formation of a nitrogen base salt rather than the carbonium ion of other *p*-doped polymers. The conductivity of PANI depends on both the oxidation state of the polymer and its degree of protonation. The oxidation state of PANI that can be doped to the highly conducting state is *emeraldine*. Protonic doping in PANI can be achieved through the protonation of the imine nitrogens of the polyleucoemeraldine

form of PANI using strong acids (Pud et al., 2003). This leads to the production of highly conductive, delocalized, stable polysemiquinone radical cation, the polyemeraldine salt form of PANI. It has also been reported that the conductivity of PANI is dependent on the solvent it is cast from or exposed to. This phenomenon has been referred to as “secondary doping.” The solvent causes a change in the polymer conformation that result in increased conductivity. However, the most significant dependence of the conductivity of PANI is upon the proton doping level. The maximum conductivity occurs when PANI is 50% doped by protons (Wallace at al., 2003). At doping levels higher than 50%, some amine sites are protonated, and at levels lower than this some imine sites remain unprotonated. In both instances, delocalization of the charge carriers over the polymer backbone is disrupted, thereby reducing the polymer conductivity.



2.4.3.2 pH sensitivity and switching properties of polyaniline

Polyaniline undergoes two distinct redox processes as well as pH switching between unprotonated and protonated states (Wallace at al., 2003; Lange et al., 2008). The influence of pH on the redox processes of PANI was investigated by MacDiarmid and co-workers (MacDiarmid et al., 1985). It was found that the potential of the second redox transition shifts cathodically with increasing of pH for 0.12 V/pH. The reason for this behaviour is the release of protons in the redox conversion from emeraldine salt to pernigraniline base. The redox processes are readily observed using cyclic voltammetry. The most conductive form of PANI, *emeraldine salt* occurs

between approximately + 0.20 and +0.60 V vs. Ag/AgCl. At less positive potentials, the fully undoped form (*leucoemeraldine*) is much less conductive, as is the fully oxidized form (*pernigraniline*) at higher potentials. If PANI is exposed to potentials higher than the second oxidation process, a third voltammetric response appears upon cycling the potential. This is due to oxidation/reduction of a degradation product (Watanabe et al., 1989). The insoluble degradation products are formed, probably due to chain scission by hydrolysis of amine groups to form benzoquinone and acrylamine terminations. The chemical properties of PANI can be controlled by application of potential, base or acid. Not only do the conductivity and chemical properties of PANI change, the colour of the polymer also changes between each of these states. It is transparent in the reduced state and when oxidized, it changes to green (at $\sim +0.2$ V) and then to blue upon further oxidation. High colour contrast is usually observed for thick films ($> 1 \mu\text{m}$) of PANI but it is achieved at the expense of switching speed (Deepa et al., 2007).

It has been reported that the rate of switching of PANI depends on the electrolyte used (with smaller ions the switching is faster), the solvent employed and the protonation level of the solution while the peak potentials vary with the pH (Bartlett & Wallace, 2000). It has also been observed that, when polyelectrolytes are incorporated as dopants in PANI, the switch from conducting to non-conducting material is shifted to very high pH solutions, enabling electrochemistry to be carried out on polyaniline in neutral solutions (Bartlett & Wallace, 2000). Polyaniline can be “switched” by the addition of acids and bases that protonate and deprotonate the base

sites within the polymer. This leads to the dependence of the polymer states, and thus the reactions, upon the pH of the solutions. In solutions of pH greater than 4, PANI loses its electroactivity entirely because the *emeraldine salt*, the only conducting form of the polymer is dedoped to form the insulator *emeraldine base* (EB) (Wallace et al., 2003). The doping reaction of PANI is the same as the one that occurs during polymerization process, and the dedoping reaction is the reverse process.

The pH and potential dependencies of conductivity and optical absorption of PANI at 420nm were reported. Later such investigations were extended to other spectral ranges and also for derivatives of PANI (Lange et al., 2008). The largest spectral changes due to deprotonation of emeraldine salt are usually observed between pH 5 and pH 8, whereas only small changes are observed between pH 2 and pH 5. Because of hysteresis in the transfer between different forms of PANI, the main spectral changes during decrease of pH are observed between pH 6 to pH 3. This leads to strong limitation of the working range of such sensors (Lange et al., 2008). Polyaniline has been shown to exhibit the same redox behaviour in both aqueous and non-aqueous media (Watanabe et al., 1989). However, in organic solvents, the second (more positive) oxidation response is irreversible, due to the lack of protons in such media.

2.4.3.3 Spectroscopic determination of the redox states of polyaniline

The common spectroscopic techniques, such as Fourier transform infrared (FTIR) and UV-Vis spectroscopy have been used to provide qualitative indication of the intrinsic redox states of conducting polymers and to predict successful doping (Patil et al., 2004; Cataldo & Maltese, 2002). It has generally been observed that the FTIR and UV-Vis spectra of unsubstituted PANI are similar to those of substituted PANI though with slight band shifts. Earlier studies suggested that the IR absorption modes at about 1500 cm^{-1} and 1600 cm^{-1} are associated with aromatic ring stretching. Tang et al. (1988) assigned the 1600 cm^{-1} peak to the quinonoid ring and the 1500 cm^{-1} peak to the benzenoid ring. The IR absorption spectrum of *leucoemeraldine* indeed exhibits a very low intensity ratio of the 1600 cm^{-1} : 1500 cm^{-1} peaks, consistent with the presence of predominantly benzenoid units. On the other hand, *emeraldine base*, which consists of about equal amounts of benzenoid (B) and quinonoid (Q) units, has about equal intensities for the 1600 cm^{-1} and 1500 cm^{-1} absorption bands. Furthermore, the IR absorption spectra of *pernigraniline* exhibits an enhanced quinonoid to benzenoid band intensity ratio (MacDiarmid et al., 1991; Cao, 1990; Sun et al., 1990). Another informative peak in the IR absorption spectra of PANI is the weak C-N stretching absorption in QBQ units at about 1380 cm^{-1} . *Leucoemeraldine* does not absorb at this frequency while *emeraldine* does. The appearance of a small amount of quinonoid imine units in partially oxidized *leucoemeraldine* is accompanied by the appearance of a weak 1380 cm^{-1} absorption band. However, upon acid protonation of *emeraldine base*, the quinonoid units are

believed to be converted to benzenoid units by a proton-induced spin-unpairing mechanism and the absorption band at 1380 cm^{-1} disappears (Kang et al., 1990). In the case of protonated *emeraldine*, the long absorption tail above 2000 cm^{-1} , which masks the NH stretching vibration in the $3100\text{-}3500\text{ cm}^{-1}$ region, and the appearance of the intense broad band at about 1150 cm^{-1} , have been associated with high electrical conductivity and a high degree of electron delocalization in the polysemiquinone forms of the doped PANI (Kang et al., 1998). Patit et al. (2004) reported the manifestation of the ‘electronic like band’ associated with high conductivity of PANI due to polarons at ca. 1100 cm^{-1} . Table 2.2 summarizes the assignments of IR absorption bands for PANI (Kang et al., 1998).

For UV-Vis spectroscopy, the lowest energy absorption band for *leucoemeraldine base* (LEB) occurs at ca. 320 nm and may be assigned to the $\pi\text{-}\pi^*$ electronic transition, i.e., between the valence and conduction bands. For *emeraldine base* (EB), there occurs a similar low wavelength $\pi\text{-}\pi^*$ band as well as a strong band at ca. 600 nm that has been attributed to a local charge transfer between a quinoid ring and the adjacent imine-phenyl-amine units giving rise to an intramolecular charge transfer exciton ($\pi\text{-}\pi^*$ quinoid ring) (Zhang et al., 2005; Wallace et al., 2003; Cho et al., 2004; Norris et al., 2000). *Pernigraniline base* (PNB) also exhibits two absorption peaks: a $\pi\text{-}\pi^*$ band at ca. 320 nm and a band at ca. 530 nm assigned to a Peierls gap transition (Wallace et al., 2003). However, in the presence of dopants, new electronic energy levels are introduced within the polymer sub-gap energies due to more energetically favourable intra-gap transitions (Fernandes et al., 2005). This corresponds to the

appearance of polaronic and bipolaronic bands in their spectra and the consequential introduction of charge carrier-electrons or holes within the polymer chain. Protonation of PNB causes a violet-to-blue colour change due to the formation of *pernigraniline salt* (PNS). This change is associated with the loss of the PNB band at 530 nm and the appearance of a strong PNS peak at ca. 700 nm. *Emeraldine salts*, on the other hand typically exhibit three peaks in their “compact coil” conformation: a π - π^* (band gap) at ca. 330 nm and two visible region bands at ca. 430 and 800 nm that may be assigned as π →polaron band and polaron→ π^* band transitions, respectively (Wallace et al., 2003; Malinauskas, 2005). The appearance of the quinoid π - π^* transition band at ca. 600 nm in the spectra of doped PANI is however indicative of incomplete doping (Geng et al., 1999).

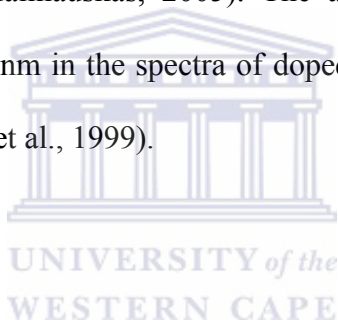


Table 2.2. Assignments for FTIR absorption bands for polyaniline

Frequency (cm ⁻¹)	Assignment
3460	NH ₂ asymmetric stretching
3380	NH ₂ asymmetric stretching, NH stretching
3310	H-bonded NH stretching
3170	=NH stretching
2930	Impurity or sum frequency
2850	Impurity or sum frequency
1587	Stretching of N=Q=N
1510	Stretching of N-B-N
1450	Stretching of benzene ring
1380	C-N stretching in QB _t Q
1315	C-N stretching in QB _c Q, QBB, BBQ
1240	C-N stretching in BBB
1160	A mode of N=Q=N
1140	A mode of Q=N ⁺ H-B or B-NH-B
1220	C-H in-plane bending of 1,4-ring
1105	
1010	
1115	C-H in-plane bending of 1,2,4-ring
1060	
960	
910	C-H out-of-plane bending of 1,2,4-ring
895	
850	
830	C-H out-of-plane bending of 1,4-ring
740	C-H out-of-plane bending of 1,2-ring
690	
645	Aromatic ring deformation
530	
500	

Abbreviations: B, benzenoid unit; Q, quinonoid unit; t, *trans*; c, *cis*

2.4.4 Nanostructured conducting polymers

Nanotechnology is an emerging field having a vast potential for bringing revolution in the development and advancement of the techniques involved in the fabrication of

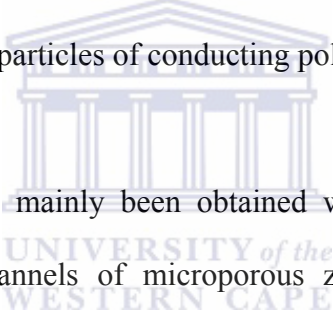
sensors and devices. Nanofabrication refers to the tools and techniques that can be put to use for changing the structure and the properties of matter at the nano (less than 100 nm) scale. With grain sizes in the order of a billionth of a meter, nanomaterials exhibit excellent mechanical, catalytic, magnetic and optical properties. Their scope of applications extends across a variety of fields including chemistry, physics, electronics, optics, material science and biomedical sciences. If the recent developments are indicators, then this technology assures taking this idea to its ultimate extreme-components fabricated from atom by atom. Materials with nanoscopic dimensions not only have potential technological applications in various areas but also are of fundamental interest in that the properties of a material can change in this regime of transition between the bulk and molecular scales (Chakarvarti and Vetter, 1998). It has been well known that performing reactions in a confined micrometer and nanometre sized environment (nanoreactor) may yield new nanostructured materials that exhibit excellent mechanical, catalytic, magnetic and optical properties. A wide range of nanomaterials including semiconductors, magnetic multilayered nanowires, metals, polymers, inorganic oxides, glasses, and nanotubules have been produced using various nanoreactor systems, such as micelles or reverse micelles, liquid crystals, microemulsions, microgels, amphiphilic polymers or block copolymers, liposomes and dendrimers (Hingorani et al., 1995; Zhao et al., 1998; Balogh and Tomalia, 1998; Bronstein et al., 1999; Sangregorio et al., 1999; Balogh et al., 1999; Ingert and Pileni, 2001; Samuelson et al., 2001; Dellinger and Braun, 2001; Forster and Konrad, 2003; Shi et al., 2004). Different nanoreactor systems are able to create nanomaterials with intriguing properties

having both the guest (nanomaterials) and host (nanoreactors) material characteristics (Chakarvarti and Vetter, 1998)

Sumio Iijima introduced the terms nanotubes and nanowires to the world of science from his discovery of carbon nanotubes in 1991 (Iijima, 1991). During the past decade, there has been a great technological focus on the production of nanostructured materials with defined sizes, shapes and geometry such as nanoparticles, nanotubes, nanorods, nanobelts, nanofilms, nanowires, nanocables, and nanocomposites (Pan et al., 2001; Feng et al., 2003; Shi et al., 2007; Malinauskas et al., 2005; Welch and Compton, 2006). The nanomaterials have found tremendous interest in diversified technological applications including biosensing, medicine, catalysis, optics, electronics, etc. (Alivisatos, 2001; Lieber, 2001; Whitesides and Love, 2001). The advantages derived from the use of nanostructured materials over micro/macroparticles as an electrode material includes high effective surface area, better mass transport, better catalysis and control over local microenvironment. Nanoparticles with sizes of about 100 nm have been reported to produce seventy times magnitude of current when applied in electroanalysis compared to that from a micro electrode (Welch and Compton, 2006).

In general, “template synthesis” is the most common and effective method for synthesizing nanostructures of conducting polymers such as polyacetylene (PAC), polypyrrole (PPy), poly(3-methyl thiophene) and PANI. If present in the polymerization solution, templates avail nanoscopic void spaces for structurally

moulding the morphology of the resultant polymers into defined nanoshapes. Besides template synthesis, various synthetic routes for the preparation of π -conjugated polymeric nanostructures have been reported. For instance, traditional methods, including chemical or electrochemical oxidative polymerization of the monomers, electrospinning or drop cast methods have been reported (Kobayashi et al., 1984; Qiu et al., 2001). The new advances in this area include the use of “template-free method” (Huang and Wan, 1999), electrochemical polymerization with a scanning micro-needle electrode, chiral nematic reaction (Akagi et al., 1998), seeding (Fukushima et al., 2003) and humidity control (Deepa et al., 2006) for synthesizing micro- or nanotubes, nanofibers and nanoparticles of conducting polymers.



Nanostructured PANI has mainly been obtained with the aid of template-guided polymerization within channels of microporous zeolites, electrodes, and porous membranes or via chemical routes in the presence of self-organized supramolecules or stabilizers (Nandi et al., 2008). According to Huang and Kaner, the nanofibrillar morphology of PANI does not require any template or surfactant, and appears to be intrinsic to PANI synthesized in water. The nanofibers that form the basic unit for PANI is naturally formed at the early stage of the polymerization reaction and are much smaller in diameter than most templated or electrospun fibres (Huang and Kaner, 2006). However, there have been a number of methods reported for the synthesis of PANI nanofibers using templates as well as other synthetic methods (Li et al., 2006). In comparison with PANI nanoparticles, which are mainly synthesized by dispersion technique and electrochemical methods, one-dimensional

nanostructured PANI, including nanofibers, nanowires, nanorods, nanotubes, nanofibrils, nanobelts and nanoribbons, presents several advantages in fabricating nanodevices and in preparing nanoscale electrical connections in highly conducting polymer composites, etc (Zhang and Wang, 2006).

2.4.5 Synthesis of nanostructured polyaniline

The processability and applicability of the synthesized conventional PANI have been mostly hampered by its infusibility or insolubility in organic solvents due to its rigid π - π conjugation system. Several strategies have therefore been employed to overcome and improve the solubility of PANI in organic solvents to enable its utilization for suitable applications. Accordingly, synthesis of nanostructured PANI has become the key step in preparing highly dispersed blends of PANI with other processable polymers, and thus the improvement of the processability of PANI. Apart from the physical routes like electrospinning, mechanical stretching, and the doping induced solution route, the chemical approaches adopted for production of one-dimensional nanostructured PANI can be generally categorized into the chemical oxidative way and the electrochemical oxidative way, just as the ones employed for the synthesis of the conventional PANI powders (Zhang and Wang, 2006).

The template synthesis method commonly used for the production of one-dimensional nanostructured PANI is further subdivided into hard template (physical template) synthesis and soft template (chemical template) synthesis approach

according to the solubility of the templates in the reacting media. Non-templated routes for the synthesis of one-dimensional nanostructured PANI such as rapid mixing reaction method, radiolytic synthesis, interfacial polymerization, and sonochemical synthesis have also been reported (Zhang and Wang, 2006). Other approaches like combined soft and hard template synthesis are also known.

2.4.5.1 Hard template synthesis

In this technique, materials can be deposited within the pores of the template membranes by either electrochemical or chemical (electroless) reduction of the appropriate metal ion. The generated structures can both be homogeneous or heterogeneous (including multilayered) short, squat fibrils, long needle-like fibrils, tubules, tapered conical (single or double cones) and geometries, with complete control over the aspect ratio (length and diameter ratio). Intrinsically conducting polymers such as PANI, PPy as well as other materials including metals, carbon, can be obtained by chemically derivating the pore walls, i.e. by providing molecular anchors or channels of hard templates such as membranes, zeolites, anodic aluminium oxides (AAO), track-etched membranes, etc., so that the electrodeposited material preferentially deposits on the pore walls (Chakarvarti and Vetter, 1998; Zhang and Wang, 2006). The technique is simple, yet nanostructures with extraordinary low dimensions (ca. 3 nm) have been reported to be produced. For example, PANI filaments with diameters of 3 nm have been achieved in the hexagonal channels of mesoporous aluminosilicate (Wu and Bein, 1994). However, the disadvantage of this

method is that, a tedious post-synthesis process is required in order to remove the templates and the nanostructured polymers may be destroyed or form undesirable aggregated structures after being released from the templates (Zhang and Wang, 2006). The requirement of ‘molecular anchors’ to maintain the nanostructured shapes is in itself a challenge. The need for the post synthesis template dissolution is also a limiting factor because only the templates with a corresponding dissolving solvent can be used (Wei et al., 2002; Long et al 2003).

The fabrication of conductive polymeric nanostructures by this method can be achieved by oxidative polymerization of the corresponding monomer which can be accomplished either electrochemically or chemically or by using chemical oxidizing agents. For example, during the chemical synthesis of PANI, the hard templates were first immersed in a pre-cooled acidic solution of aniline monomer, and then the oxidant solution at the same temperature was added to start the polymerization. During the procedure, PANI was produced and deposited within the pores or channels of the templates. With the templates eliminated, partly or completely, one-dimensional nanostructured PANI was isolated. Occasionally, the templates were not removed; giving rise to the one-dimensional nanostructured PANI filled composite materials. In some cases, aniline was adsorbed from vapour phase into the channels of the templates, and polymerization was then carried out in an identical fashion as mentioned above. PANI nanotubules were also synthesized by placing solutions of aniline and ammonium peroxydisulfate (APS), the oxidant, in a two-compartment cell with the particle track-etched membrane (PTM) as the dividing wall, which serves as

the hard template. The monomer and the oxidant diffused toward each other through the membrane and reacted, yielding the PANI nanotubules in the pores of the membrane (Zhang and Wang, 2006). In addition to the above-mentioned chemical oxidative polymerization, PANI nanofibers, nanotubules and nanoribbons were also prepared by electrochemical oxidative polymerization with hard templates such as PTM, AAO and enclosed nanochannels. Polymers generated using electrochemical oxidative polymerization within PTM is associated with increased electric conductivity because the polymerization is confined to the pore spaces and electrostatic interactions between the ionic species allow alignment on the walls of the pores (Malinauskas et al., 2005). While using electrochemical method, one surface of the membrane is coated with a metal film which acts as an anode and the polymer is grown within the pores. It has been reported that if the membrane is a polycarbonate material, then the polymer preferentially nucleates and grows on the pore walls, producing polymeric tubules whose wall thickness can be controlled by controlling the polymerization time. In some polymers like PPy, the tubules end up closed to form solid fibrils, while in PANI, the tubules do not close up even after long polymerization time (Chakarvarti and Vetter, 1998). Maceij et al., (2003) prepared PANI and poly-*o*-methoxyaniline nanotubes in polycarbonate membranes through the chemical in situ deposition method.

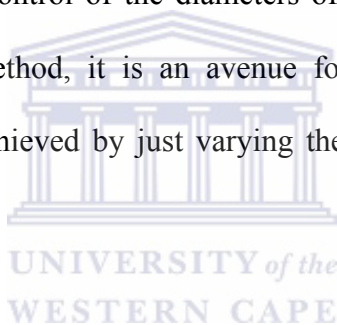
The hard template method is expected to be a very promising and powerful tool in producing crystalline nanomaterials to be used in biosensing and light-emitting

diodes. This may prove to be the turning point in the device-making technology (Chakarvarti and Vetter, 1998).

2.4.5.2 Soft template synthesis

Due to the limitations presented by the hard template method, new approaches towards PANI dispersibility through nanostructurization are now focused on the use of soft templates. The soft template synthesis method, referred to as the “template-free” method (in that no hard template is used) entails synthesizing PANI and its derivatives, in the presence of structure-directing molecules such as surfactants, polyelectrolytes, deoxyribonucleic acid (DNA), thiolated cyclodextrins, sulfonated porphyrins, liquid crystalline, and ethanol, which act as templates for production of the one-dimensional nanomaterials (Zhang and Wang, 2006). The surfactants are often complex acids with bulky side groups, such as the naphthalenesulfonic acid (NSA) (Wei et al., 2002), camphorsulfonic acid (CSA) (Zhang et al., Wan, 2005), dodecyl benzenesulfonic acid (DBSA) (Han et al., 2002), 5-aminonaphthalene-2-sulfonic acid (ANSA) (Wei and Wan, 2003), etc. The surfactant molecules in solution exist in micellar form leaving nanoscopic spaces available for monomer polymerization. In this way, surfactants act as soft templates for nanostructurization. The polyelectrolytes include poly(acrylic acid), poly(styrenesulfonic acid), poly(vinylsulfonic acid) etc. The “template-free” method is simple and cheap in comparison with the hard template method because it does not require post synthesis processing. It results into nanostructured materials with improved processability,

conductivity and morphology. Also, through the “template-free” method, several dispersible one-dimensional structures taking various forms depending on the nature of template can be obtained. The formation of the dispersible one-dimensional nanostructured PANI depends on the reaction conditions, such as the concentration of the monomer, the molar ratio of the monomer to oxidant or the soft template, type of templating molecule, synthesis temperature and time. Generally, the lower concentrations of aniline favoured the formation of nanotubes or nanofibers, while the higher concentrations favoured the formation of granular PANI (Zhang and Wang, 2006). Although control of the diameters of the nanostructures is not easily achieved through this method, it is an avenue for the fabrication of new smart materials (composites) achieved by just varying the contents of the polymerization solution.



In a typical surfactant based procedure, aniline and surfactants such as CSA, NSA, ANSA, *o*-aminobenzenesulfonic acid, etc. with different molar ratios are added to a certain amount of distilled water. A transparent solution of aniline/surfactant salt formed is brought to a specified temperature, and then an aqueous solution of the oxidant, usually ammonium peroxydisulfate (pre-cooled to the same temperature) added to initiate the polymerization. After a predetermined period of reaction time, the mixture is filtered, washed, and dried to obtain the one-dimensional nanostructured PANI (Zhang and Wang, 2006). For instance, Huang and Wan (Huang and Wan, 1999) synthesized microtubes of PANI by this method, using $(\text{NH}_4)_2\text{S}_2\text{O}_8$ as an oxidant in the presence of β -naphthalene sulfonic acid (NSA) as a

dopant. It was proposed that the formation of these PANI microtubes can be attributed to self-assembling of β -NSA molecules and/or their aniline salts into microstructural intermediate (Wan and Li, 2000) which acts as both a super molecular template (Qiu et al., 2001) and a self-doping agent. The reliability and practicability of this method have been proven through changing polymer chains (Huang and Wan, 1999; Liu and Wan, 2001; Shen and Wan, 1999; Wan and Li, 1999), dopants (Wan et al., 2001; Qiu and Wan, 2001; Qiu et al., 2001) and using different polymerization methods (Yang and Wan, 2002). At the same time, the size of the tubes, from micrometer to nanometer (100-300 nm), could be controlled through changing the synthesis conditions (Qiu and Wan, 2001; Qiu et al., 2001). Furthermore, it was discovered that the diameter and length of the tubes strongly depended on the polymerization conditions (Qiu and Wan, 2001; Shen and Wan, 1999). Zhang and Wan (Zhang and Wan, 2002) report composite films of nanostructures (e.g. nanotubes or nanorods of 60-80 nm) of PANI blended with water-soluble poly(vinyl alcohol) (PVA) as a matrix. The PANI nanostructures were synthesized by a “template-free” method in the presence of β -NSA as a dopant. The authors believe that blending with soluble polymers is suitable for improving the processability of PANI micro- or nanotubes. Yang et al. synthesized chiral PANI nanotubes with inner diameter of 50–130 nm, outer diameter of 80–220 nm and aspect ratio of 6–10, with chiral 2-pyrrolidone-5-carboxylic acid (PCA) as the template (Zhang and Wang, 2006). Nickels et al. and Ma et al. synthesized nanowires of PANI with DNA as the template, and the nanowires were immobilized on silicon surface with pre-stretched strand DNA as the template (Zhang and Wang, 2006).

Michira, et al. (2007) synthesized nanofibrils of PANI with diameters less than 200 nm using anthracenesulfonic acid (ASA) as the structure-directing molecule. It was proposed that the ASA micelles formed guided the formation of the fibrillar morphology. Similar structures were reported for CSA doped PANI (Zhang and Manohar, 2004). Elsewhere, the chemical oxidative polymerization of aniline was performed in a micellar solution of DBSA to obtain nanoparticles with enhanced thermal stability and processability (Han et al., 2002). The average size of the PANI particles was between 20-30 nm.

In a polyelectrolyte based procedure, the polyelectrolyte is first dissolved in an organic solvent, such as tetrahydrofuran, to give a homogeneous solution then aniline is added to the solution to form a gel composed of a molecular complex of aniline and the polyelectrolyte. After washing with tetrahydrofuran to eliminate the excess aniline, the gel complex is re-dissolved in an acidic aqueous solution. Polymerization is initiated following addition of the oxidant solution, and then PANI nanofibers collected by filtration after a specific period of reaction time. As far as the mechanism is concerned, Liu and Yang, Hwang and Yang in independent studies suggested that aniline was firstly bound onto the polyelectrolytes, followed by polymerization of aniline attached to the polyelectrolyte templates. Therefore, PANI nanofibers with diameters of 50 nm are produced when the template molecule is an extended linear chain of poly(acrylic acid), while globular morphology is obtained when the random coil conformation of poly(styrenesulfonic acid) is used as the template (Zhang and Wang, 2006).

PANI/PANI related materials, by themselves, reveal redox functions only in acidic media, $\text{pH} < 4$ (Wallace et al., 2003), a feature that limits its broad use, specifically in combination with biomolecules which normally require a neutral pH environment. It was, however, reported that the doping of PANI or its derivatives with anionic species or the formation of composite polymer blends between PANI and negatively charged polymers such as poly(styrenesulfonate), poly(vinylsulfonic acid) or poly(acrylic acid) switches the redox activity of PANI to neutral pH values and also leads to the increase in its structural stability and conductivity at a broader range of pH values in aqueous media (Iwuoha et al., 1997; Wallace et al., 2003; Grennan et al., 2006). This is attributed to the effective doping (protonation) of PANI by the trapped polyelectrolytes in a broad pH range. Employing a polyelectrolyte to bind to and preferentially align the aniline monomers prior to polymerization has also shown promise in facilitating the desired head-to-tail coupling of the aniline substrates. During polymerization, the anionic polyelectrolytes such as poly(styrenesulfonate) and poly(acrylate) also provide the required counterions for charge compensation in the doped PANI products. This can lead to water-soluble or water-dispersed emeraldine salt products (Wallace et al., 2003). PANI may be deposited onto electrode surfaces through chemical or electrochemical means. Electrochemical polymerization, through galvanostatic, potentiostatic or potentiodynamic means, offers the potential to incorporate a wider range of dopant ions, since the reaction is carried out in the presence of an appropriate electrolyte rather than a chemical oxidant. Electrochemical oxidation also gives better control over film properties, such as thickness and morphology (Grennan et al., 2006). For these reasons, this work has

focused on the synthesis of nanostructured poly(2,5-dimethoxyaniline) to be employed for the construction of an electrochemical enzyme biosensor for the detection of the herbicides glufosinate, glyphosate and AMPA. Nanostructured (nanofibers, nanoparticles and nanotubes) poly(2,5-dimethoxyaniline) (PDMA) have been electrochemically synthesized by the soft-template ('template-free') method using the dopant and structure-directing molecule, poly(4-styrenesulfonic acid) (PSS).

2.4.5.3 Electrochemical no-template synthesis

To distinguish between the commonly called "template-free" synthesis of the soft template method, the term "no-template" was coined here to name the method for synthesizing one-dimensional nanostructured PANI without any templates, hard or soft. One-dimensional nanostructured PANI can also be synthesized by electrochemical no-template approaches (Okamoto et al., 1998; Li et al., 2004). Langer et al. obtained PANI nanofibrils, as well as microfibrils or rods, by electrochemically synthesizing PANI from an aqueous medium at pH~1 without any templates. The nanofibrils doped with fullerene derivatives exhibited diameters of 10–100 nm and lengths of 500–2000 nm (Langer et al., 2001). Both single nanofibrils and their networks were obtained with controlled charge flows (Langer et al., 2001). Large arrays of uniform and oriented nanowires of PANI with diameters less than 100 nm were synthesized by Liang et al. (2002) and Liu, et al. (2003) on a variety of

substrates by a three-step electrochemical deposition procedure, without using any templates.

2.4.6 Properties of nanostructured polyaniline and its derivatives

FTIR and UV-Vis spectroscopy studies have revealed that all PANI nanotubes, nanofibers, nanowires, nanorods, as well as microtubes, have backbone structures similar to that of the conventionally prepared granular PANI (Zhang and Wang, 2006, Michira et al., 2007). In some cases, the Einstein shifts observed in the FTIR and UV-Vis spectra originated from the interaction between the PANI chains and some small molecules, such as ethanol, not from the chemical structures. Conductivity measurement of the hard-template synthesized PANI nanotubules showed that the conductivities decreased with the increase of the diameters, and finally reached the conductivity of the conventional PANI powder (Zhang and Wang, 2006).

2.4.7 Conclusions and future trends

The documented health effects and the occurrence of glyphosate, glufosinate and AMPA in foods and the environment raises particular concern in view of the anticipated human exposure to these herbicides and their formulations which are reported to be more toxic than the herbicides themselves. Generally, the residues of these herbicides are not adequately monitored in food and the environment since the methods of their analysis are complex and costly and cannot be applied on a regular

basis. The review indicates that biosensors can meet the need for continuous environmental monitoring of these herbicides to replace or complement the intermittent analytical techniques due to their low cost of analysis, ease of operation, high sensitivity and minimization of sample pre-treatment. Biosensors have undergone rapid development over the last few years due to the combination of new bioreceptors with the ever-growing number of transducers and materials for transducer modification. By combining the use of electronically conducting polymers with immobilized enzymes and by making use of the particular properties of conducting polymers, it is possible to develop biosensors with enhanced performances. Great progress in this field has shown that the modification of electrode surfaces using proper matrices provide a favourable micro-environment for the enzyme to exchange its electrons directly with the underlying electrode and thus affords a new opportunity for the detailed study of the enzyme electrochemistry and its direct electron transfer.

Despite the vast amount of research conducted on biosensors, their use is still against many unresolved technical problems and a number of factors such as sensitivity, selectivity, miniaturization for in-vivo applications, integration of signal processing steps on a chip, building of arrays for more complex pattern recognition analysis, biocompatibility, stability and response time still require investigation. Currently, the research is focused on improving biosensor sensitivity through the use of nanostructured materials as mediators. Nanostructured PANI is one of the most promising candidates for the development of nanobiosensor due to their high surface

area, versatile synthesis approaches, high conductivity, as well as the controllable chemical and physical properties by oxidation and protonation, and the good environmental stability. Nanostructurization has mainly been achieved by use of hard and soft templates. Although various kinds of synthesizing methods have been established, preparation of one-dimensional nanostructured PANI with controllable morphologies and sizes, especially well oriented arrays on a large scale is still a major challenge and therefore new synthetic methods are required.

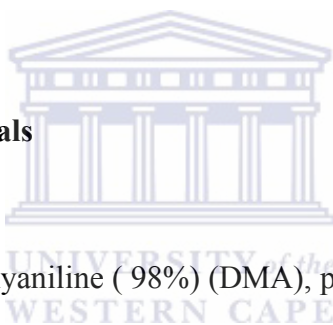


CHAPTER 3

Experimental Section

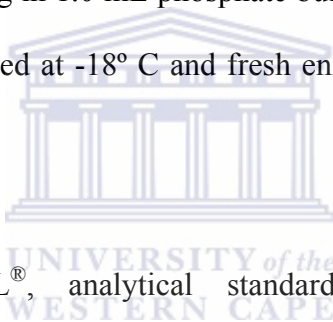
This chapter describes the various analytical techniques employed, detailed research methodology and general experimental procedures for the electrochemical synthesis of nanostructured conducting polymer, biosensor construction, characterization and application of the developed biosensor for the determination of selected herbicides.

3.1 Reagents and materials



The reagents 2,5-dimethoxyaniline (98%) (DMA), poly(4-styrenesulfonic acid) (18% w/v solution in water) (PSS), N,N-dimethylformamide (spectrophotometric grade, $\geq 99.8\%$) (DMF), chloroform (CHCl_3), hydrochloric acid (HCl) ($\geq 32\%$), sulfuric acid (H_2SO_4), fuming (20% SO_3), disodium hydrogen phosphate (98+%), potassium dihydrogen phosphate (99+%), acetic acid, sodium acetate and hydrogen peroxide (30%) were all obtained from Sigma-Aldrich, South Africa. All chemicals were of analytical reagent grade and were used without further purification. The hydrogen peroxide (30%) stock solution was refrigerated at 4° C. Deionized water (18.2 M Ω cm) purified by a Milli-QTM system (Millipore) was used as reagent water for aqueous solution preparation.

Phosphate buffer solution of 0.1 M was prepared by dissolving 3.549 g of disodium hydrogen phosphate and 3.4023 g of potassium dihydrogen phosphate separately in 250 mL deionized water, then mixing the salt solutions according to Henderson-Hasselbalch equation to obtain the required pH values. The phosphate buffer solution (PBS) was refrigerated at 4° C. The hydrogen peroxide working solution of 0.01 M was freshly prepared by dilution from its stock solution. Horseradish peroxidase (E.C. 1.11.1.7, 169 U/mg powder) was obtained from Sigma-Aldrich, South Africa and refrigerated at -18° C. Stock solutions of horseradish peroxidase (HRP) were prepared by dissolving 2.0 or 4.0 mg in 1.0 mL phosphate buffer (pH 7.01) in eppendorf vials. The stocks were refrigerated at -18° C and fresh enzyme solutions prepared prior to experiments.



Glyphosate (PESTANAL[®], analytical standard) and glufosinate-ammonium (PESTANAL[®], analytical standard) were obtained from Fluka, South Africa while aminomethylphosphonic acid (AMPA) (> 99%) was obtained from Aldrich, South Africa. Glyphosate, glufosinate-ammonium and AMPA were used to prepare the standard stock solutions of 1000 mg L⁻¹ (refrigerated at 4° C) by dissolving them in deionized water. The working solutions of glyphosate, glufosinate-ammonium and AMPA were freshly diluted from their stocks.

Analytical grade argon gas was purchased from Afrox Company, South Africa. Alumina polishing pads and powder (0.05, 0.3 and 1.0 μm) were obtained from Buehler, Illinois, USA. The screen-printed carbon electrodes obtained from National

Centre for Sensor Research, Dublin City University, Ireland were cut from the printed sheet then pre-treated in 0.2 M H₂SO₄ solution before use. Carbon films were obtained from Agar Scientific, South Africa.

3.2 Sample preparation

Dry corn samples were purchased from the local stores, ground to fine powder (<200 mesh) then 1.0 g extracted with 20 mL of water: chloroform mixture (5:3) overnight. The contents were transferred to centrifuge tubes and centrifuged (10,000 rotations per minute, 25° C) for 10 min to remove solid particles. The supernatant of the water phase was transferred to clean centrifuge tubes, and 20 mL of deionized water was added to repeat the extraction procedure. The supernatants of the water phase obtained in the two runs were mixed, filtered through 0.45 µm pore membrane filters and stored at 4° C. The working sample solutions were spiked with appropriate volumes of stock solutions of glyphosate or glufosinate and topped up to mark with PBS for subsequent biosensor analysis.

3.3 Measurement and instrumentation

The detection method widely employed in this study involves the combination of enzymatic biosensors with electrochemical techniques such as amperometry, cyclic voltammetry (CV) and rotating disk electrode (RDE). Generally, electrochemical techniques are based on the transformation of chemical information into an

analytically useful signal. This section describes the instrumentation, principles and practical aspects of the electrochemical techniques as well as the enzyme biosensors employed in this study.

The other techniques used include transmission electron microscopy (TEM), scanning electron microscopy (SEM), ultra violet-visible (UV-Vis) and Fourier transform infrared (FTIR) spectroscopy.

3.3.1 Electrochemical techniques

3.3.1.1 Instrumentation



The basic components of a modern electroanalytical system for voltammetric and amperometric measurements are a potentiostat, a computer, and the electrochemical cell. The potentiostat plays the role of applying accurate and controlled potential and monitoring the current produced. The most widely used potentiostats are assembled from discrete integrated-circuit operational amplifiers and other digital modules. In many cases, especially in the larger instruments, the potentiostat package also includes electrometer circuits, analog-to-digital converter (ADC) and digital-to-analog converter (DAC), and dedicated microprocessors with memory. In the computer-controlled instruments, the properties of the modulation and the waveform are under software control and can be specified by the operator. The most commonly used waveforms are linear scan, differential pulse, and square wave. The use of

micro- and nanometre-size electrodes has made it necessary to build potentiostats with very low current capabilities. Microelectrodes routinely give current responses in the pico- to nanoampere range. High-speed scanning techniques such as square-wave voltammetry require very fast response times from the electronics. These diverse and exacting demands have pushed potentiostat manufacturers into providing a wide spectrum of potentiostats tailored to specific applications.

The electrochemical cell, where the electrochemical measurements are carried out, consists of a working (indicator) electrode, a reference electrode, and usually a counter (auxiliary) electrode. In general, an electrode provides the interface across which charge can be transferred or its effects felt. Because the working electrode is where the reaction or transfers of interest takes place, whenever we refer to the electrode, we always mean the working electrode. The reduction or oxidation of a substance at the surface of a working electrode, at the appropriate applied potential, results in the mass transport of new material to the electrode surface and the generation of current. The three electrodes are presented in Fig. 3.1 and are described below:

- i. **Working electrode** – this is the electrode at which the redox of the analyte or the electrochemical phenomena being investigated takes place. The commonly used materials for working electrodes include platinum, gold and glassy carbon;

- ii. **Reference electrode** – this is the electrode whose potential is known and is constant. Its potential is taken as the reference, against which the potentials of the other electrodes are measured. The most commonly used reference electrodes for aqueous solutions are the saturated calomel electrode (SCE) and silver/silver chloride electrode (Ag/AgCl);
- iii. **Auxiliary electrode** – it serves as a sink for electrons so that current can be passed from the external circuit through the cell. Reactions occurring at the auxiliary electrode surface are unimportant as long as it continues to conduct current well. To maintain the observed current, this electrode will often oxidize or reduce the solvent or bulk electrolyte though the reactions occur over short periods of time and rarely produce any appreciable changes in bulk concentrations. Most often the auxiliary electrode consists of a metallic foil or thin platinum wire, although gold and sometimes graphite have also been used.

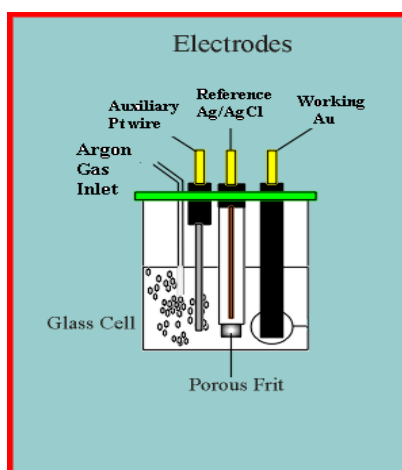


Figure 3.1. Schematic representation of an electrochemical cell consisting of three electrodes.

Figure 3.2 illustrates the setup for the electroanalytical system used in this study. The cyclic voltammetry (CV), amperometry and rotating disk electrode (RDE) measurements were performed using a potentiostat BAS 100B/W electrochemical analyzer from Bioanalytical Systems, Inc. (West Lafayette, IN) with a conventional three-electrode system consisting of gold disk (1.6 mm diameter, 3.0 mm diameter for rotating disk electrode) as the working electrode, platinum wire as the auxiliary electrode, and Ag/AgCl (saturated 3 M NaCl) as the reference electrode. Prior to experiments, the bare gold electrodes were polished with aqueous slurries of 1.0, 0.3 and 0.05 μm alumina powder, rinsing with distilled water after polishing with each grade of alumina. The polished electrode was then sonicated in water and absolute ethanol. The auxiliary electrode was cleaned by burning in a flame for several minutes and the Ag/AgCl electrode was cleaned by rinsing with copious amounts of distilled water. All potentials were quoted with respect to Ag/AgCl. The potentiostat was computer-controlled therefore the experimental modes were selected from the software and specified during its operation. Phosphate buffer solution (0.1 M PBS, pH 6.10) was used as the supporting electrolyte except for the pH dependent experiments which were performed in PBS at various pH values. All experimental solutions were purged with high-purity argon gas for 10 min and blanketed with argon atmosphere during measurements. The experiments were carried out at controlled room temperature of 22 $^{\circ}\text{C}$.

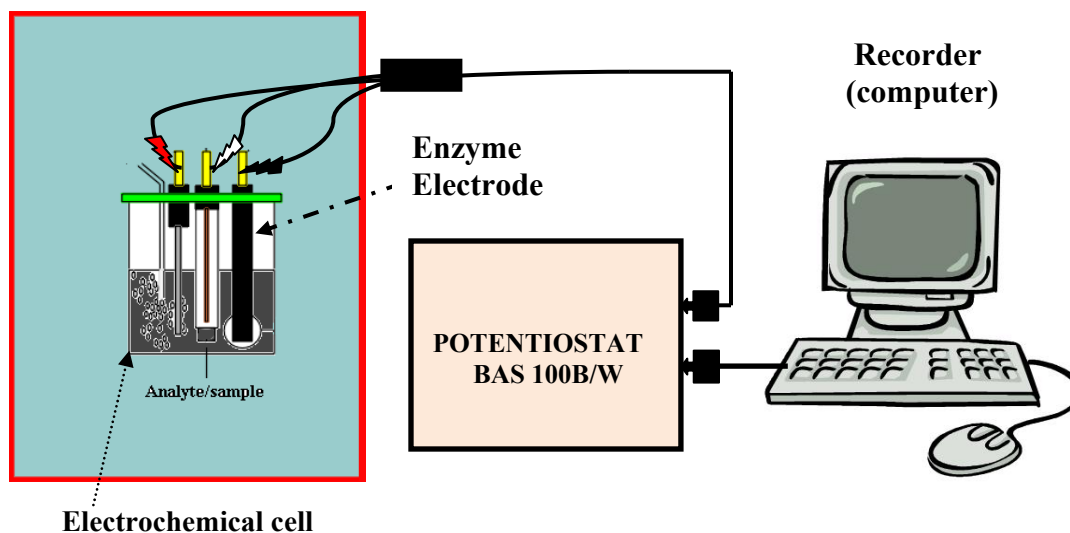


Figure 3.2. Schematic representation of the major components of the electroanalytical system used for the electrochemical measurements.

3.3.1.2 Principles of cyclic voltammetry

The common characteristics of all voltammetric techniques is that they involve the application of a potential (E) to an electrode and the monitoring of the resulting current (I) flowing through the electrochemical cell. In many cases, the applied potential is varied or the current is monitored over a period of time (t). Thus all voltammetric techniques can be described as some function of E , I , and t . They are considered as active techniques (as opposed to passive techniques such as potentiometry) because the applied potential forces a change in the concentration of an electroactive species at the electrode surface by electrochemically reducing or oxidizing it.

Cyclic voltammetry (CV) is a widely used electroanalytical technique. It has wide applications in the study of redox processes, electrochemical properties of analytes in solution, and for understanding reaction intermediates (Bard & Faulkner, 2001). In CV, the electrode potential is ramped linearly at a scan rate of v . The resultant trace of current against potential is termed as a voltammogram. During cyclic voltammetry measurement, the potential is ramped from an initial potential, E_i to a more negative potential but, at the end of its linear sweep, the direction of the potential scan is reversed, usually stopping at the initial potential E_i (or it may commence an additional cycle) (Monk, 2001). The potential is usually measured between the reference electrode and the working electrode and the current is measured between the working electrode and the auxiliary electrode, also known as the counter electrode. This data is then plotted as current versus potential as shown in Fig. 3.3. The forward scan produces a current peak for any analytes that can be reduced (or oxidized depending on the initial scan direction) through the range of the potential scanned. The current increases as the potential reaches the reduction potential of the analyte, but then decreases as the concentration of the analyte is depleted close to the electrode surface. If the redox couple is reversible, then reversing the applied potential makes it reach a potential that re-oxidizes the product formed in the first reduction reaction, thus producing a current of reverse polarity from the forward scan. The oxidation peak usually has the same shape as that of the reduction peak. As a result, the information about the redox potential and the electrochemical reaction rates of compounds can be obtained. For instance, if the electronic transfer at the

surface is fast and the current is limited by the diffusion of species to the electrode surface, then the current peak will be proportional to the square root of the scan rate.

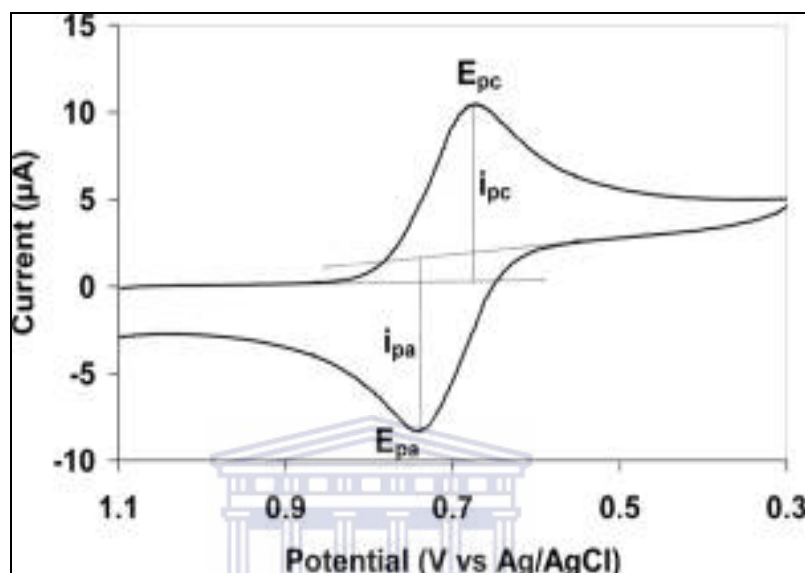


Figure 3.3. A typical cyclic voltammogram.

The important parameters in a cyclic voltammogram are the peak potentials (E_{pc} , E_{pa}) and peak currents (I_{pc} , I_{pa}) of the cathodic and anodic peaks, respectively. If the electron transfer process is fast compared with other processes (such as diffusion), the reaction is said to be electrochemically reversible, and the peak separation is

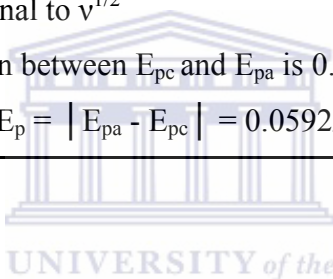
$$\Delta E_p = |E_{pa} - E_{pc}| = 2.303 RT / nF \quad (3.1)$$

Thus, for a reversible redox reaction at 25 °C with n electrons ΔE_p should be $0.0592/n$ V or about 60 mV for one electron. In practice this value is difficult to attain because

of such factors as cell resistance. Irreversibility due to a slow electron transfer rate results in $\Delta E_p > 0.0592/n$ V, greater, say, than 70 mV for a one-electron reaction. The diagnostic tests for electro-reversibility are listed in Table 3.1.

Table 3.1. Diagnostic tests for the electrochemical reversibility of a redox couple, carried out by cyclic voltammetry

1.	$ I_{pa} / I_{pc} = 1$
2.	The peak potentials, E_{pc} and E_{pa} , are independent of the scan rate v
3.	The formal potential (E°) is positioned midway between E_{pc} and E_{pa} , so $E^\circ = (E_{pa} + E_{pc}) / 2$
4.	I_p is proportional to $v^{1/2}$
5.	The separation between E_{pc} and E_{pa} is $0.0592/n$ V for an n-electron couple (i.e. $\Delta E_p = E_{pa} - E_{pc} = 0.0592/n$ V)



For a reversible reaction, the concentration is related to peak current by the Randles–Sevcik expression (at 25 °C) (Monk, 2001; Bard & Faulkner, 2001):

$$I_p = 2.686 \times 10^5 n^{3/2} A c^0 D^{1/2} v^{1/2} \quad (3.2)$$

where I_p is the peak current in amperes, n is the number of electrons transferred, A is the electrode area (cm^2), D is the diffusion coefficient ($\text{cm}^2 \text{s}^{-1}$), c^0 is the concentration in mol cm^{-3} , and v is the scan rate in V s^{-1} . Cyclic voltammetry is carried out in quiescent solution to ensure diffusion control. A three-electrode arrangement is used. The utility of cyclic voltammetry is highly dependent of the

analyte being studied. The analyte has to be redox active within the experimental potential window. It is also highly desirable for the analyte to display a reversible wave. A reversible wave is displayed when an analyte is reduced or oxidized on a forward scan and is then re-oxidized or re-reduced in a predictable way on the return scan as shown in Fig. 3.3. For a multi-oxidation state electroactive species like PANI and its derivatives, several redox couples are recorded in the voltammogram and the critical potentials at which these limiting currents occur are related to the standard electrode potentials for the specific chemical system. Electrochemical reactions sometimes show non-reversible or quasi-reversible waves with deviation from the above reversibility behaviours. For quasi-reversible systems for instance, the peak separation (ΔE_p) is greater than $59 \text{ mV}/n$ and increases with increasing v ; the peak current I_p increases with $v^{1/2}$ but is not proportional to it and the cathodic peak potential shifts negatively with increasing v . In this study, CV was employed for the synthesis of the polymer and to investigate the redox processes and the electrochemical properties of analytes in solution.

3.3.1.3 Principles of amperometry

Amperometry is based on measurement of the intensity of the current resulting from the electrochemical oxidation or reduction of an electroactive species under an imposed potential. The change in current is usually measured as a function of time. It is usually performed by maintaining a constant potential at a platinum, gold or glassy carbon working electrode where the oxidation or reduction of a species takes place

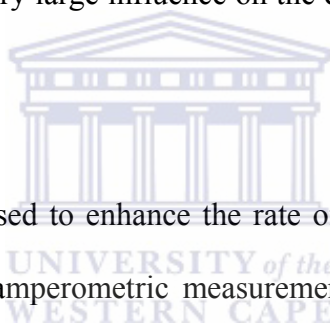
with respect to a reference electrode. A three electrode conventional system can be used as in voltammetry. During electrolysis, the working electrode may act as an anode or a cathode, according to the nature of the analyte. The potential of the working electrode is adjusted to a value of the plateau of the voltammetric wave.

For a simple electron transfer process, it is always possible, by applying a sufficiently high overpotential, to make the rate of the electron transfer step greater than the mass transport. The current flowing in the cell will then reach a mass transport limited plateau value which will increase in magnitude if the solution is stirred, or the electrode is rotated or vibrated as in the case of rotating disk electrode (RDE). The resulting current is directly correlated to the bulk concentration of the electroactive species or its production or consumption rate within the adjacent biocatalytic layer. As biocatalytic reaction rates are often chosen to be first order dependent on the bulk analyte concentration, such steady-state currents are usually proportional to the bulk analyte concentration. Amperometry is the technique widely employed in this study. It was used for the direct determination of glyphosate, glufosinate and AMPA.

3.3.1.4 Principles of the rotating disk electrode (RDE)

Rotating disk electrode (RDE) is a hydrodynamic device that uses convection to enhance the rate of mass transport to and from the electrode surface thus offering advantages over techniques which operate in stationary solution. The faster rate allows steady state conditions to be rapidly achieved (i.e., the rates of mass transport

and electron transfer are balanced). The introduction of convection (usually in a manner that is predictable) helps to remove the small random contribution from natural convection which can complicate measurements performed in stationary solutions as in the case of voltammetry. In analytical applications it is much more common to stir or agitate the electrolyte or to flow the electrolyte through the cell. It is also possible to vary the rate of reaction at the electrode surface by altering the convection rate in the solution and this can be usefully exploited in mechanistic analysis and electroanalytical applications. When these forms of forced convection are present, they have a very large influence on the current density and the sensitivity of the biosensor.



In this study, RDE was used to enhance the rate of mass transport to and from the electrode surface during amperometric measurements. The convective flow during measurements with RDE is illustrated in Fig. 3.4. In this arrangement, the injected analytes were brought to the surface by the gold disk electrode rotating in solution. Experiments were performed to determine the optimum rotation speeds for the RDE and 400 rotations per minute (rpm) was selected as the optimum rotation speed for the enzyme biosensor. It was applied throughout all the experiments. For measurements involving the use of immobilized biomolecules, it is important that the rotation speed chosen should result in laminar flow of the solution. This is in order to avoid the physical removal of the biomaterials.

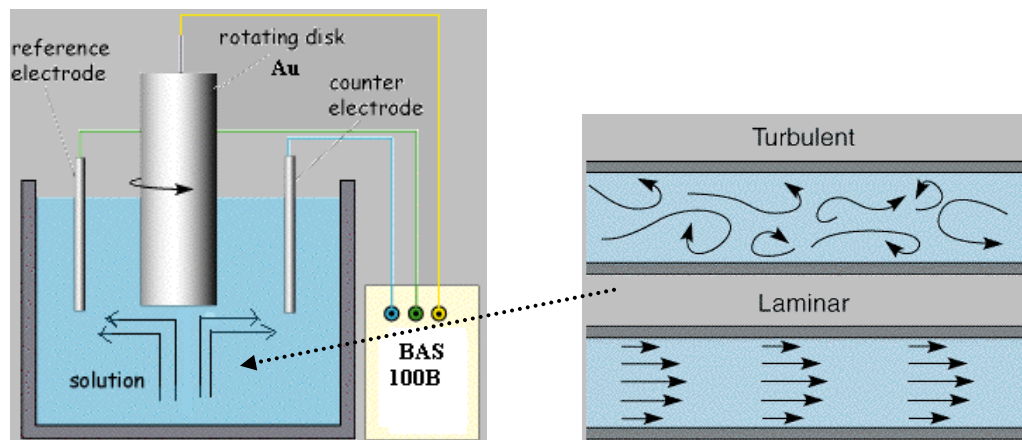


Figure 3.4. Convective flow resulting from the rotation of a rotating gold disk electrode.

3.3.1.5 Electrochemical enzyme biosensors

Most electrochemical biosensors make use of the existing transducers, the instrumentation and techniques already associated with them. The transducers can be connected to a millivoltmeter for potentiometric measurements, or to a potentiostat for amperometric or voltammetric measurements (see Fig. 3.2). The system is then connected to a recorder which monitors the biosensor signal and progression of its response curve towards steady state. The principle modifications are mostly made to the part of the transducer where the enzyme is to be immobilized. An enzyme biosensor is usually constructed by immobilization onto the electrode surface a thin enzymatic layer, which measures the concentration of a substrate. The enzymatic reaction transforms the substrate into a reaction product that is detectable by the electrode. The enzyme biosensors therefore require a recording system to decode the

signal produced during the enzymatic reaction. The signal (current) measured is usually proportional to the concentration of analyte in the solution. The enzymes used in these systems do require periodical renewal to maintain their optimal activity.

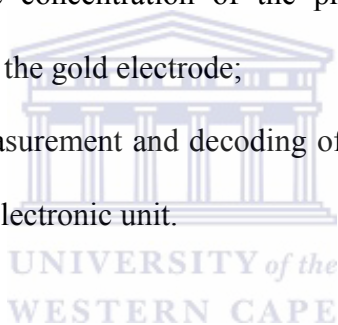
3.3.1.5.1 Principles of operation

A schematic representation of an enzyme biosensor setup used in this study is given in Fig.3.5. The sensitive gold electrode surface is in contact with an enzymatic layer incorporated in PDMA-PSS nanostructures, and it is assumed that there is no mass transfer across this surface. The external surface of the enzymatic layer is immersed in a solution containing the substrate or analyte under investigation. The substrate or analyte migrates towards the interior of the layer and is converted into reaction products when it reacts with the immobilized enzyme. In order to achieve rapid equilibrium of concentrations, the polymer film and the enzymatic membrane must be as thin as possible. The solution must also be well stirred to ensure constant supply of the analyte and proper mixing of the solution when the analyte is introduced. In summary, the steps during the operation of an enzyme electrode are as follows:

- i. Transport of the substrate or analyte from the bulk of the solution towards the enzymatic layer;
- ii. Diffusion of the substrate or analyte within this layer, accompanied by the enzymatic transformation of the substrate or analyte into reaction product.

Diffusion is the movement of a species down a concentration gradient and it occurs whenever there is a chemical change at an electrode surface;

- iii. Migration of the product towards the gold electrode surface. Migration is the movement of charged species due to a potential gradient, and it is the mechanism by which charge passes through the electrolyte. For the electroactive species, the forces leading to migration are purely electrostatic, and hence the charge can be carried by any ionic species in the solution (Greef et al., 1990);
- iv. Conversion of the concentration of the product at this interface into an electrical signal by the gold electrode;
- v. Amplification, measurement and decoding of the signal (current or potential) by an appropriate electronic unit.



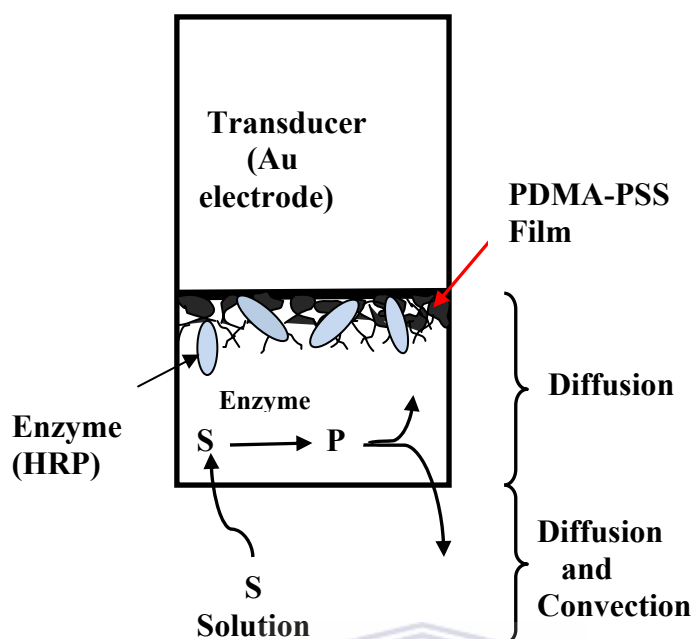
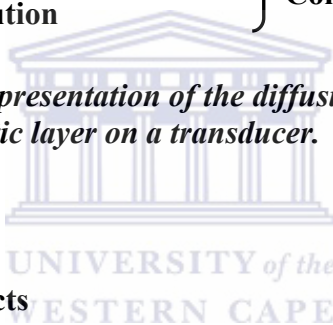


Figure 3.5. Schematic representation of the diffusion of the substrate S and the product P in the enzymatic layer on a transducer.



3.3.1.5.2 Practical aspects

Once the biosensor has been conceived and constructed, it can be installed in a number of different ways according to the objective required. It may be simply immersed into the sample medium, placed in a cell into which the sample is injected, or integrated into an automated system. In this study, the enzyme biosensor constructed was immersed into the cell, connected to the instrumentation for the electrochemical measurements, and voltammetric or amperometric detections performed. For voltammetric measurements, a magnetic stirrer was used to stir the solution at 400 rpm after injection of the substrate then the solutions left to stand still

before the voltammograms were recorded. The amperometric experiments were performed while stirring at 400 rpm with a magnetic stirrer or using RDE. Specific application of an enzyme biosensor requires precise information about its response time, the range and the reproducibility of its calibration curve, its detection limit, and any other parameters that determine the stability of its response. Appropriate experiments were therefore conducted to optimize the enzyme biosensor parameters.

For inhibitor determination, the economic advantages are not so compelling because inhibition implies the decay of the enzyme activity and therefore a limited number of consecutive measurements can be achieved with the same batch of immobilized enzyme. Based on this, the practical application of the inhibitor biosensor is stated primarily for reversible inhibitors. More precisely, the initial response of a biosensor devoted to field applications should be recovered after inhibition in a reasonably short period of time. For reversible inhibition the initial response can be recovered with a washing out procedure after contact with inhibitor. For irreversible inhibitors, complexing reagents or reactivators can be used to recover the response of the enzyme biosensor.

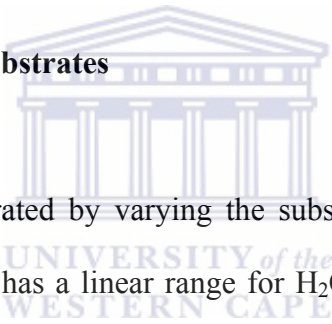
3.3.1.5.2.1 Response time

The response time of a biosensor is the time taken for it to reach a steady state where it is no longer possible to detect any variation in the signal. The response time is very difficult to evaluate precisely in steady state so the t_{98} value corresponding to the time

taken to reach 98% of the sensor response is often used instead of the response time (Tran-Minh, 1993). In practice, the transducer does not transform a chemical signal into an electric one immediately, but requires a certain time, which depends on the transducer used. It is reported that stirring the sample medium or using forced convection reduces the response time of a biosensor since it favors the movement of the substrate or analyte towards the active enzymatic membrane (Tran-Minh, 1993).

3.3.1.5.2.2 Biosensor calibration

(a) Determination of substrates



A biosensor can be calibrated by varying the substrate concentration as shown in Figure 3.6. The biosensor has a linear range for H₂O₂ concentrations between 1.3 x 10⁻³ M and 3.6 x 10⁻³ M. The curve flattens out on both sides of the linear zone. The upper plateau corresponds to high concentrations of H₂O₂ ([S] >> K_m), a situation which saturates the active sites of the enzyme while the lower plateau corresponds to the detection limit of the transducer. The important part of the curve is usually the linear range where variation in substrate concentration gives a variation in the current. The slope of the curve in the linear zone corresponds to the sensitivity of the biosensor because it expresses a variation in the signal obtained as a function of the analyte concentration.

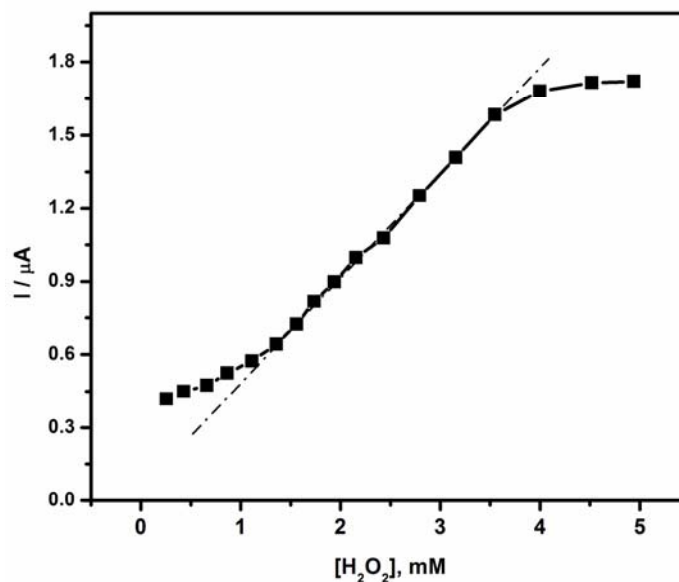


Figure 3.6. Calibration of an amperometric enzyme electrode for H₂O₂.

(b) Determination of inhibitors

Inhibitors reduce the signal of a biosensor by reducing the activity of the immobilized enzyme on the transducer. This modifies a biosensor calibration curve that is plotted as a function of substrates concentration. The curve is usually displaced according to the mode of inhibition. When an enzyme biosensor is intended for the determination of a species that inhibits an enzymatic reaction, the substrate concentration is fixed at a given value, and the inhibitor concentration is varied (Tran-Minh, 1993). The inhibitor is added in increasing concentrations to determine the percentage inhibition at various concentrations. For reversible inhibitors, the indirect determination of the inhibiting effect and the inhibitor concentration, respectively, involves at least three stages:

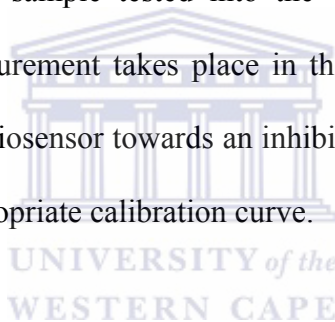
- i. Determination of the enzymatic activity by measuring the initial response of the biosensor to the enzyme substrate;
- ii. The contact of a biosensor with an inhibitor solution (incubation stage). For reversible inhibitors, the inhibition procedure is usually performed in the presence of the substrate and the resulting decay of the enzyme activity and of the response of the biosensor increase with the duration of the contact (i.e. with the time of incubation);
- iii. The repeated determination of a reduced response of the biosensor followed by calculation of the inhibition degree as the relative decrease of the response value. The inhibition degree (percentage inhibition, $I\%$) is calculated as follows:


$$I\% = \frac{I_0 - I_i}{I_0} \times 100 \quad (3.3)$$

where I_i and I_0 are the current differences obtained for the biosensor in the presence and absence of an inhibitor respectively. The advantage of using $I\%$ is its dimensionless character.

Enzyme biosensors are capable of determining a compound directly in a sample or analyte medium (the batch method). Figure 3.2 illustrates an example of direct measurement in a batch system using an enzyme electrode and its associated analytical apparatus. In this method, the volume of the sample may vary a great deal,

with a minimum of a few microlitres. If the volume is too small, however, the consumption of the substrate by the enzyme biosensor may result in a drift in its response. The sample medium can simply be changed by rinsing the biosensor. It is desirable to place the sample in a measuring cell that allows the normal working conditions of the biosensor such as pH and temperature to be achieved. The direct measurement is generally more useful for studying the response time, plotting the calibration curve and calculating the detection limit of the biosensor. In this study, the direct determination of the inhibiting effect of the herbicides was achieved by injecting the inhibitor or sample tested into the working solution after substrate addition so that the measurement takes place in the presence of the substrate. The sensitivity of an enzyme biosensor towards an inhibitor is also defined as the slope of the linear zone of the appropriate calibration curve.



3.3.2 Other techniques

3.3.2.1 Fourier transform infrared (FTIR) spectroscopy

The FTIR spectra were recorded on a PerkinElmer Spectrum 100, FT-IR spectrometer. The specimen were prepared by first electrodepositing doped or undoped PDMA on the gold electrode surface, then immobilizing HRP onto PDMA-PSS (in the case of HRP/PDMA-PSS films), followed by scrapping them gently from the electrode surface. The spectra of the specimen were recorded in the region 400-4000 cm^{-1} directly without mixing with KBr. The spectra obtained were used to

identify the various functional groups in the polymer as well as those in the backbone chain of HRP.

3.3.2.2 Ultra violet-visible (UV-Vis) spectroscopy

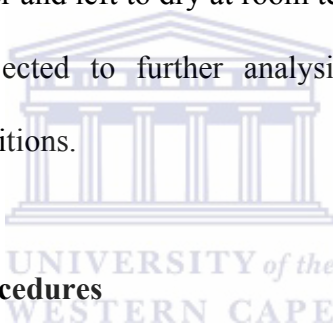
The UV-Vis spectra were recorded on a Nicolet Evolution 100 Spectrometer (Thermo Electron Corporation, UK). After electrodeposition of doped or undoped PDMA and immobilization of HRP onto the PDMA-PSS (in the case of HRP/PDMA-PSS films), the samples were dissolved in DMF, placed in 4 cm³ quartz cuvettes and their UV-Vis spectra recorded. Free HRP sample was dissolved in PBS, pH 6.10 and its spectrum recorded. The spectra were recorded in the region of 300-1000 nm. The obtained spectra were then used to characterize the absorption bands of the heme HRP as well as those of the polymers.

3.3.2.3 Transmission electron microscopy (TEM)

Transmission electron microscopy (TEM) image was acquired using a Hitachi H-800 electron microscope operated at acceleration voltages of 175 keV. It was used to characterize the morphology of PDMA-PSS. The specimen was prepared by dispersing the particles of the electrosynthesized PDMA-PSS in N, N-dimethylformamide, placing a few drops of the particle solution onto carbon films, then leaving the films to dry at room temperature for about 30 min.

3.3.2.4 Scanning electron microscopy (SEM)

Scanning electron microscopy was used to characterize the morphology of PDMA, PDMA-PSS and that of HRP immobilized on the PDMA-PSS film. The images were acquired using either a Gemini LEO 1525 Model or a Hitachi X-650 analyzer employing the secondary electron (SE) mode with interchangeable accelerating voltages of 25 kV. Screen-printed carbon electrodes were used for electrodeposition of samples for SEM analysis. After electrodeposition of samples, the electrodes were rinsed with deionized water and left to dry at room temperature for about 30 min. The same samples were subjected to further analysis by EDX to determine their percentage atomic compositions.



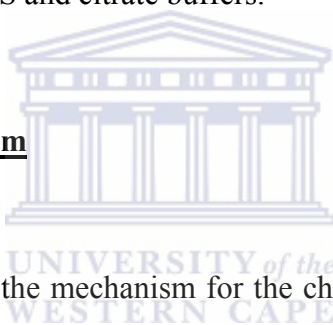
3.4 Electrochemical procedures

3.4.1 Electrochemical synthesis and characterization of poly(2,5-dimethoxyaniline) doped with poly(4-styrenesulfonic acid) (PDMA-PSS)

Poly(2,5-dimethoxyaniline) nanostructures (nanofibers, nanoparticles and nanotubes) were synthesized electrochemically by the soft-template ('template-free') method using the dopant and structure-directing molecule PSS. 0.1 M 2,5-dimethoxyaniline (DMA) in 1.0 M HCl solution was electropolymerized on gold disk electrodes in absence and presence of PSS (DMA-PSS ratio of 2:1) by cycling the potential repeatedly from -0.2 to +0.8 V using cyclic voltammetry (CV) mode, at a scan rate of

40 mV s⁻¹ for 7 cycles. After electropolymerization, the gold electrodes coated with PDMA or PDMA-PSS films were rinsed with 1.0 M HCl. The same electrochemical synthesis procedure was employed for the deposition of the polymer on screen-printed carbon electrodes for SEM analysis. The electrochemical behaviour of the gold electrodes coated with nanostructured PDMA-PSS films (PDMA-PSS/Au electrodes) were then investigated in 1.0 M HCl solution by cyclic voltammetry (CV) at various scan rates in the potential range between -0.2 and +0.8 V. The electrochemical behaviour and redox properties of the PDMA film was investigated at various pH values in PBS and citrate buffers.

Polymerization mechanism



It is generally agreed that the mechanism for the chemical/electrochemical oxidative polymerization of aniline related monomers is similar to that of aniline (Bejan & Duca, 1998). The proposed mechanism for the electrochemical synthesis of nanostructured PDMA in absence and presence of a dopant anion is therefore illustrated in Fig. 3.7. During electrochemical synthesis, the DMA monomers at the gold electrode surface undergo oxidation to form radical cations that react with other DMA monomers or radical cations, forming nanostructured PDMA and PDMA-PSS chains on the gold electrode surface. The first step is the formation of the radical cation of DMA by oxidation on the gold electrode surface. This is followed by dimer formation as a result of coupling of radicals by the so-called “head to tail” reaction and elimination of two protons. The dimer (oligomer) formed is oxidized on the

electrode surface along with DMA. The radical cation of the oligomer couples with a DMA radical cation, resulting in propagation of the chain. The formed PDMA polymer is doped by the PSS (HA) present in the solution (step 4).

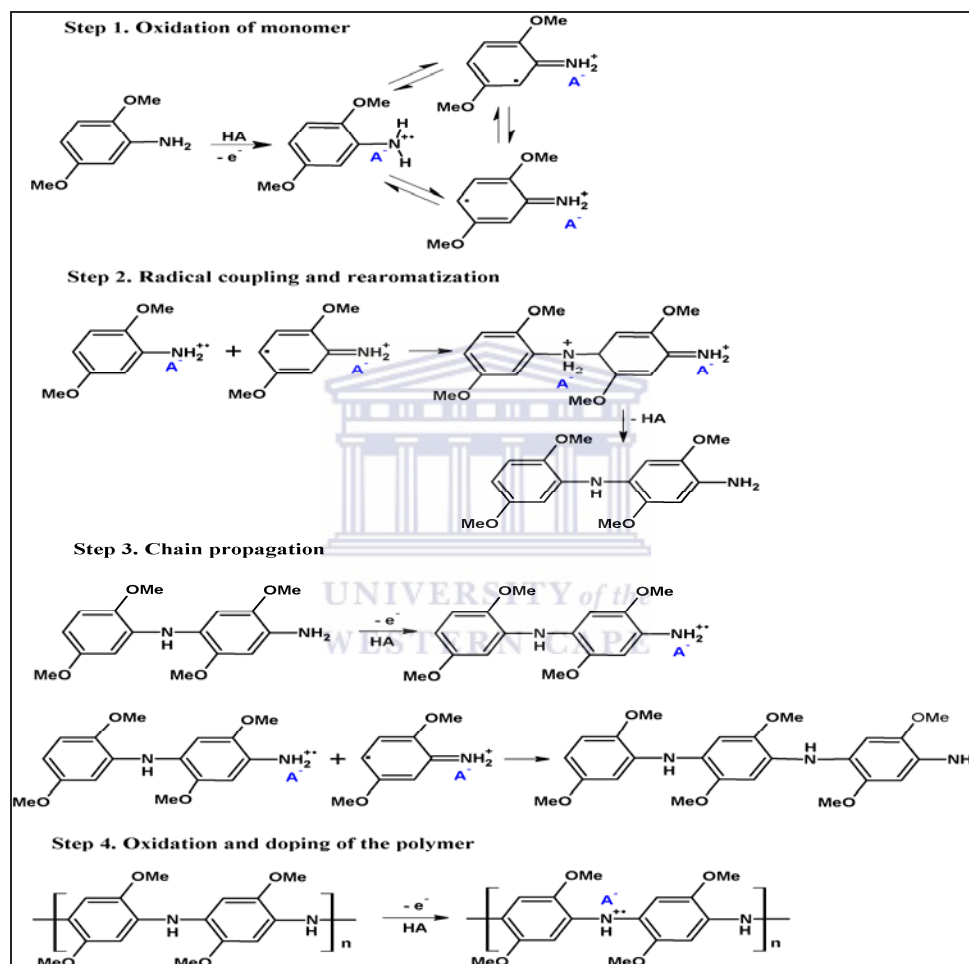


Figure 3.7. Electrochemical synthesis of nanostructured poly(2,5-dimethoxyaniline) in the presence of a dopant anion, A^- (PSS).

3.4.2 Preparation and characterization of the enzyme biosensor

Following electrodeposition of nanostructured PDMA-PSS film onto the gold electrode surface, the electrode was transferred to a 20 mL batch cell containing 5.0 mL PBS and the polymer surface reduced using time based modes at a constant potential of -0.5 V until the reduction attained steady state. 60 μL of 2.0 mg/mL or 4.0 mg/mL buffer solution of HRP was then added to the cell containing 1.0 mL fresh PBS and the PDMA-PSS film oxidized for 20 min at +0.65 V. During the oxidation process, the heme protein HRP became electrostatically attached onto the PDMA-PSS film. For RDE measurements, 600 μL of 2.0 mg/mL buffer solution of HRP was added to the cell containing 10 mL PBS and the procedure for HRP immobilization carried out. The biosensor was stored in PBS at 4 °C when not in use. The same procedure was applied for immobilization of HRP onto the surface of PDMA-PSS modified screen-printed electrodes used for SEM analysis. The electrochemical behaviour of the biosensor (HRP/PDMA-PSS/Au) electrodes were investigated by CV in the potential range between -0.6 and +0.2 V. The characterization by CV was carried out at various scan rates. The effect of pH on the direct electrochemistry of HRP/PDMA-PSS biosensor was investigated by CV in PBS at various pH values. Other biosensor parameters such as stability and sensitivity were investigated and optimized.

3.4.3 Detection of herbicides

3.4.3.1 Detection of glyphosate by cyclic voltammetry (incubation method)

Cyclic voltammetry was used to measure the responses of the HRP/PDMA-PSS biosensor to the substrate H_2O_2 before and after its incubation in glyphosate standard solutions at controlled room temperature of 22 °C. The biosensor was placed in PBS (pH 6.10), 0.7 μM H_2O_2 solution added and stirred then the initial response of the biosensor measured in a quiescent solution and recorded. The reduction current generated is proportional to the concentration of H_2O_2 before incubation of the biosensor in glyphosate standard solution and it is a measure of the activity of the immobilized enzyme. Various concentrations of glyphosate standard solutions were then added to the working PBS solution containing the 0.7 μM H_2O_2 while stirring, followed by incubation of the biosensor for 20 min after successive additions of glyphosate. The response of the biosensor was measured again in a quiescent solution after successive incubations and recorded. The current generated (after incubation of the biosensor) as a result of the reduction of H_2O_2 is correlated to the glyphosate concentrations. Glyphosate was added in increasing concentrations in order to determine the percentage inhibition at the various concentrations. From the data obtained, the percentage inhibition of activity of HRP, I %, corresponding to various concentrations of glyphosate were calculated using equation 3.3. Calibration curves representing the variation in current and the variation corresponding to the percentage inhibition (I %) with various inhibitor concentrations at a fixed concentration of

substrate were therefore plotted and information regarding the type of inhibition and the detection limit of the biosensor derived from the plots.

3.4.3.2 Amperometric detection of glyphosate, glufosinate and aminomethylphosphonic acid

- a) Amperometric detection of glyphosate and AMPA was carried out in PBS at applied potential of -0.28 V while stirring with a magnetic stirrer at 400 rpm. After background current reached a considerably steady value, an appropriate amount of H_2O_2 (0.01 M standard solution) was added to give a final concentration of 0.25 mM, and a steady state current (I_0) at this concentration recorded. Finally, increasing concentrations of standard solutions of glyphosate or AMPA were successively injected into the batch cell containing the working solution, and the steady state currents (I_i) produced recorded as response. Amperometric responses of the biosensor to H_2O_2 were measured before addition of the herbicides in order to measure the activity of the enzyme. This was followed by detection of the standard herbicide solutions in the presence of H_2O_2 . The decreased current (I_i), generated is proportional to the final concentration of the inhibitor in solution. The percentage inhibition of activity of HRP, $I \%$, corresponding to various concentrations of glyphosate or AMPA were calculated using equation 3.3. Calibration curves for the HRP/PDMA-PSS biosensor were plotted and used to determine the

sensitivity, linear range and the detection limits of the biosensor to glyphosate and AMPA.

- b) Amperometric detection of glyphosate and glufosinate was carried in PBS using RDE at 400 rpm and applied potential of -0.1 V. This potential was chosen because it is the potential at which the reduction of H_2O_2 occurred when HRP was immobilized on RDE. After background current reached a considerably steady value, an appropriate amount of H_2O_2 (0.01 M standard solution) was added to give a final concentration of 0.06 mM and a steady state current (I_0) at this concentration recorded. Finally, increasing concentrations of standard solutions of glyphosate or glufosinate were successively injected into the batch cell containing the working solution, and the steady state currents (I_i) produced recorded as response. The detection of the herbicide standard solutions took place in the presence of H_2O_2 . The decreased current (I_i), generated is proportional to the final concentration of the inhibitor in solution. The percentage inhibition of activity of HRP, $I\%$, corresponding to various concentrations of glyphosate or AMPA were calculated using equation 3.3. For the detection of glyphosate and glufosinate in samples, the spiked corn and soya bean samples were injected into the batch cell containing PBS and the measurement carried out in presence of the substrate. The currents produced were then recorded as response. Calibration curves for the HRP/PDMA-PSS biosensor were plotted from the data obtained

and used to determine the sensitivity, linear range and the detection limits of the biosensor to glyphosate and glufosinate

3.5 Graphing and data analysis

After collecting the data in an experimental setup using BAS Programs, OriginLab and SigmaPlot 8.0 software were used for graphing and data analysis.

3.6 Determination of the limit of detection (LOD)

The limits of detection (LOD) for the biosensor towards the substrate and inhibitors were calculated as:

$$LOD = \frac{3 \times \text{Standard Deviation (S.D.) of replicate analyses of the Blank}}{\text{Sensitivity}} \quad (3.4)$$

Sensitivity is defined as the slope of the linear calibration curve of the biosensor.

In the case of determination of analytes that are inhibitors of an enzymatic activity, the limit of detection can also be defined as the concentration of the inhibitor required to obtain 10-20% of inhibition considering the error of the measurements (Yang et al., 2004; Amine et al., 2006).

CHAPTER 4

Synthesis and Characterization of Poly(2,5-dimethoxyaniline) Doped with Poly(4-styrenesulfonic acid)

4.1 Introduction

As mentioned earlier, PANI and its derivatives have been studied extensively since its discovery in the 1980s. The interest in this material and its derivatives is mainly due to their interesting electrical and optical properties together with its chemical tunability, ease of derivatization, processability into fibres and films, as well as its stability. It has generally been agreed that the chemical/electrochemical oxidative polymerization of monomers of substituted aniline is similar to that of the parent (unsubstituted) aniline and that the properties of substituted PANIs including their nanostructures are similar to those of the parent PANI (Wallace et al., 2003; Bejan & Duca, 1998). During the past two decades, PANI has been synthesized and its chemical and physical properties studied extensively under different conditions, and tremendous advances in the chemistry, electrochemistry, physics, and processing of PANI have been achieved. However, solubility of PANI has been of concern and studies are now directed towards the improvement of its solubility. In light of this, attention is now diverted to synthesis of derivatized, doped or nanostructured PANI materials which are believed to produce soluble and more processable PANI for

various applications including biosensor applications. Although PANI is generally regarded to have three main stable oxidation states, i.e. *leucoemeraldine base (LEB)* form, *emeraldine base (EB)* form and the *pernigraniline base (PNB)* form, each of the above insulating base forms can be transformed into the corresponding *emeraldine salt (ES)* form either by redox doping or non-redox doping (cf. chapter 2).

In this study, the electrochemical synthesis of nanostructured (nanofibers, nanoparticles and nanotubes) poly(2,5-dimethoxyaniline) (PDMA) was achieved by the soft-template ('template-free') method in absence and presence of a structure-directing molecule, poly(4-styrenesulfonic acid) (PSS). The polyelectrolyte PSS acted as a dopant and a structure-directing molecule providing the template for the production of the nanostructured materials. Firstly, the properties of the synthesized PDMA and PDMA-PSS films in acidic and neutral conditions were investigated in order to lay a good foundation for the subsequent studies of the properties of PDMA-PSS film in neutral conditions and its potential biosensor application. The electropolymerization and doping properties of PDMA-PSS films were investigated by a combination of electrochemical techniques such as cyclic voltammetry (CV) and spectroscopic techniques such as Fourier transform infrared (FTIR) and UV-Vis spectroscopy and the results are presented in this chapter. In addition, transmission electron microscopy (TEM) and scanning electron microscopy (SEM) were used to investigate the morphology of the polymers and for estimation of their sizes. The undoped PDMA was used as a reference to study the effect of doping and to ascertain if doping indeed took place.

4.2 Electrochemical synthesis and characterization of PDMA-PSS

Electrochemical polymerization of the monomer 2,5-dimethoxyaniline on gold electrode surfaces in absence and presence of the polyelectrolyte PSS was achieved by cycling the potential repeatedly between -0.2 and 0.8 V at a scan rate of 40 mV s⁻¹ (cf. chapter 3, section 3.4.1). The cyclic voltammograms for the electrodeposition of PDMA and PDMA-PSS films on the gold electrode surfaces are shown in Fig. 4.1. The electrodeposition of PDMA on the gold electrode surface proceeds via a radical cation mechanism (cf. chapter 3, section 3.4.1). Two pairs of redox peaks centred at ca. 0.17 V (a/a') and 0.55 V (c/c'), corresponding to transition from leucoemeraldine to emeraldine and emeraldine to pernigraniline states (Morrin et al., 2005) respectively, were observed for both the doped PDMA (PDMA-PSS) and the undoped PDMA. This indicates the presence of discrete electroactive regions in the films. The origin of another pair of redox peaks observed at ca. 0.40 V (b/b') for both PDMA-PSS and PDMA is much more complex and it can be attributed to many different intermediates and degradation products (cross-linked polymer, benzoquinone, etc.) (Watanabe et al., 1989; Hong et al., 2005).

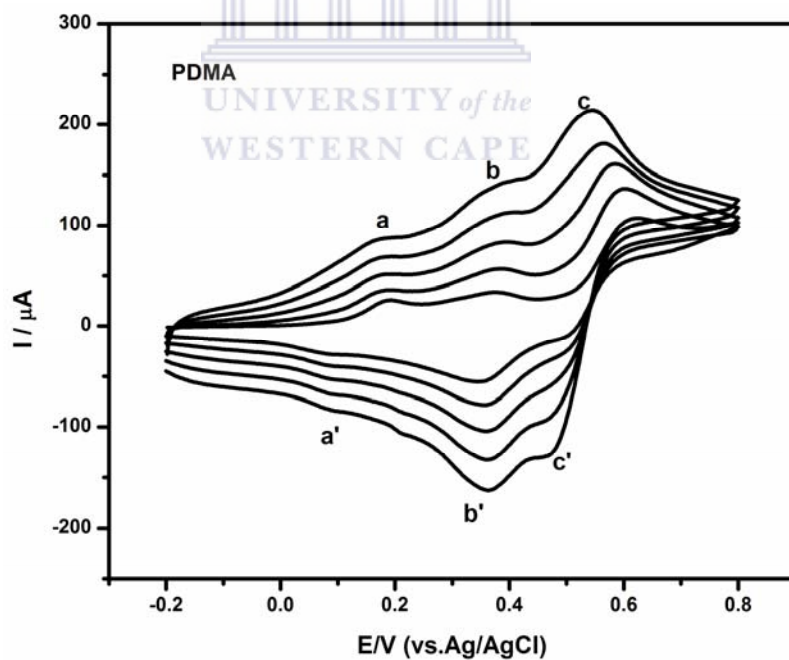
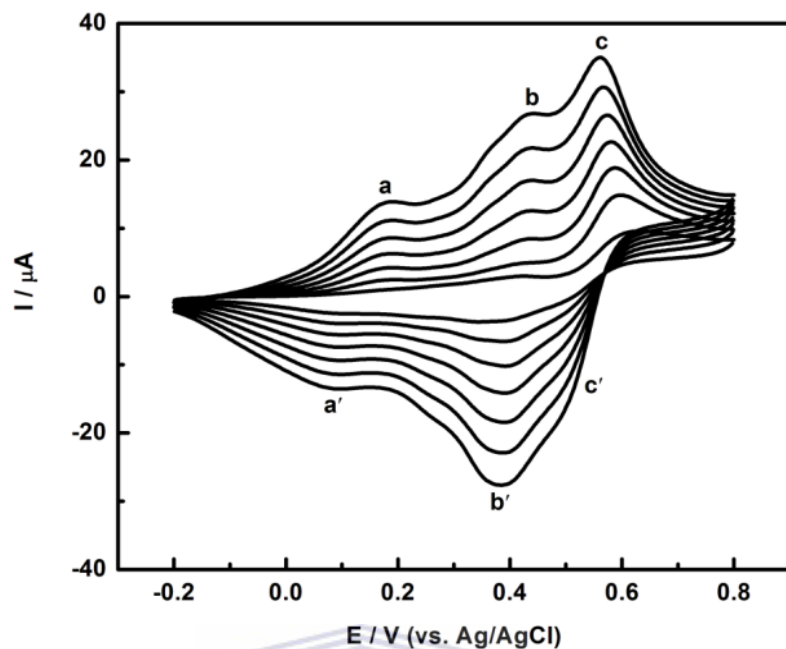
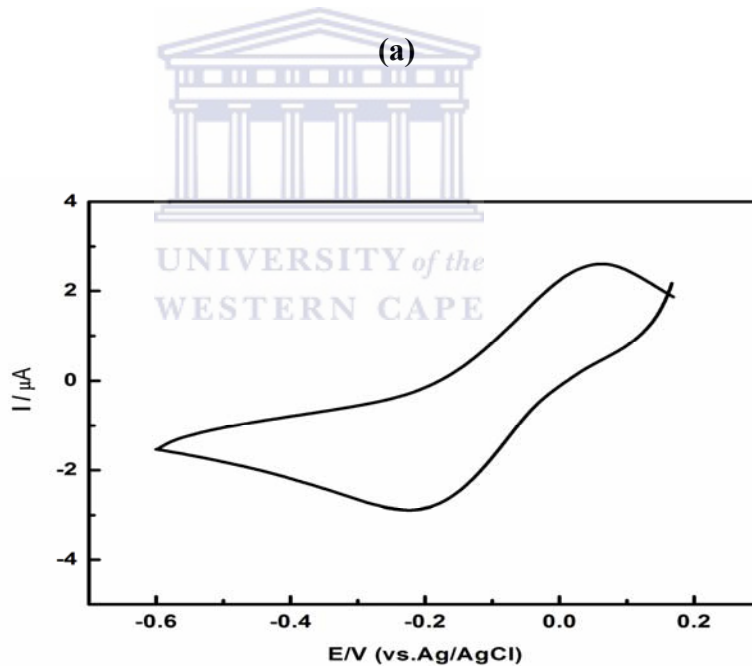
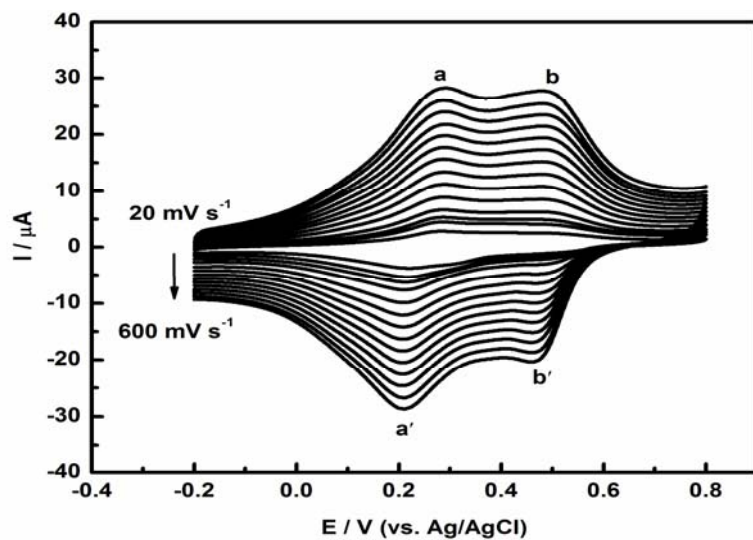


Figure 4.1. Cyclic voltammograms for electrochemical synthesis of (a) PDMA-PSS and (b) PDMA films in 1.0 M HCl at a scan rate of 40 mV s^{-1} .

The electrodeposited PDMA-PSS film was further subjected to characterization by CV in 1.0 M HCl at various scan rates and in 0.1 M PBS (pH 6.10) at a scan rate of 5 mV s⁻¹ and the results are shown in Fig. 4.2. Only two pairs of redox peaks centred at ca. 0.20 V (a/a', corresponding to the transformation of leucoemeraldine base to emeraldine salt) and at ca. 0.50 V (b/b', corresponding to transformation of emeraldine salt to pernigraniline salt) (Morrin et al., 2005) can be observed for the PDMA-PSS modified electrode in 1.0 M HCl (Fig. 4.2a). It was also observed that the peak currents increased with increase in scan rates while the redox peaks that correspond to incorporation of degradation products disappeared. These results confirm that PDMA-PSS film was successfully attached onto the gold electrode surface. PDMA being a PANI derivative, it reflects features and properties similar to those of PANI. The voltammogram for PDMA-PSS film in PBS (Fig. 4.2b) showed that it exhibited good electroactivity at pH 6.10 and within the potentials closer to 0 V which is the potential range mostly employed for studies of direct electron transfer of enzymes. This makes PDMA-PSS a perfect candidate for use as a mediator in enzyme biosensors. Broad redox peaks, with a large peak separation ($\Delta E_p = E_{pa} - E_{pc}$) of 0.2 V, are observed for PDMA-PSS film in 0.1 M PBS which may be attributed to the superposition of two redox processes usually observed for PANI in strong acidic solutions (such as those in Fig. 4.2a), i.e., a doping/dedoping and a deprotonation/protonation process. At low pH values, two separate redox peaks can clearly be seen (Fig. 4.2a). The redox peak at the low potential corresponds to the doping/dedoping process, while the one at higher potential corresponds to the deprotonation/protonation process which is highly pH dependent.



(b)

Figure 4.2. Cyclic voltammograms of electrodeposited PDMA-PSS film in (a) 1.0 M HCl solution at scan rates 20-600 mV s^{-1} and (b) 0.1 M PBS (pH 6.10), scan rate of 5 mV s^{-1} .

4.3 Spectroscopic characterization of PDMA-PSS films

4.3.1 Fourier transform infrared (FTIR) spectroscopy

FTIR spectroscopy has been used extensively for characterization of conducting polymers in order to depict their conducting states as well as to ascertain their successful doping (Patil et al., 2004; Cataldo & Maltese, 2002). Doped PANI and its derivatives exist in the emeraldine salt forms which are essentially delocalized polysemiquinone radical cations whose stability is maintained by the presence of dopant anions. It is expected that the interaction between an organic polymer and the dopant would bring about structural and electronic modifications in their polymer backbone. The modifications manifest themselves in the appearance of new bands in the FTIR spectra of the polymers. This is due to the displacement of the positions of the double bonds leading to the formation of quinoid structures upon doping. It has been reported that the resultant dopant modification is independent of the dopant used and can serve as spectroscopic signatures for successful doping (Fernandes et al., 2005). The degree of electron delocalization in the polysemiquinone forms of the doped PANI is manifested by the appearance of the intense broad band at ca. 1150 cm^{-1} , which has been associated with high electrical conductivity and a high degree of electron delocalization in the polysemiquinone forms of the doped PANI (Kang et al., 1998). Other studies have reported the appearance of this band at ca. 1100 cm^{-1} and the authors associated it with the presence of polarons (Patil et al., 2004).

In this study, the electropolymerized PDMA and PDMA-PSS films were subjected to FTIR spectroscopy analysis to ascertain the incorporation of the dopant PSS during electropolymerization. The results were verified by comparing the FTIR spectrum of undoped PDMA with that of doped PDMA (PDMA-PSS). Figure 4.3 shows the FTIR spectra of PDMA and PDMA-PSS films. PDMA-PSS spectrum shows the introduction of PSS bands at 1170 cm^{-1} and 1050 cm^{-1} as a result of the asymmetric and symmetric stretching modes of the $-\text{SO}_2\text{-OH}$ group respectively (Cataldo & Maltese, 2002). This confirms successful doping of PDMA by PSS during electropolymerization. The appearance of the band close to 1100 cm^{-1} could be associated with the high electrical conductivity and a high degree of electron delocalization in the polysemiquinone forms of the doped PANI and PANI derivatives. Michira et al. (2007) observed the presence of the electronic band at ca. 1100 cm^{-1} when PANI was doped with anthracenesulfonic acid. This indicates that the dopant modification is indeed independent of the dopant used and can serve as a signature for successful doping. The PDMA-PSS film also shows a strong band at 1500 cm^{-1} due to the *para*-linked polymerization and confirms the presence of 1,4-amino (-NH-) substituted aromatic compound ($1525\text{-}1485\text{ cm}^{-1}$). This suggests that the anionic polyelectrolyte PSS, served a role of preferentially aligning the dimethoxyaniline monomers prior to polymerization promoting a more ordered *para*-linked reaction (Kim et al., 2007; Songa et al., 2009). The PDMA spectrum only the other hand shows two weak bands in the $1525\text{-}1485\text{ cm}^{-1}$ region suggesting that the monomers were not aligned prior to polymerization. As observed, PDMA-PSS spectrum shows the double bond character of C=N stretching frequency at 1663 cm^{-1}

suggesting that PSS played a role in doping the synthesized PDMA to the highly conducting emeraldine salt form (Kim et al., 2007). The presence of sharp duplex peaks at 1321 and 1251 cm^{-1} for PDMA-PSS is characteristic of C-O groups. The C-O duplex peaks for PDMA appear at 1330 and 1298 cm^{-1} but with lower intensity than that of PDMA-PSS.

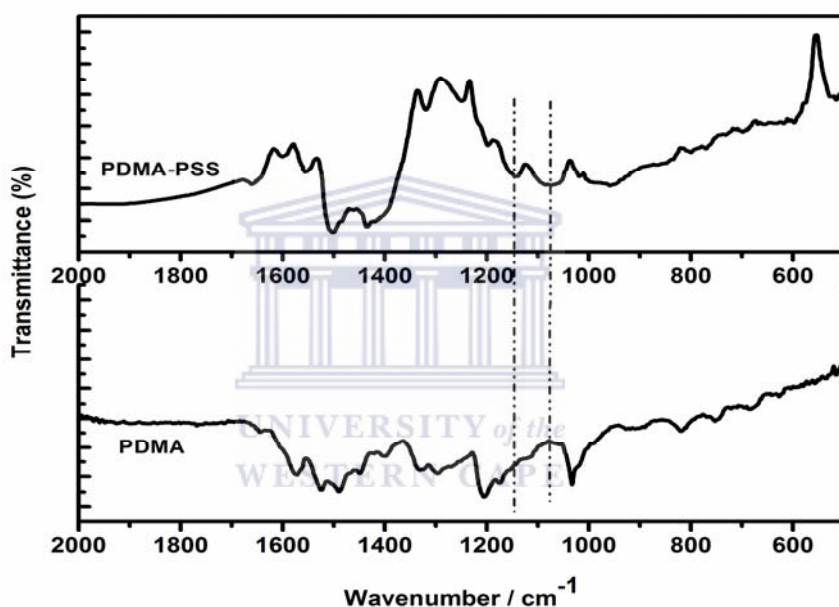


Figure 4.3. FTIR spectra of undoped PDMA and doped PDMA (PDMA-PSS) films.

4.3.2 UV-Vis spectroscopy

UV-Vis spectroscopy is a common technique that is used to give qualitative indication of the intrinsic redox states of conducting polymers. In this study, UV-Vis has been used to give an indication of the redox state of PDMA-PSS and to study the changes that occur as a result of doping. The electropolymerized PDMA and PDMA-

PSS films were dissolved in DMF and subjected to UV-Vis analysis. The UV-Vis spectra are presented in Fig. 4.4. Differences in the positions of absorption bands are observed when UV-Vis spectrum of undoped PDMA is compared with that of PDMA-PSS. The UV-Vis spectrum of PDMA-PSS film shows only one strong peak in the region ca. 800 nm due to the polaron $\rightarrow\pi^*$ band transition for emeraldine salt form of PANI. This confirms the effective doping of PDMA during electropolymerization. Michira (2007) also observed the same kind of behaviour for PDMA doped with naphthalene sulfonic acid (NSA) in which only one polaron band appeared at ca. 780 nm. This polaron band is a diagnostic test for the conformation of the PANI chains and it appears in the region 750-850 nm (Kim, et al., 2007). The undoped PDMA on the other hand displays a strong band at ca. 600 nm that is characteristic of emeraldine base. This can be attributed to a local charge transfer between a quinoid ring and the adjacent imine-phenyl-amine units giving rise to an intramolecular charge transfer exciton (Wallace et al., 2003).

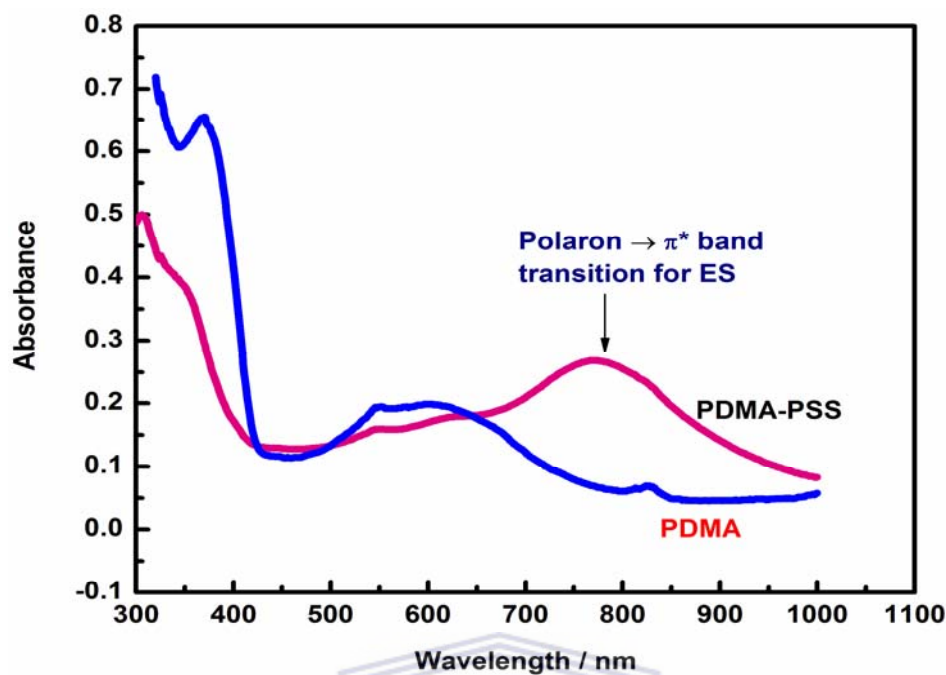
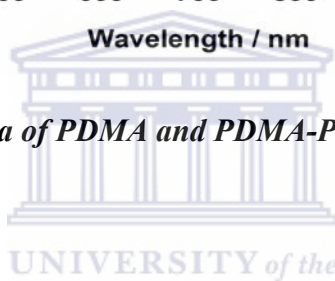


Figure 4.4. UV-Vis spectra of PDMA and PDMA-PSS films.



4.4 Characterization of PDMA-PSS by scanning electron microscopy (SEM) and transmission electron microscopy (TEM)

The chemical and electrochemical synthesis of PANI and PANI derivatives result in different kinds of morphologies depending on the synthesis conditions such as the nature of dopant, solvent used, synthesis temperature, the type of template used, the monomer: dopant ratio, synthetic route used etc. One-dimensional nanostructured PANI have mostly been synthesized by the use of hard and soft templates either chemically or electrochemically. On the contrary, the PANI nanoparticles can be synthesized chemically or electrochemically without employing templates. The

scanning electron microscopy (SEM) and transmission electron microscopy (TEM) images of the electrosynthesized PDMA and PDMA-PSS films are shown in Fig. 4.5. The SEM image of the PDMA film synthesized by the electrochemical “no-template” method i.e. without employing any template is shown in Fig. 4.5a. ‘Flower-like’ microfiber aggregates with diameters less than 200 nm are observed on the image. The SEM image of PDMA synthesized by the electrochemical “soft template” method (PDMA-PSS), employing the polyelectrolyte PSS to act as a structure-directing molecule shows globular morphology with buds of polymer having diameters less than 100 nm. As observed, there is a change in morphology when PSS is incorporated into PDMA (Fig. 4.5b) indicating that PSS played a role in directing the structure and morphology and aligning the monomers to form more ordered structures. The TEM image (Fig. 4.5c) of the PDMA synthesized by the electrochemical “soft template” method (PDMA-PSS) shows nanotubular structures with diameters ranging from 10-40 nm. This indicates that PSS can be used to direct the synthesis of both nanoparticles and one-dimensional nanostructured substituted PANI such as PDMA.

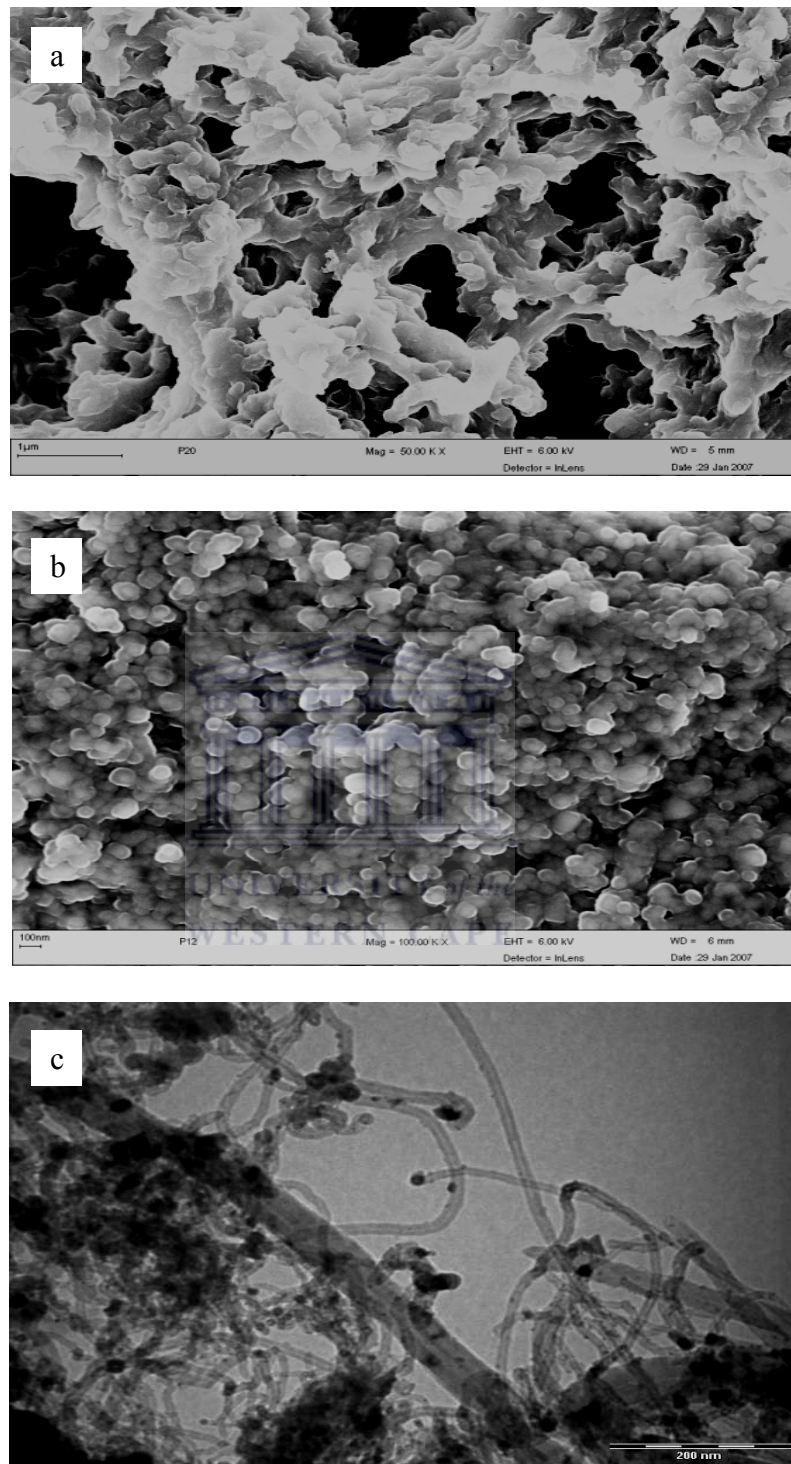
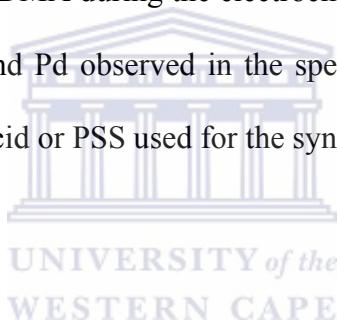


Figure 4.5. (a) SEM image of PDMA microfibers (b) SEM image of PDMA-PSS nanoparticles and (c) TEM image of PDMA-PSS nanotubes (magnification of 100 000 x).

The micro/nano-structured PDMA and PDMA-PSS films were then subjected to EDX analysis to determine the percentage atomic composition of the atoms present in them. By comparing the EDX spectra of undoped PDMA (Appendix A1) with that of doped PDMA (Appendix A2), it was possible to confirm that the doping successfully took place. PDMA exhibited percentage atomic compositions of 62.16 C, 16.39 O and 19.48 Cl whereas the PDMA-PSS spectra showed the introduction of 6.09 S as a result of doping with PSS. The other atoms present in PDMA-PSS were 63.95 C, 16.87 O and 8.20 Cl. The EDX results correlates with those of FTIR in confirming the successful doping of PDMA during the electrochemical polymerization. The trace amounts of Mo, Ga, Si and Pd observed in the spectra may have been due to their impurities present in the acid or PSS used for the synthesis of the polymer.



4.5 Conclusions

Nanostructured PDMA-PSS materials (nanotubes and nanoparticles) were successfully prepared by the electrochemical “soft template” method in which PSS acted as a dopant and provided the template for the synthesis of the nanomaterials. The results indicate that when PSS is used as a polyelectrolyte, it can direct the synthesis of both nanotubes and nanoparticles with diameters less than 100 nm. The spectroscopic techniques revealed that the PDMA-PSS materials exhibited properties similar to those of the parent doped PANI (unsubstituted) and they have backbone structures similar to that of the conventionally prepared granular doped PANI. Successful electrochemical doping was confirmed by the spectroscopic techniques as

well as EDX. The nanostructured PDMA-PSS materials synthesized by the electrochemical ‘soft template’ method also presented highly attractive features such as ease of synthesis, high solubility in N,N-dimethylformamide, good structural stability and conductivity in neutral pH which are suitable for their application as biosensor materials.



CHAPTER 5

HRP/PDMA-PSS Biosensor Characterization and Optimization

5.1 Introduction

The direct electron transfer between an electrode and a redox enzyme is very important for the fundamental studies and the construction of biosensors. However, because of the unfavorable orientation of the enzyme on the bare electrode surface or the adsorption of impurities that denature it, the enzyme often exhibits sluggish electron transfer at conventional electrode surfaces. As discussed earlier (cf. chapter 2, section 2.3), modification of the electrode surface using suitable compatible matrices are known to provide a favorable micro-environment for the protein to exchange its electrons directly with the underlying electrode and thus the study of enzyme electrochemistry can be achieved. Horseradish peroxidase (HRP) is an important heme-containing enzyme that has been studied for more than one century (Veitch, 2004). Although HRP has been intensively studied by electrochemical methods, its direct electrochemistry is relatively difficult to be investigated. As discussed previously (cf. chapter 2, section 2.3), the direct electron transfer of HRP at a bare electrode surface is usually very slow and difficult to observe. Therefore, a mediator is required to realize the direct electron transfer of HRP at an electrode

surface. Nanostructured conducting polymers and in particular, PANI and PANI derivatives have attracted much more attention with this regard in recent years especially in biological and chemical researches because of their biocompatibility. It is well-known that the nanostructured polymers possess interesting features including high electrical conductivity, stability, improved processability and solubility in a variety of solvents which are superior to those of the parent polymers. On the other hand, they can act as tiny conduction centers to facilitate electron transfer between the enzyme and the electrode surface. They are also known to provide a suitable micro-environment for enzyme immobilization during biosensor construction enabling direct communication between the immobilized enzyme and the electrode surface. In most cases, biosensors have been constructed by electrodeposition of nanostructured polymers onto the electrode surface, followed by electrostatic attachment of the enzymes to the polymer layers.

In this study, the interesting features of the nanostructured PDMA-PSS materials synthesized by the “soft template” method, such as ease of synthesis, good structural stability, conductivity in aqueous media at neutral pH and high solubility in N,N-dimethylformamide were investigated for their possible application as mediators in the construction of HRP/PDMA-PSS biosensor. After their electrodeposition on gold electrode surface, the model enzyme HRP was immobilized by the electrostatic attachment method resulting to an enzyme biosensor, HRP/PDMA-PSS. The direct electron transfer of HRP on nanostructured PDMA-PSS matrix was then investigated and the biosensor parameters characterized by cyclic voltammetry (CV), as well as

the spectroscopic techniques such as FTIR and UV-Vis spectroscopy. Finally, the biosensor operating parameters were studied and optimized then applied for the evaluation of its electrocatalytic activity for the reduction of H_2O_2 . This chapter therefore presents the results for the characterization of the HRP/PDMA-PSS biosensor as well as those for its optimization for the detection of H_2O_2 .

5.2 Spectroscopic analysis of PDMA-PSS and HRP/PDMA-PSS films

5.2.1 Fourier transform infrared (FTIR) spectroscopy

It is well known that the shapes and positions of the amide I and amide II infrared absorbance bands of proteins provide detailed information regarding the secondary structure of peptide backbone chain $\{-(\text{C}=\text{O})-\text{NH}-\}$ in both naturally occurring and artificial proteins (Li and Hu, 2003; Liu et al., 2005). The amide I band ($1700\text{-}1600\text{ cm}^{-1}$) is caused by $\text{C}=\text{O}$ stretching vibrations of the peptide linkages. The amide II band ($1620\text{-}1500\text{ cm}^{-1}$) results from a combination of N-H in plane bending and C-N stretching vibrations of the peptide groups (Sun et al., 2004). These two amide bands are sensitive markers for protein conformational changes. The sensitive technique widely used to probe into the secondary structure of the proteins is FTIR spectroscopy. Studies have shown that when enzymes are immobilized on substrates by electrostatic forces, there is usually a little change in their FTIR spectra (Kumar and McLendon, 1997; He et al., 2004). In this study, FTIR spectroscopy has been employed to probe into the secondary structure of HRP in order to evaluate its

interaction and compatibility with the PDMA-PSS film. The FTIR spectra for the free HRP and that of HRP/PDMA-PSS film are presented in Fig. 5.1. The results indicated that HRP did not denature and its integral structure was not altered during its immobilization onto PDMA-PSS/Au electrode. This conclusion was verified by comparing the FTIR spectra of free HRP with that of the HRP/PDMA-PSS film. Free HRP showed an IR signal at 1643 cm^{-1} for amide I band, and another one at 1528 cm^{-1} for amide II band (Fig. 5.1c), whereas the amide I band for HRP/PDMA-PSS film appeared at 1642 cm^{-1} and the amide II band at 1530 cm^{-1} (Fig. 5.1b). It was observed that PDMA-PSS did not show absorbance in the amide I and amide II band regions as those of HRP and HRP/PDMA-PSS. The IR peaks at 1642 and 1530 cm^{-1} for HRP/PDMA-PSS film were thus attributed to those of amide I and II bands of HRP indicating that the nanostructured PDMA-PSS film provided a biocompatible environment for HRP immobilization enabling it to retain its integral structure.

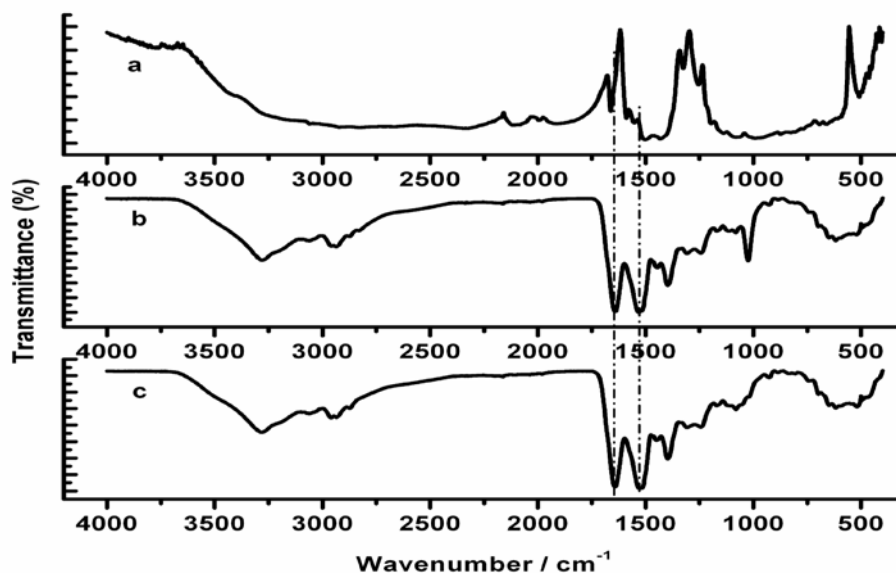


Figure 5.1. FTIR spectra of (a) PDMA-PSS film, (b) HRP/PDMA-PSS film and (c) free HRP.

5.2.2 UV-Vis spectroscopy

The position of the Soret absorption band of the heme provides information regarding the tertiary structure of heme proteins; especially with regards to conformational changes in the heme region (George and Hanania, 1953; Ma et al., 2007). UV-Vis spectroscopy is therefore an effective means for monitoring the possible changes of the Soret absorption band in the heme group region. Figure 5.2 shows the UV-Vis spectra of free HRP in PBS (pH 6.10) and that of HRP/PDMA-PSS film in PBS-DMF mixture. The Soret band for free HRP appears at 409 nm with high absorbance while for HRP/PDMA-PSS it is slightly shifted to 415 nm. The slight shift in the Soret band for HRP/PDMA-PSS and the decrease in its absorbance may be due to the interaction between PDMA-PSS film and HRP during immobilization. Such

interactions do not destroy the structure of the biomolecules, thus the results are an indication that HRP was successfully attached and retained its biological activity after immobilization on PDMA-PSS modified electrode. The spectrum of PDMA-PSS film does not show any absorption near absorption wavelength of HRP, thus the band of HRP/PDMA-PSS at 415 nm is entirely due to the HRP Soret band. This leads to the conclusion that the nanostructured PDMA-PSS film provides a suitable micro-environment for the immobilization of HRP and can be used as a mediator to aid its direct electron transfer on the gold electrode surface.

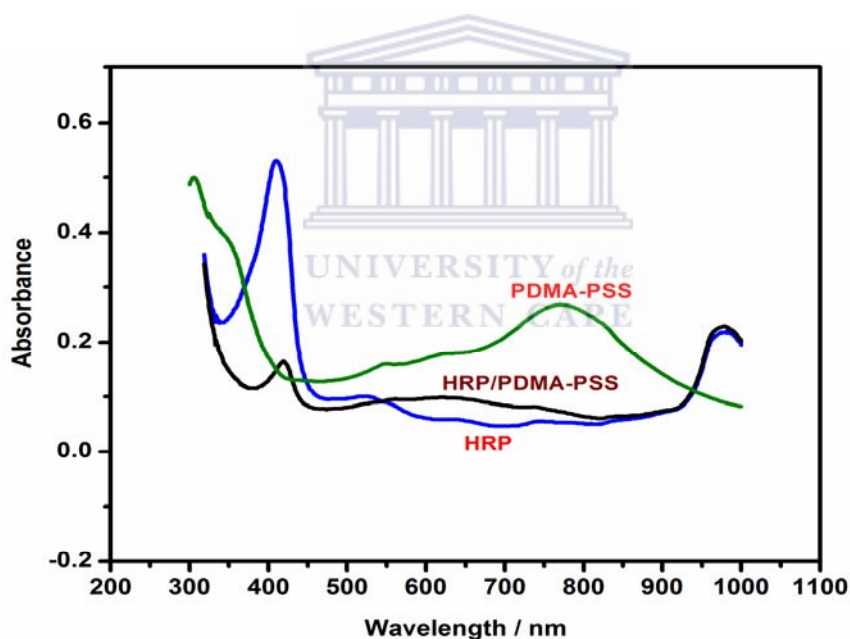


Figure 5.2. UV-Vis spectra for HRP in PBS pH 6.10, HRP/PDMA-PSS and PDMA-PSS films in PBS-DMF solution.

5.3 Direct electrochemistry of HRP and electrochemical characterization of the HRP/PDMA-PSS biosensor

After ascertaining that HRP was successfully immobilized on PDMA-PSS and that it did not denature during this process, the developed HRP/PDMA-PSS biosensor was subjected to characterization by CV. The cyclic voltammograms of HRP/PDMA-PSS biosensor in PBS (pH of 6.10) at various scan rates (2-10 mV s⁻¹) are shown in Fig. 5.3. It was observed that the cathodic peak potential (E_{pc}) shifted negatively while anodic peak potential (E_{pa}) shifted positively with increasing scan rate. The separation between the anodic and cathodic peak potentials ($\Delta E_p = E_{pa} - E_{pc}$) was calculated to be 248 ± 5 mV. The large peak separation observed for the biosensor is contributed by the redox process of PDMA-PSS in PBS that can be attributed to the superposition of its two redox processes usually observed in strong acidic solutions (cf. chapter 4, section 4.2). Hong et al. (2007) also observed a large peak separation of 256 ± 4 mV for HRP immobilized on Nafion-cysteine/Au electrode. This suggests that the materials onto which the enzymes are immobilized play a major role in determining the resulting features of the biosensor. At very high scan rates, the wave shape was distorted, and E_{pa} and E_{pc} values shifted to more positive and negative potentials. The peak currents increased linearly and were directly proportional to the scan rates (Fig. 5.3b), consistent with thin layer electrochemical behaviour (Murray, 1984). Additionally, the slope of the plot of log peak current versus log of scan rate was found to be 0.6 which is close to the expected value of 1, for redox processes that involve surface-bound species. Thus, it can be concluded that HRP immobilized on

the surface of the nanostructured PDMA-PSS film undergoes a quasi-reversible electrochemical reaction at lower scan rates.

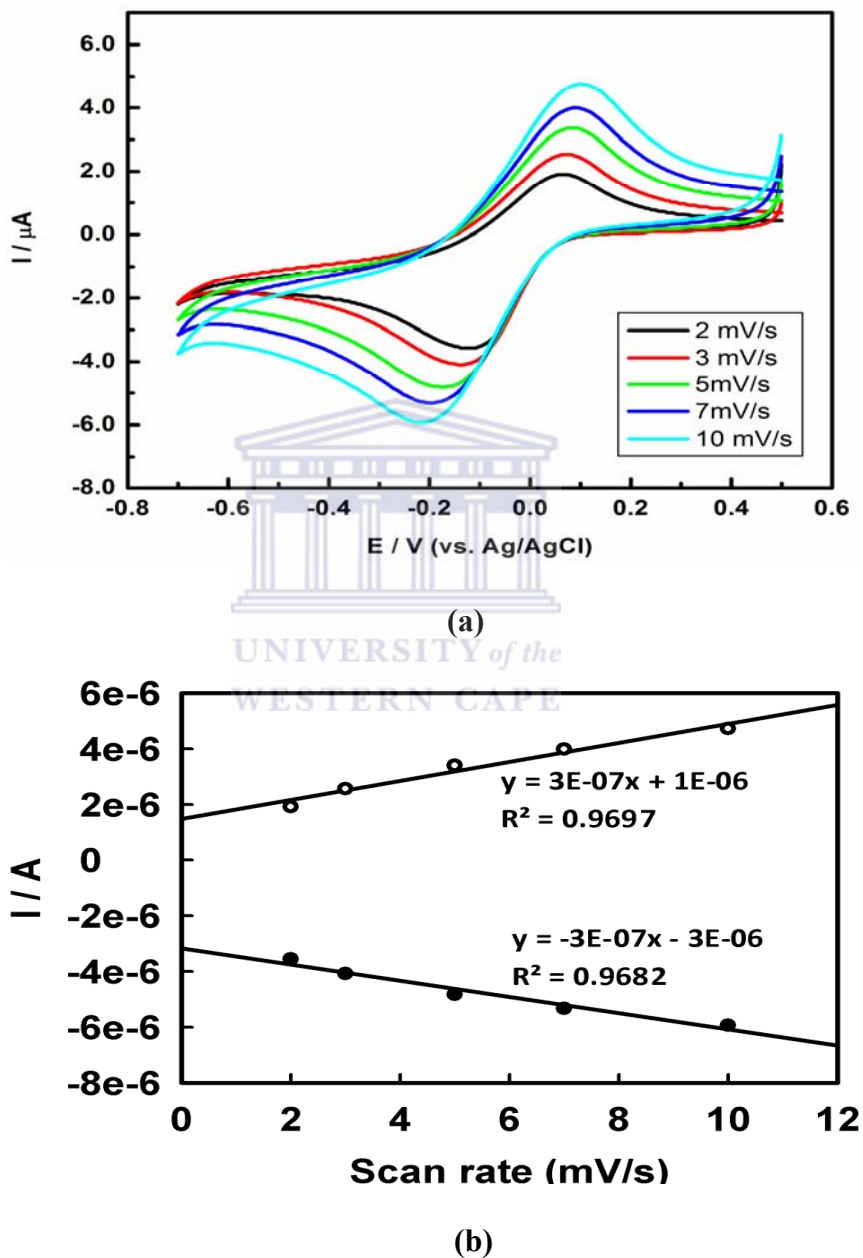


Figure 5.3. (a) Cyclic voltammograms of HRP/PDMA-PSS biosensor in PBS (pH 6.10) at scan rates 2, 3, 5, 7, 10 mV s^{-1} and (b) the plot of cathodic and anodic peak currents versus scan rates.

The solution pH is an important factor to consider during the study of electrochemical behaviour and direct electrochemistry of proteins. In this study, the formal potential (E°) of the redox couple was found to be dependent on the solution pH. Figure 5.4 shows the dependence of formal potential, E° (defined as the average of E_{pa} and E_{pc}) on the solution pH. E° shifted linearly to the negative direction with increasing pH from 5.51-7.96 with a slope of $-57.19 \text{ mV pH}^{-1}$. This value is in close agreement with the theoretical value of -58.5 mV pH^{-1} (at $22 \text{ }^{\circ}\text{C}$) for a proton-coupled single electron transfer electrochemical reaction (Sun et al., 2004). It suggests that a single protonation accompanies the single electron transfer between the PDMA-PSS/Au electrode and the heme Fe (III) of HRP. Thus, the redox reaction between the HRP and the gold electrode surface through the mediator PDMA-PSS is a single electron transfer process. The value estimated for the number of electrons, $n = 1$, was therefore used to calculate the surface concentration of electroactive HRP in the PDMA-PSS film.

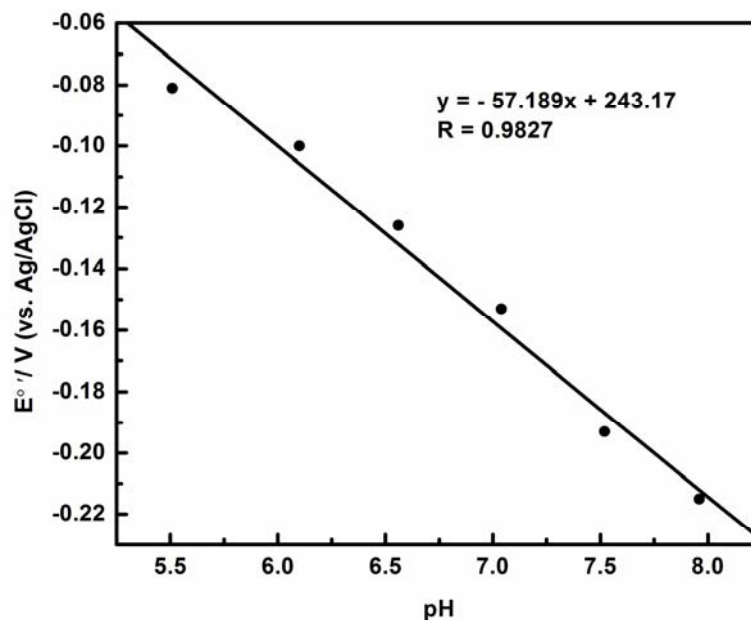


Figure 5.4. The dependency of the formal potential (E°) on the pH of PBS.

For thin layer electrochemical behaviour like that exhibited by HRP, the surface concentration (Γ) of its electroactive species in the mediator or promoter used can be deduced by integration of the peaks of the cyclic voltammograms of the biosensor and using Faraday's law according to the following equation (Hong et al., 2007):

$$I_p = \frac{n^2 F^2 A \Gamma \nu}{4RT} \quad (5.1)$$

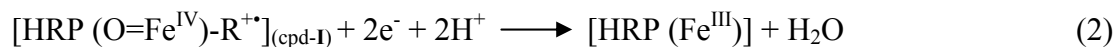
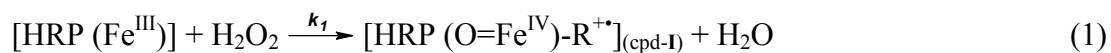
where I_p is the reduction (or oxidation) peak current, n is the electron transfer number, F is the Faraday constant (96493 C/mol), A denotes the geometric area of the working electrode (cm^2), ν is the scan rate (V s^{-1}), T is the temperature in Kelvin

and R is the gas constant ($8.314 \text{ J mol}^{-1} \text{ K}^{-1}$). Equation 5.1 illustrates the variation of peak currents with scan rates.

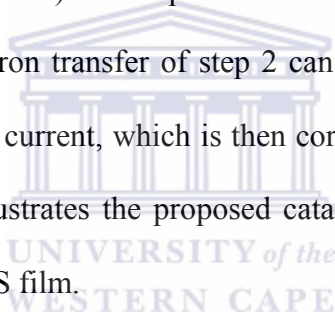
Considering that the integrated reduction peak of the cyclic voltammogram for the biosensor = $4.5755 \times 10^{-6} \text{ A}$, $\nu = 0.01 \text{ V s}^{-1}$, $T = 295\text{K}$, $A = 0.02 \text{ cm}^2$, and $n=1$, the surface concentration of the electroactive HRP in the PDMA-PSS film (Γ) was estimated to be $2.41 \times 10^{-8} \text{ mol cm}^{-2}$. The calculated value was found to be higher than the Γ value of $5.0 \times 10^{-11} \text{ mol cm}^{-2}$, reported for the saturated concentration of HRP in monolayer coverage (Liu et al., 2006; Xiao et al., 2000). This suggests that multiple layers of HRP were immobilized on the nanostructured PDMA-PSS film.

5.4 Investigation of the electrocatalytic activity of the HRP/PDMA-PSS biosensor

The electrocatalytic activity of the HRP/PDMA-PSS biosensor for the reduction of H_2O_2 was investigated by cyclic voltammetry and steady-state amperometry. Figure 5.5 shows the CV responses of HRP/PDMA-PSS biosensor to H_2O_2 in PBS (pH 6.10) at 5 mV s^{-1} . It was observed that when 0.4, 0.5 and 0.7 of μM H_2O_2 were successively added into the PBS solution, the biosensor showed remarkable increase in response and cathodic peak currents indicating that the immobilized HRP retained its bioelectrocatalytic activity and was not denatured. The electrocatalytic process can be expressed as follows (cf. chapter 2, section 2.3.1.3):



The direct (mediatorless) heterogeneous electron transfer from the bare electrode surface to the active site of the enzyme (step 2) is usually hampered by its low rate resulting from the deep burying of the electroactive groups within the protein structure due to unfavourable orientations of the molecules at the electrode surface and the long electron transfer distance between the electrode surface and the active site of HRP (Zhang et al., 2007; Ferapontova et al., 2002). In the presence of nanostructured PDMA-PSS film, the heterogeneous direct electron transfer of step 2 can be carried out at a reasonable rate. This results in a reduction current, which is then correlated to the concentration of H_2O_2 in solution. Figure 5.6 illustrates the proposed catalytic cycle of HRP immobilized on nanostructured PDMA-PSS film.



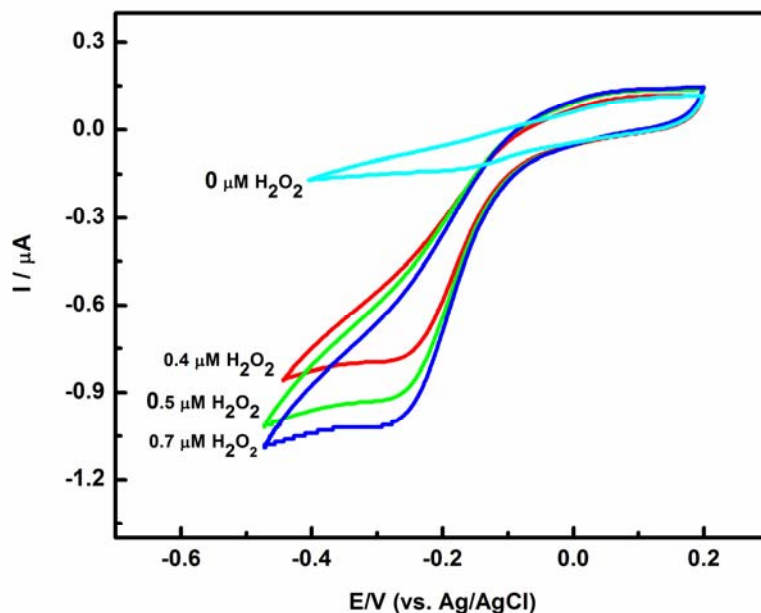


Figure 5.5. Cyclic voltammograms of HRP/PDMA-PSS biosensor in PBS (pH 6.10) in response to various concentrations of H_2O_2 at a scan rate of 5 mV s^{-1} .

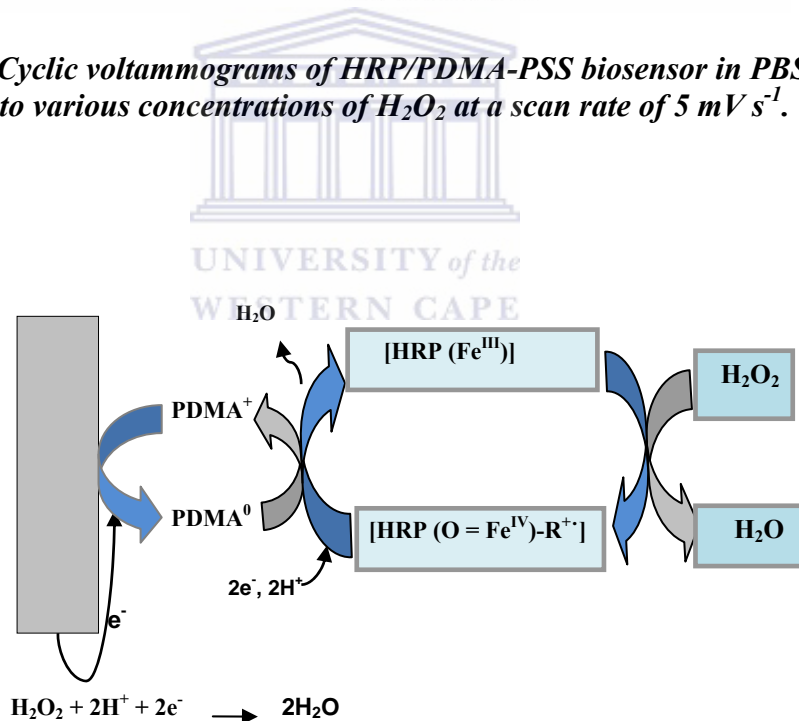


Figure 5.6. The proposed mechanism for the nanostructured PDMA-PSS/HRP biosensor in anaerobic medium. $\text{PDMA}^{0/+}$ are the nanostructured PDMA-PSS-bound redox sites.

It has been reported that the reduction of H_2O_2 starts at a potential close to the formal potentials of $\text{Fe}^{2+}/\text{Fe}^{3+}$ in the active centre of HRP, which were determined by potentiometric studies to be in the range of -0.15 to -0.64 V (vs. SCE, pH 6-7) (Sun et al., 2004). In this study, the reduction of H_2O_2 occurred at a cathodic peak potential of -0.28 V (Fig. 5.5) which is within the range of the formal potential obtained from other studies. This confirms that the immobilized HRP was responsible for the reduction of H_2O_2 . Hence, the potential of -0.28 V was selected as the optimized monitoring potential and was applied throughout this study when a magnetic stirrer was used to introduce convection into the solution. Figure 5.7 shows the typical steady-state amperometric responses of the HRP/PDMA-PSS biosensor to successive additions of H_2O_2 into PBS pH 6.10. Working and calibration curves are presented in the insets. Catalytic characteristics of the biosensor and increase in current illustrated in Fig. 5.7, were observed for successive additions of H_2O_2 into the electrolyte solution. A linear range from 1.0×10^{-7} - 7.0×10^{-7} M was observed for the biosensor ($r = 0.9995$), with a sensitivity of $5.0 \times 10^{-2} \mu\text{A} \mu\text{M}^{-1}$ and a detection limit of 3.5×10^{-8} M (based on equation 3.4) when low enzyme loading of 60 μL of 2.0 mg mL^{-1} buffer solution of HRP was used (Fig. 5.7a). When the enzyme loading was increased to 60 μL of 4.0 mg mL^{-1} , higher concentrations of H_2O_2 were used and therefore the biosensor exhibited a linear range of 5×10^{-5} - 2.5×10^{-4} M ($r = 0.9924$), sensitivity of 1.8 mA mM^{-1} and a detection limit of 5.8×10^{-9} M (Fig. 5.7b). Sensitivity is the slope of the linear calibration curves. It was observed that a higher detection limit could be achieved at higher enzyme loading though the sensitivity decreased at such

concentrations. The detection limits achieved by the HRP/PDMA-PSS biosensor were lower than most HRP biosensors for the detection of H_2O_2 . For instance, a detection limit of 4.01×10^{-7} M was achieved by Xu et al. (2006) when HRP was incorporated on carboxymethyl chitosan–gold nanoparticles modified electrode while that of 1.3×10^{-6} M was achieved by Hong et al. (2007) when HRP was incorporated on nafion-cysteine modified gold electrode. This indicates that the nanostructured PDMA-PSS materials played a role in enhancing the sensitivity and response of the biosensor due to their nano-sizes.



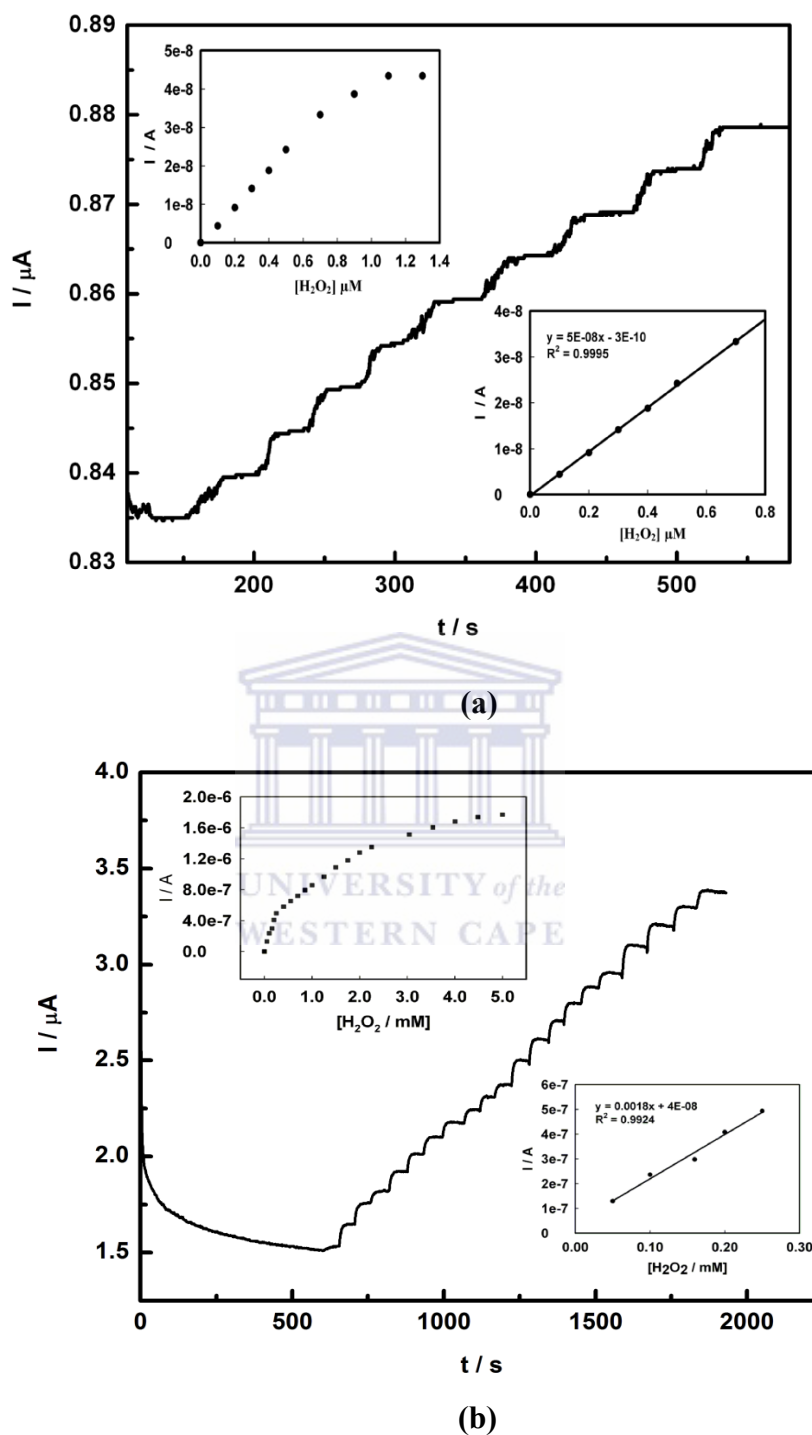


Figure 5.7. Biosensor responses to successive injections of H_2O_2 in stirring PBS (applied potential of -0.28 V). Insets are the calibration curves for the responses. In (a) $60 \mu\text{L}$ of 2.0 mg/mL and (b) $60 \mu\text{L}$ of 4.0 mg/mL buffer solution of HRP was used.

5.5 Response time of the HRP/PDMAP-PSS biosensor

As discussed in chapter 3, section 3.3.1.5.2.1, the response time of the biosensor is estimated as the time taken to reach 98% of its steady state current. The response time of the HRP/PDMA-PSS biosensor was calculated to be 17 ± 3.0 s ($n=10$) based on this estimation.

5.6 Reproducibility and stability of the HRP/PDMAP-PSS biosensor

It has been reported that the stability of the enzyme sensor increases with the enzyme concentration (Tran-Minh, 1993). When the membrane contains more active enzyme, the biosensor is more stable and has a longer lifetime. In this study, the long-term stability of the HRP/PDMA-PSS film was investigated by evaluating the response of the same biosensor (stored at 4 °C and at room temperature of 22 °C in PBS) to 0.1 mM H₂O₂. The biosensor containing more active enzyme was very stable at both temperatures, showed good response and there was no significant change in its catalytic activity during repetitive measurements over a period of one week. In addition, the biosensor could be used to perform up to three amperometric measurements with many additions of H₂O₂ such as those of Fig. 5.7b, with a decrease in current response by only 5% of the original value after one week. For reproducibility studies, amperometric responses of three HRP/PDMA-PSS biosensors (fabricated the same way) to H₂O₂ additions in the range of 0.05-0.25 mM were measured. The relative standard deviation for the repeat measurements was found to

be less than 5%. The stable electrocatalytic activity and sensitivity of the HRP/PDMA-PSS/Au electrodes used in this study was certainly facilitated by the good mediating capabilities of the conducting nanostructured PDMA-PSS films capable of fast electron transfers.

5.7 Conclusions

Nanostructured PDMA-PSS film proved to be an attractive material for immobilization of HRP, promoting its direct electron transfer on gold electrode. The FTIR and UV-Vis results indicated that the protein HRP immobilized on PDMA-PSS film retained its bioelectrocatalytic activity towards the reduction of H_2O_2 and was not denatured. This proves that the immobilization procedure used in this study allows for the construction of stable enzyme membranes. It also proves that the PDMA-PSS film provided a suitable microenvironment for immobilization of HRP and is therefore suitable for the construction of HRP/PDMA-PSS biosensor for the detection of the herbicides. The high sensitivities achieved with this biosensor can allow sensitive detection of the selected herbicides at low concentrations.

CHAPTER 6

**Application of HRP/PDMA-PSS Biosensor for the Detection of
Herbicides**

6.1 Introduction

As mentioned earlier (cf. Chapter 2, section 2.3.1.4), the ability of certain substances to inhibit the catalytic activity of enzymes can be exploited for their detection and quantification in the so-called enzyme-inhibition biosensor. In this study, the fact that herbicides suppress the activity of photosynthetic enzymes and peroxidases in plants has been exploited for the detection and quantification of glufosinate, glyphosate and its metabolite AMPA. An HRP inhibition-based biosensor has been constructed and evaluated for the detection of these herbicides. After the HRP/PDMA-PSS biosensor was constructed and optimized, it was placed into a three-electrode electrochemical cell into which the analytes and samples of interest were injected and determined. The electrodes were connected to a computer-controlled potentiostat and the determination of the herbicides glufosinate, glyphosate and AMPA achieved either directly using steady-state amperometry or by incubation method using cyclic voltammetry (CV). In both studies, the response of the biosensor before its contact with the herbicides was measured by investigating its biocatalytic activity towards the reduction of the substrate H_2O_2 . The response of the immobilized HRP to its substrate

H_2O_2 is a measure of its activity. The detection of the herbicides was carried out in the presence of a fixed concentration of H_2O_2 . This chapter presents the results of analysis of glyphosate, glufosinate and AMPA by HRP/PDMA-PSS biosensor employing voltammetric and amperometric techniques as well as those obtained from monitoring the interaction of HRP and the herbicides by SEM and FTIR techniques.

6.2 Detection of glyphosate by the incubation method

The detection principle used in this study was based on inhibition of the activity of the immobilized HRP by glyphosate. The estimation of inhibition degree or the effect of inhibitor concentration on the activity of the immobilized HRP involved measuring the decay of the biosensor after contact with glyphosate. The initial response of the biosensor, corresponding to its initial activity was measured followed by the measurement of its response after incubation in glyphosate phosphate buffer solution. Incubation was achieved as described in chapter 3, section 3.4.3.1. Incubation is the stage at which the biosensor is kept in contact with the inhibitor. It allows inhibition in spite of the low rate of complexation between the enzyme and the inhibitor. The effect of incubation time on the response of the biosensor was investigated and the results are shown in Fig. 6.1. Biosensor response was measured before and after incubation in $3.0 \mu\text{g L}^{-1}$ standard glyphosate buffer solutions in presence of $0.7 \mu\text{M}$ H_2O_2 for a period of 5 to 30 min. The percentage inhibition corresponding to incubation time was then calculated based on equation 3.3. Percentage inhibition increased with increase in incubation time while a decrease in biosensor response

characterized by a decrease in reduction current was observed. The percentage inhibition is indicated by the biosensor signal and the results in this study reveal that it is a function of the incubation time. It has been reported that an increase in incubation time leads to a higher degree of inhibition and favours the detection of the inhibitor at low concentrations (Tran-Minh, 1993). Inhibition by some pesticides requires a much longer time to reach an equilibrium state with the corresponding enzyme thus incubation is required to improve the detection limit (Tran-Minh, 1993). In order to obtain lower detection limits, incubation time that gives a percentage inhibition greater than 10% is usually preferred. In this study an incubation time of 20 min was selected for measurements and it was necessary also for the investigation of the type of inhibition by glyphosate. Once the type of inhibition by glyphosate (either reversible or irreversible) is established by measuring the biosensor response after incubation in subsequent glyphosate concentrations, it is possible to choose the detection method (either incubation or direct amperometry) suitable for its quantitative determination.

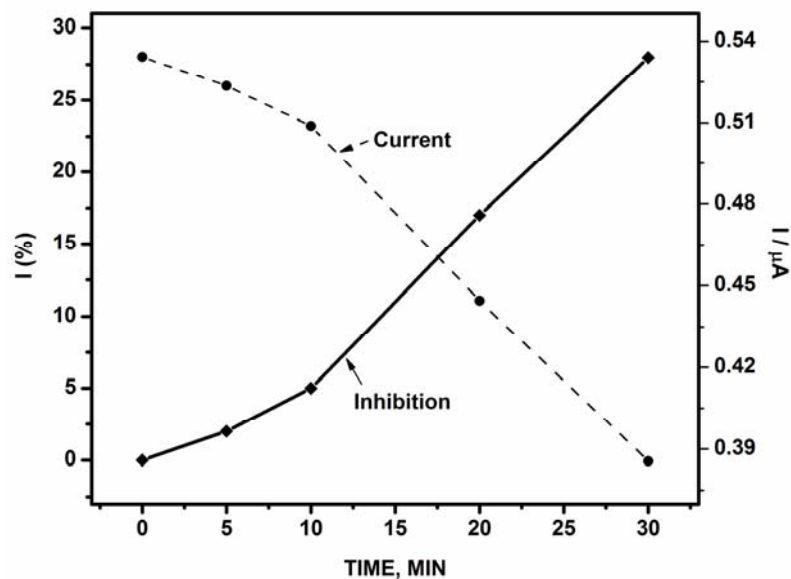
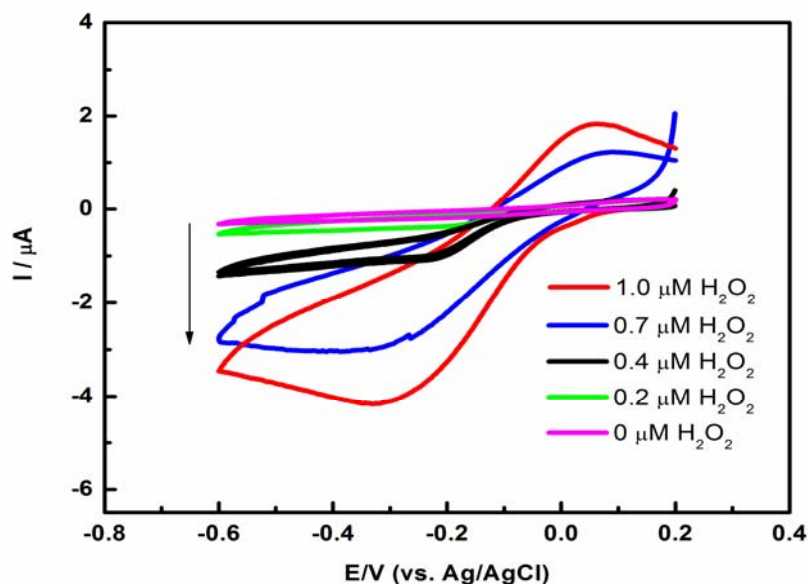


Figure 6.1. The effect of incubation time on the biosensor response and decay of enzyme activity.

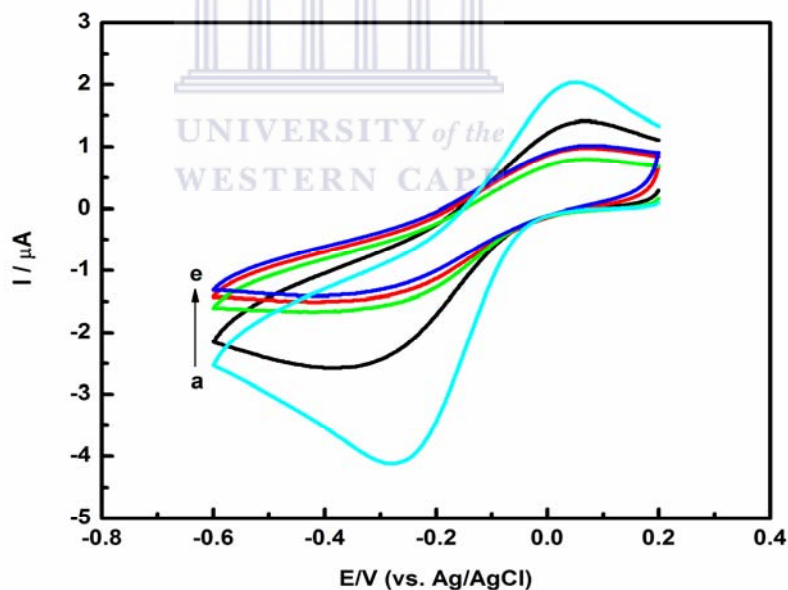
The responses of HRP/PDMA-PSS biosensor to H_2O_2 before and after incubation in subsequent concentrations of glyphosate standard solutions were investigated by CV and the results are illustrated in Fig. 6.2. Increase in cathodic peak currents were observed for successive additions of 0.2 – 1.0 μM H_2O_2 into PBS (Fig. 6.2A). The amount of H_2O_2 added during the inhibition studies must be within the linear range of the biosensor. This is because, when the substrate concentration is very high, the biosensor is no longer capable of determining the substrate but determines the inhibitor which may affect the maximal rate of the enzymatic reaction. The responses of the biosensor shown in Fig. 6.2B were measured after incubation in 0.25 -14.0 $\mu\text{g L}^{-1}$ glyphosate standard solutions in presence of 0.7 μM H_2O_2 . A decrease in cathodic peak currents and a reduction in biosensor response with increase in glyphosate

concentrations were observed. The fact that one biosensor could be used to perform five measurements presented in Fig. 6.2B suggests that glyphosate is a reversible inhibitor.

In order to obtain the glyphosate concentration that caused 50% inhibition or rate reduction (IC_{50}), the activity percent and percentage inhibition ($I\%$), were calculated and plotted against glyphosate concentrations as shown in Fig. 6.3. The percentage inhibition, expressed as a relative decay of the response value after contact of the biosensor with various concentrations of glyphosate was calculated using equation 3.3. It is observed that the IC_{50} value for both Fig. 6.3a and 6.3b is ca. $9.6 \mu\text{g L}^{-1}$. The percentage inhibition increased with increase in concentration of glyphosate and about $68 \pm 2.5\%$ of the activity of HRP was inhibited by $14.0 \mu\text{g L}^{-1}$ glyphosate. The detection limit for glyphosate by this method was found to be $1.70 \mu\text{g L}^{-1}$ ($0.01 \mu\text{M}$) based on the 10% inhibition degree described in section 3.6.



(A)



(B)

Figure 6.2. (A) Cyclic voltammograms of HRP/PDMA-PSS biosensor in PBS (pH 6.10) in response to various concentrations of H_2O_2 and (B) Cyclic voltammograms for the HRP/PDMA-PSS/Au electrode in PBS (pH 6.10) in presence of 0.7 μM H_2O_2 after incubation in 0.25, 6.0, 12.0, 13.0 and 14.0 $\mu\text{g L}^{-1}$ glyphosate solutions (a-e). Scan rate of 5 mV s^{-1} .

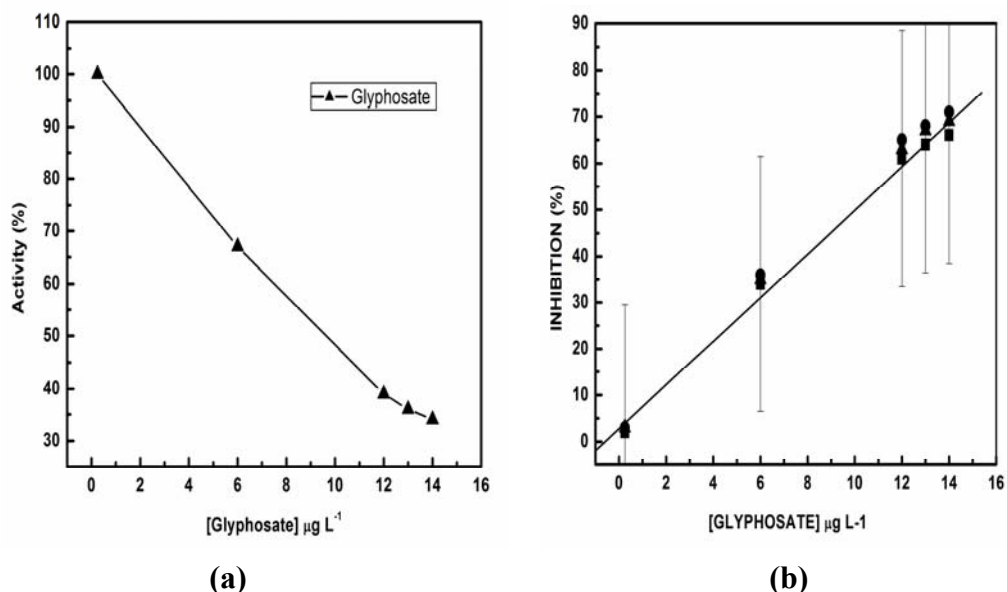
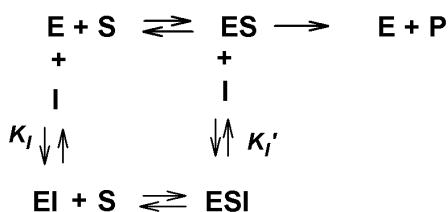


Figure 6.3. (a) The effect of inhibitor concentration on the activity of HRP and (b) Inhibition plot for the HRP/PDMA-PSS biosensor, data given as mean \pm S.D.

To study the type and kinetics of inhibition, the response of the biosensor to various concentrations of H_2O_2 was investigated by steady-state amperometry in absence and presence of $9.6 \mu\text{g L}^{-1}$ glyphosate (IC_{50} value) as shown in Fig. 6.4 and the data obtained used to plot a Lineweaver-Burk plot for the enzymatic reaction as shown in Fig. 6.5. The apparent Michaelis-Menten constant (K_m^{app}) is a reflection of both the enzyme affinity and the ratio of microscopic kinetic constants. It can be observed from the electrochemical version of the Lineweaver-Burk equation (Hong et al., 2007):

$$\frac{1}{I_{SS}} = \frac{1}{I_{max}} + \frac{K_m^{\text{app}}}{I_{max}[S]} \quad (6.1)$$

where I_{ss} is the steady-state current after addition of H_2O_2 , I_{max} is the maximum current measured under saturated substrate conditions and $[S]$ is the substrate concentration in the bulk solution. When I/I_{ss} is plotted against I/I_{max} , a straight line is obtained with a slope of K_m^{app}/I_{max} and a y-intercept of I/I_{max} ; hence both K_m^{app} and I_{max} can be obtained. From Fig. 6.5, the values of $K_m^{app} = 2.67 \mu M$ and $2.71 \mu M$ were derived for the HRP/PDMA-PSS biosensor in presence and absence of glyphosate respectively. The low K_m^{app} values obtained for the HRP/PDMA-PSS biosensor indicate a strong substrate binding. Since the K_m^{app} values are in close agreement with each other, it is concluded that it was unchanged during inhibition. The I_{max} values were calculated to be $0.18 \mu A$ and $0.12 \mu A$ in absence and presence of glyphosate respectively. This shows that inhibition by glyphosate decreases I_{max} . It is observed that the x-intercept remained the same with or without glyphosate. The general observations indicate that the inhibition of HRP by glyphosate is a non-competitive reversible type. The possible inhibitory mechanism for glyphosate can thus be deduced as:



where E represents the enzyme HRP, S represents the substrate H_2O_2 , I represents glyphosate and P is the product which in this case is H_2O . Non-competitive inhibitors bind equally well to both E and the complex ES (i.e., they have identical affinities for E and ES). This results in the formation of three complexes ES, EI and ESI, of which only ES can yield the product of enzymatic reaction, in this case it results into the formation of H_2O . The mechanism suggests that the binding of glyphosate to HRP does not affect the binding of H_2O_2 to HRP. There could be a possibility that glyphosate may be binding to a site different from that of H_2O_2 or it may be interacting with a site on HRP which is not its active site. The interaction between HRP and glyphosate is discussed at a later stage.

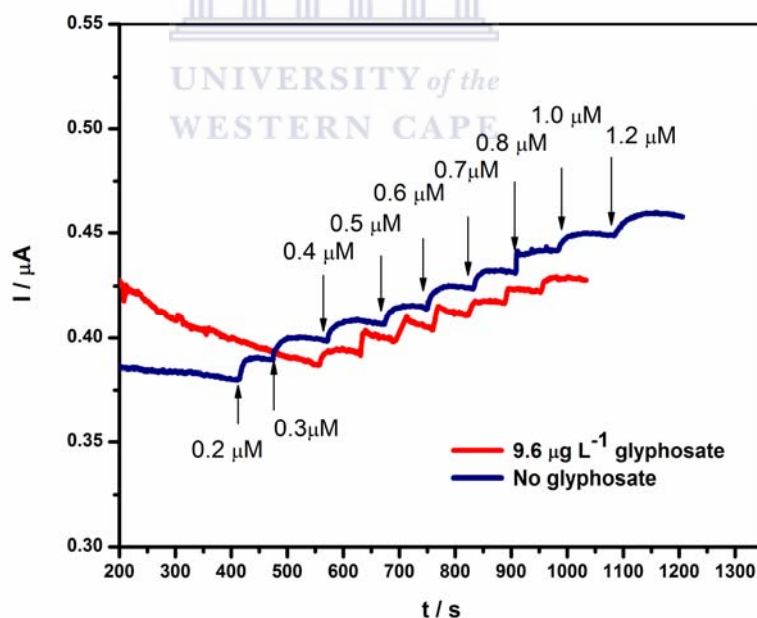


Figure 6.4. Biosensor responses to successive injections of H_2O_2 in absence and presence of $9.6 \mu\text{g L}^{-1}$ glyphosate, at applied potential of -0.28 V , in stirring PBS.

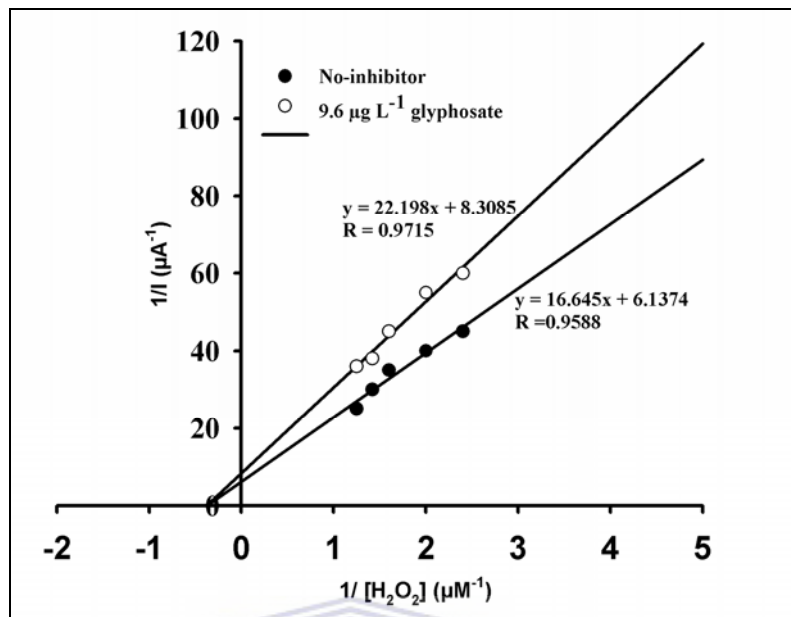
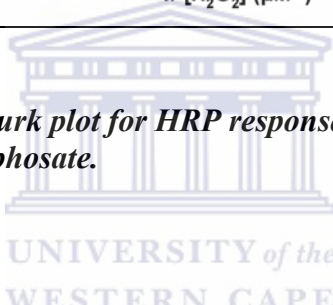


Figure 6.5. Lineweaver-Burk plot for HRP response to H₂O₂ in absence and presence of 9.6 µg L⁻¹ glyphosate.



6.3 Detection of herbicides by steady-state amperometry (direct method)

After establishing that glyphosate is a reversible inhibitor, experiments were performed to determine whether its detection can be achieved directly without incubation. This is based on the findings that the rate constant of the reaction between an enzyme (E) and a reversible inhibitor (I) is high and an equilibrium state with the complex EI can rapidly be achieved (Tran-Minh, 1993). It has been reported that the steady-state biosensor response for a given reversible inhibitor concentration does not depend on the incubation time when the enzyme is in contact with the inhibitor before the substrate is added (Tran-Minh, 1993). For instance, Yang et al. (2004) determined

sulfides directly without incubation using an amperometric HRP inhibition biosensor and a low detection limit was achieved by this method.

6.3.1 Glyphosate and aminomethylphosphonic acid standard solutions

Electrocatalytic responses of the HRP/PDMA-PSS biosensor to H_2O_2 were investigated by steady-state amperometry (at an applied potential of -0.28 V) under magnetic stirring in the presence and absence of glyphosate (or AMPA) standards in the test solutions. Figures 6.6A and 6.6B show the typical amperometric responses of the biosensor to H_2O_2 , glyphosate and AMPA standard solutions in PBS pH 6.10. Replicate experiments were performed and are denoted as Exp.1 and Exp.2 in Figs. 6.6A and 6.6B. Points a-b (Fig. 6.6A and 6.6B) correspond to successive additions of 0.05-0.25 mM H_2O_2 . Typical catalytic response of the biosensor, characterized by increase in reduction current as the concentration of H_2O_2 increases was observed, confirming the activity of the immobilized HRP. The biosensor was then applied for the detection of glyphosate and AMPA standards in the presence of 0.25 mM H_2O_2 . Points b-c in Fig. 6.6A correspond to additions of 2.0-80.0 $\mu\text{g L}^{-1}$ glyphosate standards into PBS while points b-c in Fig. 6.6B correspond to additions of 1.5-70.0 $\mu\text{g L}^{-1}$ AMPA standards. It was observed that the biosensor response reduced after successive injections of glyphosate or AMPA standards into the cell solutions leading to a decrease in the response signal (i.e. reduction current). This suggests that glyphosate and AMPA reduced the activity of the immobilized HRP. The decrease in

the response signal was found to be directly proportional to the concentrations of glyphosate and AMPA in the test solutions.

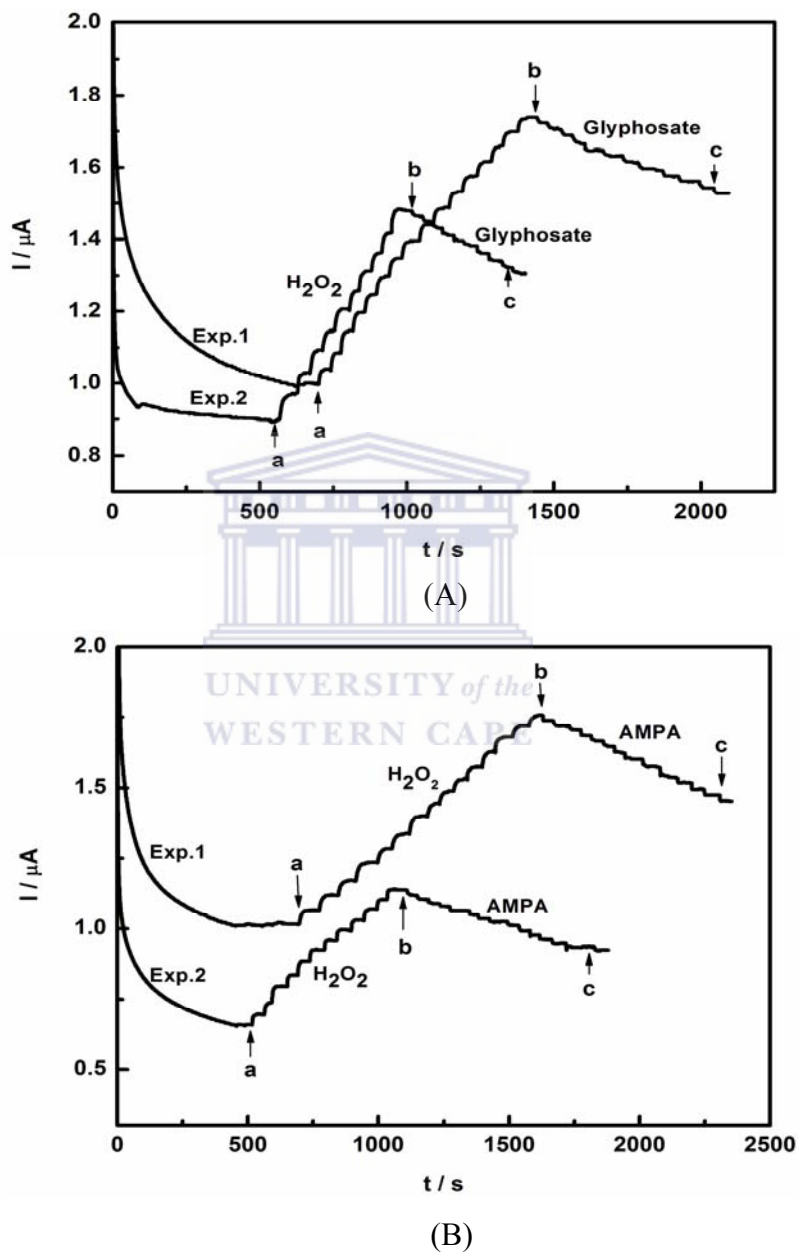


Figure 6.6. Biosensor responses to successive additions of (A) H_2O_2 (a-b) and glyphosate standard solutions (b-c) (B) H_2O_2 (a-b) and AMPA standard solutions (b-c) into PBS while stirring at 400 rotations per minute (rpm).

The results indicate that the detection of the reversible inhibitor glyphosate and its metabolite AMPA can be achieved directly without the incubation procedure which is time consuming. However, it has been observed that the degree of inhibition by this method is very low as compared to the incubation method. The inhibition plots for the HRP/PDMA-PSS biosensor obtained by the direct method using a magnetic stirrer are presented in Fig. 6.7. At glyphosate concentration of $14.0 \mu\text{g L}^{-1}$ only 8% of the enzyme activity had been inhibited as opposed to that of 68% achieved by the incubation method at the same concentration. This suggests that in order to obtain higher inhibition values by this method, higher concentrations of glyphosate must be added and this may require a long period of time. It was not possible to attain the IC_{50} value by this method in the experiments carried out in this study. Further optimization of the concentrations of added glyphosate may be required to achieve the IC_{50} value in order that the Lineweaver-Burk plot can be obtained and the K_m^{app} and I_{max} values calculated. The same behaviour was reflected by AMPA which is a metabolite of glyphosate and therefore the IC_{50} value was not achieved. The advantage of using this method is that it enables the biosensor to retain its activity for a longer period of time allowing many measurements to be carried out consecutively. Based on the experimental errors that would be encountered as a result of using very high concentrations or large volumes of glyphosate in order to achieve higher inhibition degree by this method, it is more appropriate to calculate the limit of detection using equation 3.4.

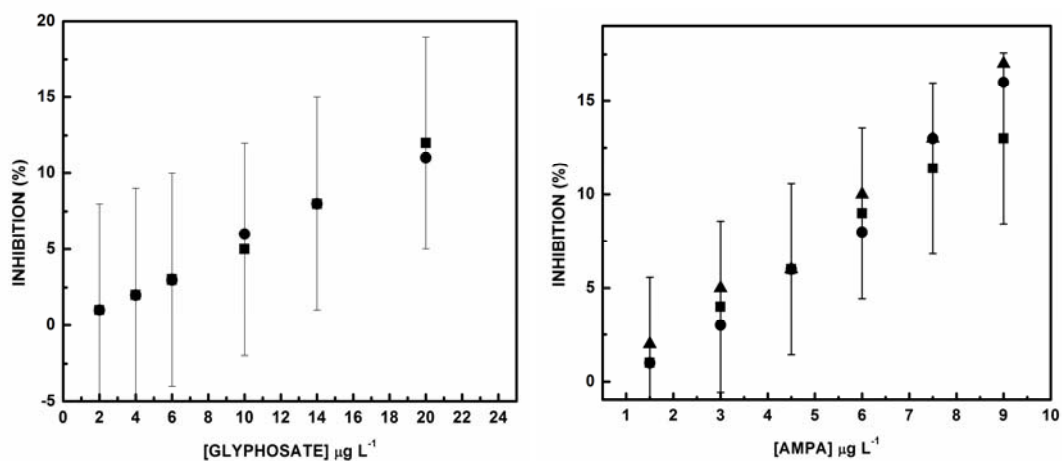


Figure 6.7. Inhibition plots showing the effects of glyphosate and AMPA on the activity of the immobilized HRP.

Using the amperometric responses obtained in the presence of glyphosate and AMPA, calibration curves (shown in Appendix A3) were plotted and used to calculate the biosensor parameters. The amperometric biosensor's dynamic linear ranges were 2.0-14.0 $\mu\text{g L}^{-1}$ for glyphosate and 1.5-7.5 $\mu\text{g L}^{-1}$ for AMPA, and nano-level sensitivities were obtained ($1.00 \pm 0.14 \text{ nA nM}^{-1}$ for glyphosate and $1.75 \pm 0.11 \text{ nA nM}^{-1}$ for AMPA, for two independent calibrations). Very low limits of detection ($0.16 \mu\text{g L}^{-1}$ for glyphosate and $1.0 \mu\text{g L}^{-1}$ for AMPA) were obtained by this method (based on equation 3.4). The reproducibility of this method was evaluated by plotting different calibration curves and using their slopes to determine the relative standard deviation (R.S.D). The low R.S.D of 5% obtained for the biosensor demonstrates that its response was highly reproducible. It was observed that the same biosensor could

be used consecutively for up to three amperometric measurements involving approximately 20 additions per measurement before surface fouling.

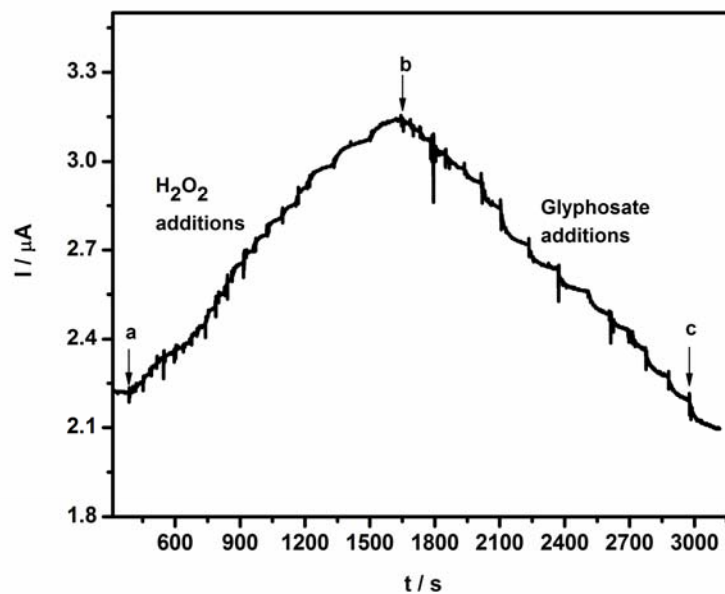
6.3.2 Detection of glyphosate and glufosinate by the rotating disk electrode

6.3.2.1 Glyphosate and glufosinate standard solutions

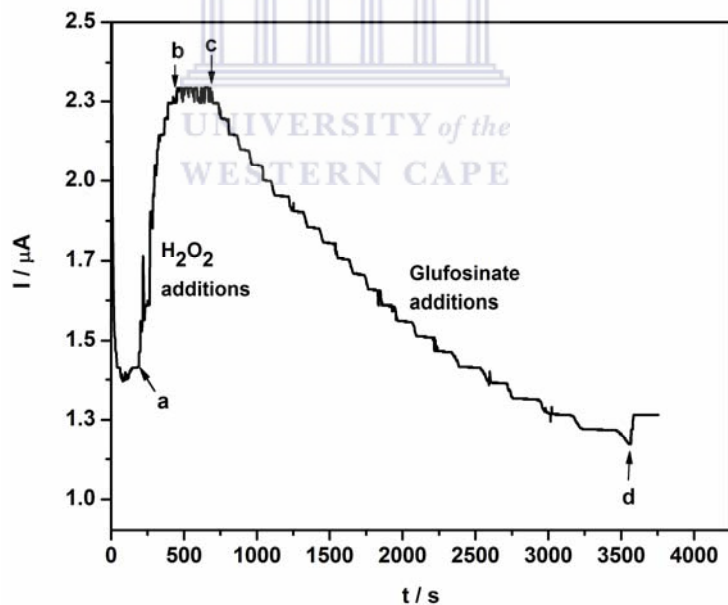
The procedure used in section 6.3.1 was applied for the detection of glyphosate and glufosinate except that a rotating gold disk electrode was used to introduce convection into the solution instead of a magnetic stirrer. The use of forced convection and in particular the rotating disk electrode is expected to enhance the sensitivity of the biosensor. Electrocatalytic responses of the HRP/PDMA-PSS biosensor to H_2O_2 were investigated by steady-state amperometry (at an applied potential of -0.1 V) in the presence and absence of glyphosate (or glufosinate) standards in the test solutions. The measurements of glyphosate and glufosinate standards were performed in the presence of 0.06 mM H_2O_2 . Typical amperometric responses of the biosensor to successive injections of glyphosate and glufosinate standard solutions, under RDE rotation of 400 rpm are illustrated in Fig. 6.8. Point b-c (Fig. 6.8A) corresponds to additions of 2.0-78.0 $\mu\text{g L}^{-1}$ glyphosate standards into PBS while point c-d (Fig. 6.8B) corresponds to additions of 2.0-70.0 $\mu\text{g L}^{-1}$ glufosinate standards. Point b-c in Fig. 6.8B corresponds to addition of blank solutions prepared the same way as the standard solutions. No significant change in current was observed when blank solutions were added. This shows that the decrease

in current or the inhibition of HRP was entirely due to the herbicides. After measurement of the biosensor response to H_2O_2 or H_2O_2 and blank, various concentrations of glyphosate and glufosinate standards were injected successively into PBS and their steady-state currents recorded as response. It was observed that the biosensor response reduced after injection of the herbicide standards into the solution leading to a decrease in signal production. The observed behaviour was similar to that reported in section 6.3.1 thus the detection of glyphosate and glufosinate by the RDE method could also be achieved without incubation.





(A)

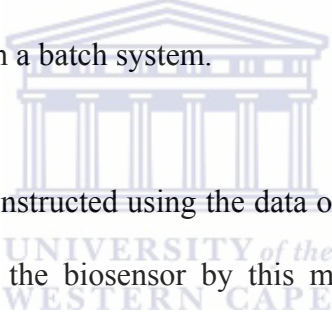


(B)

Figure 6.8. Biosensor responses to successive injections of (A) H₂O₂ (a-b) and glyphosate standard solutions (b-c) (B) H₂O₂ (a-b, d), blank solutions (b-c) and glufosinate standard solutions (c-d) into PBS under RDE rotation of 400 rpm.

Glyphosate depressed the HRP activity by 30% within 22 min after its addition to a final concentration of $78.0 \mu\text{g L}^{-1}$ while glufosinate depressed the HRP activity by 46% within 50 min at a final concentration of $70.0 \mu\text{g L}^{-1}$. Inhibition of HRP increased with increase in concentrations of the herbicides. At glyphosate concentration of $14.0 \mu\text{g L}^{-1}$, only 3% of the biosensor activity had been inhibited indicating that it could be used for a batch of experiments before its activity could be 100 % inhibited. Once again, the attainment of the IC_{50} value by this method requires higher concentrations or large volumes of standards to be injected into the detection solution. After contact of the biosensor with glyphosate for 22 minutes, the enzyme electrode was removed from the solution, rinsed with PBS and used for other sets of measurements. It was observed that the biosensor responded well to H_2O_2 after rinsing with PBS and the results obtained were consistent with those obtained previously in absence of glyphosate. When H_2O_2 was injected into fresh PBS an increase in reduction current was again observed. After addition of H_2O_2 to check the activity of the enzyme, the same procedure for addition of glyphosate was repeated as before and measurements taken. It was observed that the same biosensor could be used for over 60 measurements. After contact of the biosensor with glufosinate for 50 min, H_2O_2 was immediately injected into the solution and suddenly an increase in current was observed. This is illustrated at point d in Fig. 6.8B. This shows that not all the active sites of HRP had been blocked by glufosinate even after contact for 50 min. Alternatively, glufosinate could be binding to sites on HRP that are different from the binding sites for the substrate. This is because its binding to HRP reduced its activity but did not affect the binding of the substrate. It was also observed that the

biosensor was reactivated by transferring from the solution containing glufosinate and rinsing with PBS and one biosensor could be used for several measurements. The results therefore demonstrate that glufosinate can also be classified as a reversible non-competitive inhibitor of HRP. Reversible inhibitors bind to enzymes with non-covalent interactions such as hydrogen bonds, hydrophobic interactions and ionic bonds. Multiple weak bonds between the inhibitor and the active site combine to produce strong and specific binding. However, reversible inhibitors generally do not undergo chemical reactions when bound to the enzyme. As a result, the extent of inhibition depended only on the concentration of glufosinate. This method is suitable for sample determination in a batch system.



Calibration curves were constructed using the data obtained and are presented in Fig. 6.9. The linear ranges of the biosensor by this method were 2.0-78.0 $\mu\text{g L}^{-1}$ for glyphosate and 2.0-10.0 $\mu\text{g L}^{-1}$ for glufosinate. Correlation coefficients of 0.9992 ($n = 12$) and 0.9998 ($n = 4$) were obtained for glyphosate and glufosinate respectively. The sensor to sensor reproducibility for glyphosate and glufosinate was very good with R.S.D. values less than 10% (triplicate measurements). The biosensor sensitivities for glyphosate and glufosinate by this method were found to be at the nano-level (2.20 nA nM^{-1} for glyphosate and 4.2 nA nM^{-1} for glufosinate). The sensitivity to glyphosate by this method was found to be slightly higher than that obtained when a magnetic stirrer was used to introduce convection into the solution (i.e. 1.00 ± 0.14 nA nM^{-1}). This is probably due to the large volumes of working PBS solutions (10.0

mL) used during RDE measurements that could have contributed to large dilutions of the analytes injected.

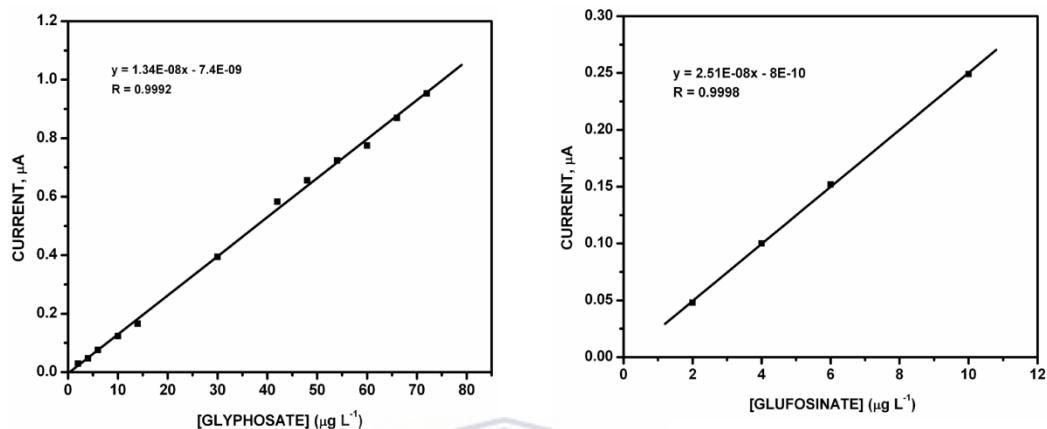


Figure 6.9. Calibration curves for biosensor response to (a) glyphosate and (b) glufosinate standards.

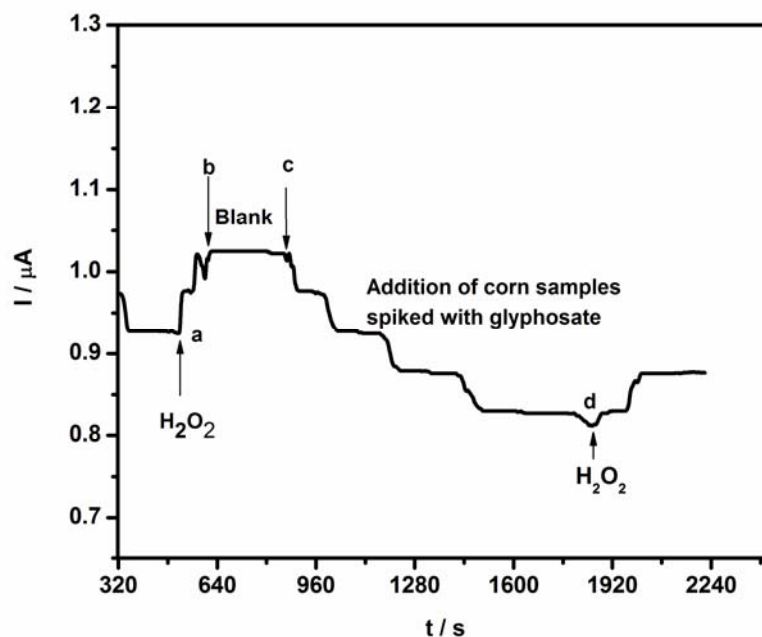
6.3.2.2 Glyphosate and glufosinate in samples

To evaluate the applicability of the HRP/PDMA-PSS biosensor in a complex sample, it was applied for the determination of glyphosate and glufosinate in spiked corn samples. It has been estimated that two-thirds of the total time required for analysis is spent in sample preparation and pre-treatment steps before the final determination. Furthermore these preparation steps are the main sources of errors in an analytical procedure (Songa et al., 2009). Therefore, the development of a method that does not require a tedious and complex sample preparation is always very attractive. In this work, the unique procedure in sample preparation was the removal of the solid

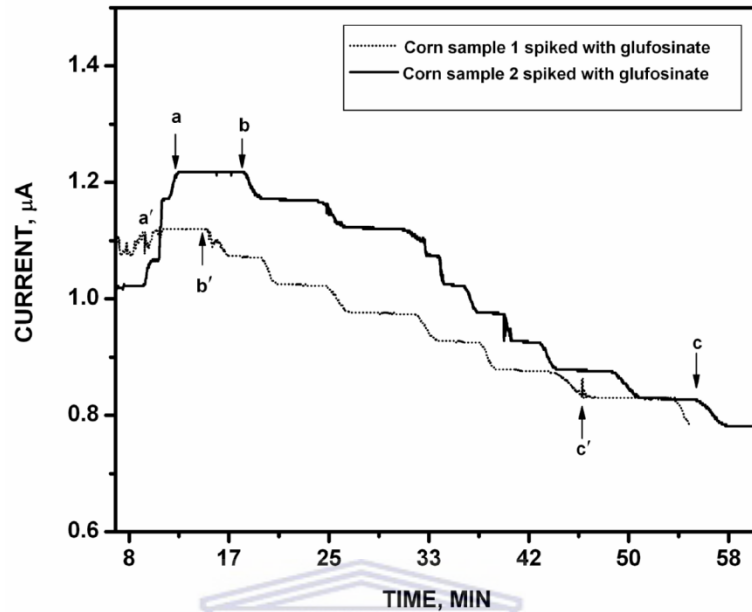
particles of the sample by centrifugation and filtration, without any kind of extraction, clean-up, derivatization, or pre-concentration step. The method of standard addition was used to determine the concentration of glyphosate and glufosinate in the samples. Standard addition is applied to most analytical techniques and is used instead of a calibration curve to solve the matrix effect problem. The matrix effect problem occurs when the sample contains many impurities. In the extraction procedure for corn, other water soluble components of foods, like amino acids, amino sugars, etc. may also have been extracted. These compounds interfere in the determination of glyphosate and glufosinate making necessary the spiking of the sample. If impurities present in the sample interact with the analyte to change the instrumental response or themselves produce an instrumental response, then a calibration curve based on pure analyte samples will give an incorrect determination. One way to solve this problem is to use standard addition. In this regard, the standard solutions (solution of known concentration of analyte) were added to the extracted corn sample solutions so that any impurities in the extracted samples were accounted for in the calibration. The concentrations of glyphosate and glufosinate in the samples were then determined by extrapolation.

Figures 6.10a and 6.10b show the amperometric responses of the biosensor to corn samples spiked with glyphosate and glufosinate respectively. H_2O_2 was first added followed by addition of blank solutions extracted using the same extraction procedure for the sample. Blank solutions were injected at points b-c (Fig. 6.10a), a-b and a'-b' (Fig 6.10b). It was observed that the addition of blank into the solution did not cause

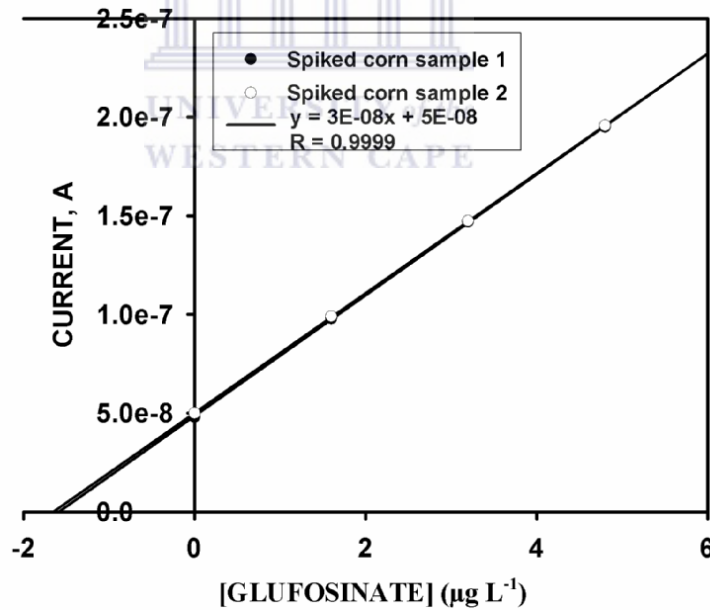
any significant change in current. This indicated that the reduction in current after injection of spiked samples was entirely due to inhibition of the enzyme by glyphosate and glufosinate present in the samples. A decrease in current was observed when corn sample spiked with 0-10.0 $\mu\text{g L}^{-1}$ glyphosate were injected into the electrolyte solution at point c-d, while an increase in current was observed when H_2O_2 was injected into the solution at point d (Fig. 6.10a). In Fig. 6.10b, a decrease in current was observed when corn samples spiked with 0-40.0 $\mu\text{g L}^{-1}$ glufosinate were injected at points b-c and b'-c'. The reduced response of the biosensor due to inhibition of the enzyme was related to the concentration of glufosinate in the test solutions and used to obtain an extrapolated plot shown in Fig. 6.10c. The extrapolated curve was found to be linear within a concentration range of 0-4.8 $\mu\text{g L}^{-1}$ and with a perfect correlation coefficient ($r = 0.9999$, $n = 4$).



(a)



(b)



(c)

Figure 6.10. (a) Biosensor responses to successive injections of corn samples spiked with glyphosate (b) response of the biosensor to injections of corn samples spiked with glufosinate (c) extrapolated linear curve for glufosinate in samples.

The detection limits for glyphosate and glufosinate in corn sample achieved by this method were both $0.1 \mu\text{g kg}^{-1}$ (calculated using equation 3.4). The RDE provided the lowest detection limit for glyphosate amongst all the other methodologies used. The biosensor reproducibility for successive blank measurements was very good with R.S.D. value of 1%. The concentration of glufosinate in replicate measurements ($n=2$) of corn samples was found to be $1.70 \mu\text{g kg}^{-1}$ while that of glyphosate in corn sample was found to be $1.50 \mu\text{g kg}^{-1}$. The absolute value of the x-intercept is the concentration of herbicide in the spiked sample solutions, in this case $1.70 \mu\text{g kg}^{-1}$ and $1.50 \mu\text{g kg}^{-1}$. The point at zero concentration added herbicide is the reading of the unknown in the sample; the other points are the readings after adding increasing amounts (spikes) of standard solution. In Fig. 6.10c, the reading of the unknown in the sample is $5.0 \text{ e}^{-8} \text{ A}$ which corresponds to glufosinate concentration of $2.0 \mu\text{g L}^{-1}$ obtained from the calibration curve of the standard method (Fig. 6.9b).

The Environmental Protection Agency (EPA, 2006) has set a maximum residue limit (MRL) of glyphosate in fruit and vegetable in the range of $0.2\text{--}5.0 \text{ mg kg}^{-1}$, in soybean at 20 mg kg^{-1} , and in drinking water at 0.7 mg L^{-1} . The FAO of the United Nations has set a MRL of glyphosate in the range of $0.1\text{--}5.0 \text{ mg kg}^{-1}$ for fruits and grains and MRL of glufosinate at 0.05 mg kg^{-1} for grains (FAO, 2006). It is observed that all the MRL values set for glyphosate and glufosinate in fruits, vegetable, grains and water are higher than the detection limits obtained in this work. The limits of detection for the HRP/PDMA-PSS biosensor were also compared to other analytical techniques as shown in Table 6.1. The values obtained for the biosensor were found

to be in good agreement with those reported for analytical techniques used in other laboratories. The limit of detection obtained for glyphosate in corn by the HRP/PDMA-PSS biosensor was found to be lower than that obtained by the MS method. The HRP/PDMA-PSS biosensor is therefore sufficient in providing high sensitivity for determination of glyphosate and glufosinate in real samples at residue levels.

Table 6. 1. Comparison of the analytical parameters of the HRP/PDMA-PSS biosensor with other analytical techniques

Compounds	Detection method	Matrix	Limits of Detection	Reference
Glyphosate	HRP/PDMA-PSS biosensor	Standard solution	0.16 $\mu\text{g L}^{-1}$	This work
		Corn	0.1 $\mu\text{g kg}^{-1}$	This work
	ELISA	Water	7.6 $\mu\text{g mL}^{-1}$	Clegg et al., 1999
	ELISA (preconcentration)	Water	0.076 $\mu\text{g mL}^{-1}$	Clegg et al., 1999
	HPLC	Water	0.22 $\mu\text{g L}^{-1}$	Piriyapittaya et al., 2008
	CE	Water	0.06 $\mu\text{g mL}^{-1}$	Chiu et al., 2008
Glufosinate	MS	Soybeans	0.6 $\mu\text{g g}^{-1}$	Chiu et al., 2008
		Corn, soya, fruits	0.01 mg kg^{-1}	Tadeo et al., 2000
	HRP/PDMA-PSS biosensor	Corn	0.1 $\mu\text{g kg}^{-1}$	This work
AMPA	GC	Crops	0.02 mg kg^{-1}	Stalikas and Konidari, 2001
	HPLC	Water	0.25 $\mu\text{g L}^{-1}$	Stalikas and Konidari, 2001
	HRP/PDMA-PSS biosensor	Standard solution	1.0 $\mu\text{g L}^{-1}$	This work
AMPA	HPLC	Water	3.40 $\mu\text{g L}^{-1}$	Piriyapittaya et al., 2008.
	CE	Water	4.04 $\mu\text{g mL}^{-1}$	Chiu et al., 2008

6.4 Evaluation of the interaction of horseradish peroxidase with the herbicides

Glyphosate and glufosinate have three reactive functional groups (amine, carboxylate and phosphonate) that can coordinate strongly or bind to metal ions as well as enzymes. They are known to inhibit the activity of photosynthetic enzymes in plants. In aqueous solutions at pH 6.3, they are dominant in ionic forms presented in Fig. 6.11 (Goodwin et al., 2003). Since glyphosate has reactive functional groups and has high affinity for iron (Fe), it could have bound strongly to the Fe in the active site of HRP blocking the active sites hence a decrease in biosensor response. The results from the inhibition experiments carried out have indicated that the binding of glyphosate to HRP did not affect the binding of the substrate to HRP thus suggesting that it could also be binding to other sites on HRP that are different from its active sites. The interaction between glyphosate and HRP was therefore investigated by FTIR and the results are presented in Fig. 6.12.

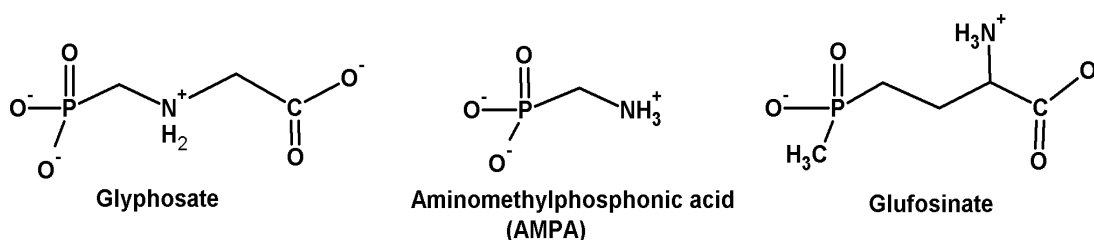


Figure 6.11 Structures of glyphosate, AMPA and glufosinate in their ionic forms dominant in aqueous solution at pH 6.3.

FTIR spectroscopy, as a sensitive technique is frequently used for investigation of the secondary structure of proteins and it can therefore be used to detect the changes that occur on HRP secondary structure as a result of its inhibition by glyphosate. The changes occurring on the peptide backbone chain of HRP were therefore monitored by recording the spectra of the native HRP, that of HRP immobilized on the PDMA-PSS modified electrode as well as recording that obtained after incubation of the immobilized HRP with known concentrations of glyphosate. The HRP immobilized on PDMA-PSS (PDMA-PSS/HRP) showed an IR signal at ca. 1642 cm^{-1} for amide I band, and another one at ca. 1530 cm^{-1} for amide II band (Fig 6.12). It was observed that the FTIR spectra recorded after the contact of the immobilized HRP with glyphosate (PDMA-PSS/HRP-Glyphosate) showed the disappearance of amide I band of HRP. This clearly indicates the binding of glyphosate to HRP. Since the amide I band is attributed to C=O stretching vibration of peptide linkage in the HRP backbone, the binding by glyphosate suggests that it coordinated with the oxygen atoms in the C=O groups of HRP through its $^+\text{NH}_2$ group, forming a complex of HRP-Glyphosate. The formation of this complex is therefore responsible for the conformational changes of HRP.

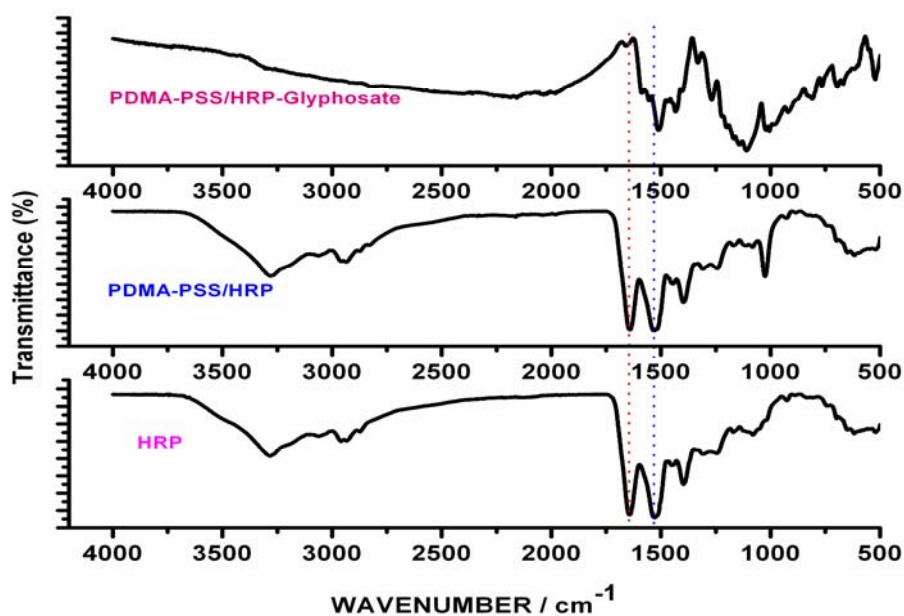
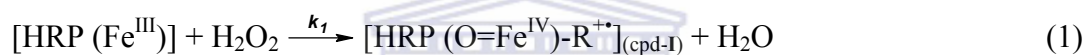


Figure 6.12. FTIR spectra illustrating the interaction of glyphosate with horseradish peroxidase.

It has been reported that the increase in the random coil content of HRP can disturb the microstructure of the heme active centre of HRP, in which the planarity of the porphyrin cycle in the heme group is increased and the exposure extent of the electrochemical active centre is decreased (Guo et al., 2008). This suggests that glyphosate can inhibit the electrochemical reaction of the HRP immobilized on the PDMA-PSS electrode and its electrocatalytic activity for the reduction of H_2O_2 through the formation of the complex with HRP. It has also been reported that the changes in the microstructure of HRP obstruct the electron transfer of Fe (III) in the porphyrin cycle of the heme group, thus HRP catalytic activity is inhibited (Guo et al., 2008). This indicates that glyphosate inhibited the activity of HRP by obstructing the electron transfer of Fe (III) in the porphyrin cycle of the heme group therefore

inhibiting its electrocatalytic activity for the reduction of H_2O_2 . The effect of glyphosate inhibition on the HRP catalytic activity was found to be increasing with increase in glyphosate concentration. Considering the reaction for the oxidation of HRP immobilized on the electrode surface by H_2O_2 to compound **I** (cpd-I) that contains an oxyferryl centre with the iron in the ferryl state ($\text{Fe}^{\text{IV}} = \text{O}$), and a porphyrin π cation radical (step 1), followed by further direct (mediatorless) electroreduction of compound **I** at the electrode surface to the initial HRP state (step 2) illustrated below:



It is expected that glyphosate would bind to compound **I** (cpd-I) in step 1 above thus hindering its electro-reduction to the initial active state of HRP (Fe^{III}). This results in the obstruction of the cycle and the electron transfer of Fe (III) leading to the inhibition of the HRP electrocatalytic activity for the reduction of H_2O_2 at the PDMA-PSS electrode surface. A similar behavior is expected for glufosinate which has the same reactive functional groups as glyphosate. AMPA being a metabolite of glyphosate, it is also expected to behave in a similar way.

The interactions of glyphosate, glufosinate and AMPA with HRP were further investigated by SEM at magnifications of 2500 and 1000x in order to observe the

changes occurring during these reactions. These changes could not be observed clearly with nano-scale dimensions and therefore the micro-scale dimensions were used for these studies. Figure 6.13 shows the SEM images of PDMA-PSS and HRP/PDMA-PSS films before and after contact with glyphosate, glufosinate and AMPA. The variation in morphologies of the films in the presence and absence of HRP, and the appearance of white HRP-like structures observed in Fig. 6.13b and 6.13c indicate that the enzyme was successfully immobilized on PDMA-PSS film. At a magnification of 1000x, more HRP-like structures were observed (Fig. 6.13b). The SEM images of HRP/PDMA-PSS film after reacting with glyphosate, glufosinate and AMPA show changes in the morphology and decrease in sizes of the HRP-like structures or their disappearance from the surface of the biosensor. The SEM images indicate that glyphosate, glufosinate and AMPA reduced the number of HRP units (i.e. the specific activity of HRP expressed in terms of pyrogallol units) in the bioelectrode, thus reducing its activity. Therefore, the reduction in the number or size of immobilized HRP units also contributed to the decrease in hydrogen peroxide signal.

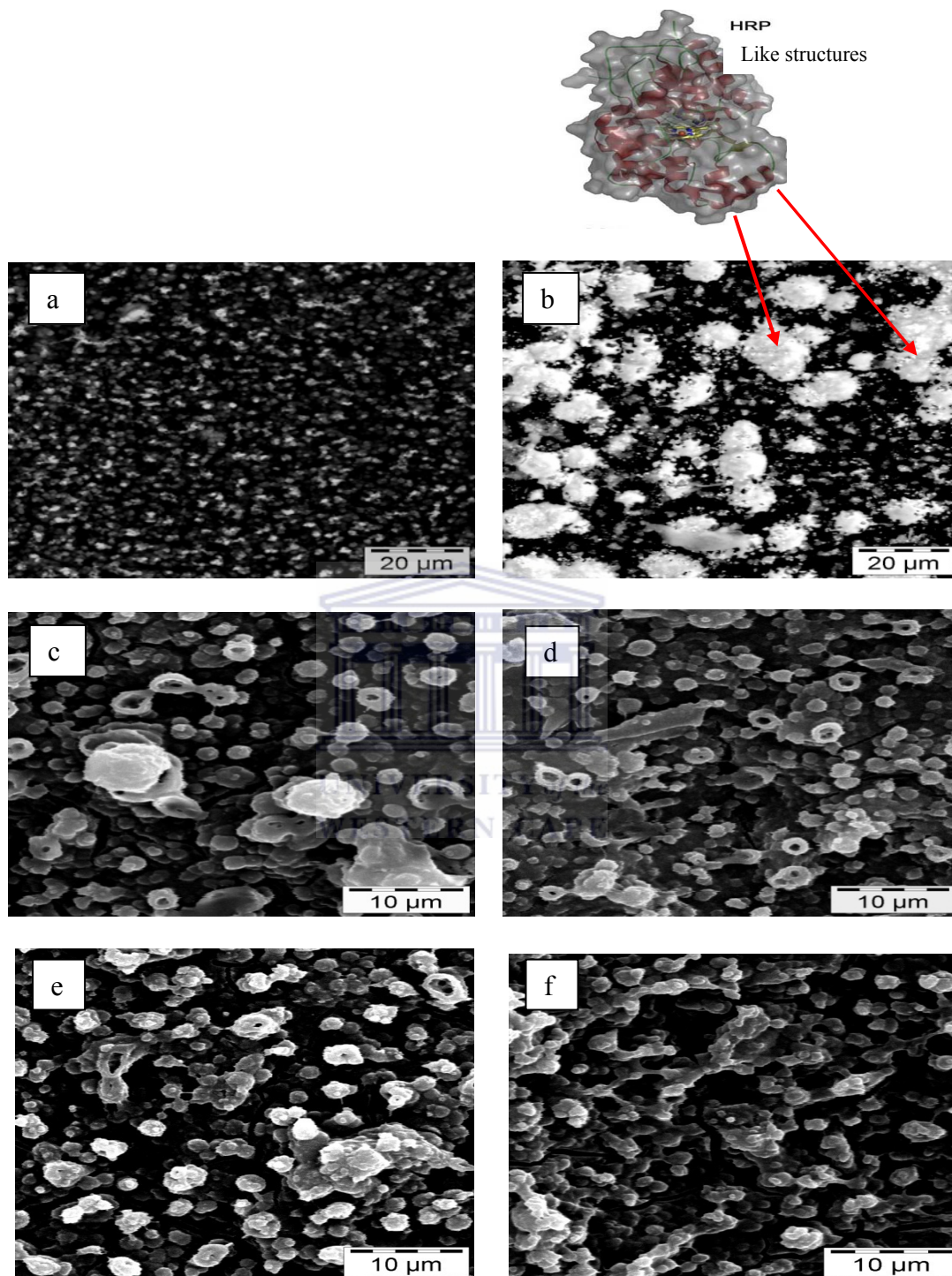


Figure 6.13. SEM images of (a) PDMA-PSS film, (b) HRP/PDMA-PSS film, (c) HRP/PDMA-PSS film (mag. 2500 x), (d) HRP/PDMA-PSS-Glyphosate, (e) HRP/PDMA-PSS-Glufosinate and (f) HRP/PDMA-PSS-AMPA (magnifications of 2500 and 1000x).

CHAPTER 7

Conclusions and Recommendations**7.1 Conclusions**

The detection and quantification of the herbicides glufosinate, glyphosate and the metabolite aminomethylphosphonic acid (AMPA) have been achieved using the developed HRP/PDMA-PSS inhibition biosensor. The detection principle was based on measurement of the reduced response of the biosensor occurring as a result of inhibition of the catalytic activity of HRP immobilized on nanostructured PDMA-PSS on gold electrode. From the results obtained it is concluded that glyphosate, glufosinate and AMPA inhibited the HRP electrocatalytic activity leading to a change in its secondary structure. The inhibition effect was found to be increasing with increase in concentrations of the herbicides and the incubation time or the time of contact of the herbicides with the biosensor. Higher inhibition degrees were realized by the incubation method in which the herbicide in question was in contact with the biosensor for 20 min before its response was measured. For the direct amperometric methods, lower inhibition percentages below the IC_{50} values were obtained after a series of measurements and therefore the calculation of the kinetic parameters in the presence of the inhibitors was not possible. This indicates that the incubation method is more appropriate for the study of enzyme kinetics.

FTIR spectroscopy was employed to study the interaction between HRP and glyphosate and the results suggested that the inhibition effect was due to the formation of the complex HRP-Glyphosate as a result of glyphosate binding to the O atoms of HRP peptide chain leading to the disappearance of amide I band of HRP and the change in its secondary structure. The binding of glyphosate to HRP is thought to have been through its $^+\text{NH}_2$ group dominant in aqueous solutions. The results suggest that the changes in the structure of HRP destructed the electron transfer of Fe (III) in the porphyrin cycle of the heme group, thus HRP catalytic activity was inhibited. The electrochemical studies of the interactions between the herbicides and HRP showed the same behavior for glyphosate, glufosinate and AMPA suggesting that they all inhibit HRP activity in a similar way given that they all have the reactive functional group $^+\text{NH}_2$, that is capable of binding with HRP. The morphological studies revealed the same behavior for all the herbicides suggesting that their inhibition mechanism is the same.

The apparent Michaelis-Menten constant (K_m^{app}) calculated for the HRP/PDMA-PSS biosensor in the presence and absence of glyphosate were found to be 2.67 μM and 2.71 μM respectively. The low K_m^{app} values obtained for the HRP/PDMA-PSS biosensor indicates strong binding to HRP by the substrates. The facts that the binding by glyphosate and glufosinate did not affect the binding of H_2O_2 and the x-intercept remained the same with or without glyphosate were used to classify them as reversible non-competitive inhibitors. Electrochemical measurements revealed the

same kind of inhibition by AMPA. Due to the reversible inhibition by these compounds and the low inhibition degrees obtained by the amperometric methods, it was possible to use the same HRP/PDMA-PSS biosensor repeatedly for up to 60 measurements without surface fouling.

The biosensor exhibited high sensitivity for glyphosate, glufosinate and AMPA and with very good reproducibility. The development of this method is a step forward in the analysis of glyphosate, glufosinate and AMPA at residue levels such as those occurring in the environment. The limit of detection of $0.1 \mu\text{g kg}^{-1}$ obtained for glyphosate and glufosinate in corn by the HRP/PDMA-PSS biosensor was found to be lower than that obtained by the MS method providing therefore, sufficient sensitivity for the determination of glyphosate in real samples without any pre-concentration step. The HRP/PDMA-PSS biosensor is therefore sufficient in providing high sensitivity for determination of glyphosate and glufosinate in real samples at residue levels. The biosensor method also demonstrated its simplicity, ease of construction, rapidity, sensitivity, and low-cost compared to the conventional analytical techniques corroborating that it can effectively be applied for environmental surveillance of these herbicides at residue levels on a regular basis.

The high sensitivity of the HRP/PDMA-PSS biosensor was provided for by the nanostructured PDMA-PSS materials used for the modification of the gold electrode surface before the immobilization of HRP. The PDMA-PSS film provided a suitable micro-environment for the immobilized HRP and acted as a mediator enhancing the

heterogeneous direct electron transfer rate of HRP. Nanostructured materials can act as tiny conduction centers to facilitate electron transfer between the enzyme and the electrode surface. The high stability of the HRP/PDMA-PSS film was due to the electrostatic attachment procedure used for the immobilization of the enzyme and the incorporation of the dopant PSS into the polymer matrix.

7.2 Recommendations

The results indicate that the HRP/PDMA-PSS biosensor is sensitive enough to detect the herbicides at low concentrations. However, in order that the biosensor can be fully applied for the detection of these herbicides in samples containing complex matrices, further optimization and selectivity studies would be required. A follow up procedure should include the studies of interfering species in the analyte solutions.

In order that the Lineweaver-Burk plot can be obtained and the K_m^{app} and I_{max} values calculated for glyphosate, glufosinate and AMPA, further optimization of their added concentrations may be required during amperometric measurements. This would be appropriate for the study of enzyme kinetics and for the investigation of the IC_{50} values.

The application of HRP/PDMA-PSS biosensor should be extended to analysis of other herbicides that can inhibit the activity of HRP. Once optimized, it is clear that

this inhibition based biosensor would provide rapid monitoring of environmental occurrence of herbicides. Integration of the HRP/PDMA-PSS biosensor into an automated system would be more attractive to provide the detection of many herbicides reducing the time of analysis. Miniaturization is further required for the biosensor to be applied for “on-site” monitoring of these herbicides.



References

Acquavella, J. F., Alexanders, B. H., Mandel, J. S., Gustin, C., Baker, B. & Chapman, P. (2004). Glyphosate biomonitoring for farmers and their families: results from the farm family exposure study. *Environ. Health Perspect.*, *112*, 321-326.

Ahuja, T., Mir, I. A., Kumar, D., & Rajesh. (2007). Biomolecular immobilization on conducting polymers for biosensing applications. *Biomaterials*, *28*, 791-805.

Akagi, K., Piao, G., Kaneko, S., & Sakamaki, K. (1998). Helical polyacetylene synthesized with a chiral nematic reaction field. *Science*, *282*, 1683-1686.

Akinyeye, R. O., Michira, M., Sekota, M., Al-Ahmed, A., Tito, D., Baker, P. G. L., Brett, C. M. A., Kalaji, M., & Iwuoha, E. I. (2007). Electrochemical synthesis and characterization of 1,2-napthaquinone-4-sulphonic acid doped Polypyrrole. *Electroanalysis*, *19*, 303-309.

Alivisatos, A. P. (2001). Less is more in medicine. *Sci. Am.*, *285*, 67-73.

Amine, A., Mohamed, H., Bourais, I., & Palleschi, G. (2006). Enzyme inhibition-based biosensors for food safety and environmental monitoring. *Biosens. Bioelectron.*, *21*, 1405-1423.

Athawale, A. A., & Kulkarni, M. V. (2000). Polyaniline and its substituted derivatives as sensors for aliphatic alcohols. *Sens. Actuators, B*, *67*, 173-177.

References

Badihi-Mossberg, M., Buchner, V., & Rishpon, J. (2007). Electrochemical Biosensors for pollutants in the Environment. A review. *Electroanalysis*, *19*, 2015-2028.

Balogh, L., & Tomalia, D. A. (1998). Poly(amidoamine) dendrimertemplated nanocomposites. 1. Synthesis of zerovalent copper nanoclusters. *J. Am. Chem. Soc.*, *120*, 7355–7356.

Balogh, L., Valluzzi, R., Hagnauer, G. L., Laverdure, K. S., Gido, S. P., & Tomalia, D. A. (1999). Formation of silver and gold dendrimer nanocomposites. *J. Nanopart. Res.*, *1*, 353-368.

Bard, A. J., & Faulkner, L. R. (2000). *Electrochemical methods: Fundamentals and applications* (2nd ed.). New York: John Wiley & Sons.

Barja, B. C., Herszage, J., & dos Santos Afonso, M. (2001). Iron (III)-phosphonate complexes. *Polyhedron*, *20*, 1821-1830.

Bartlett, P. N., & Wallace, E. N. (2000). The oxidation of β -nicotinamide adenine dinucleotide (NADH) at poly(aniline)-coated electrodes Part II. Kinetics of reaction at poly(aniline)–poly(styrenesulfonate) composites. *J. Electroanal. Chem.*, *486*, 23-31.

Bejan, D., & Duca, A. (1998). Voltammetry of aniline with different electrodes and electrolytes. *Croat. Chem. Acta*, *71*, 745-756.

Bıřak, N., Senkal, B. F., & Sezer, E. (2005). Preparation of organo-soluble polyanilines in ionic liquid. *Synth. Met.*, *155*, 105-109.

References

Bloor, D., & Movaghar, B. (1983). Conducting polymers. *IEEE Proceedings*, 130, 225–232.

Bronstein, L. H., Sidorov, S. N., Valetsky, P. M., Hartmann, J., Colfen, H., & Antonietti, M. (1999). Induced micellization by interaction of poly(2-vinylpyridine)-block-poly(ethylene oxide) with metal compounds. Micelle characteristics and metal nanoparticles formation. *Langmuir*, 15, 6259–62.

Buffin, D. & Jewell, T. (2001). Report for the Pesticide Action Network UK. From: http://www.foe.co.uk/resource/reports/impacts_glyphosate.pdf [Accessed: 20 September 2008].

Calas, A. –G., Richard, O., Meme, S., Beloeil, J. –C., Doan, B. –T., Gefflaut, T., Meme, W., Crusio, W. E., Pichon, J., & Monte cot, C. (2008). Chronic exposure to glufosinate-ammonium induces spatial memory impairments, hippocampal MRI modifications and glutamine synthetase activation in mice. *Neurotoxicology*, 29, 740-747.

Campanella, L., Favero, G., Sammartino, M. P., & Tomassetti, M. (1999). Analysis of several real matrices using new mono-, bi-enzymatic or inhibition organic phase enzyme electrodes. *Anal. Chim. Acta*, 393, 109–120.

Cao, Y. (1990). Spectroscopic studies of acceptor and donor doping of polyaniline in the emeraldine base and pernigraniline forms. *Synth. Met.*, 35, 319-332.

Castillo, J., Gáspár, S., Sakharov, I., & Csöregi, E. (2003). Bienzyme biosensors for glucose, ethanol and putrescine built on oxidase and sweet potato peroxidase. *Biosens. Bioelectron.*, 18, 705–714.

References

Cataldo, F., & Maltese, P. (2002). Synthesis of alkyl and N-alkyl-substituted polyanilines. A study on their spectral properties and thermal stability. *Eur. Polym. J.*, 38, 1791-1803.

Chakarvarti, S. K., & Vetter, J. (1998). Template synthesis - A membrane based technology for generation of nano-/micro materials: A review. *Radiat. Meas.*, 29, 149-159.

Chen, C. -C., & Gu, Y. (2008). Enhancing the sensitivity and stability of HRP/PANI/Pt electrode by implanted bovine serum albumin. *Biosens. Bioelectron.*, 23, 765-770.

Chen, S. -S., Wen, T. -C., & Gopalan, A. (2003). Electrosynthesis and characterization of a conducting copolymer having S-S links. *Synth. Met.*, 132, 133-143.

Chen, X., Peng, X. Kong, J., & Deng, J. (2000). Facilitated electron transfer from an electrode to horseradish peroxidase in a biomembrane-like surfactant film. *J. Electroanal. Chem.*, 480, 26-33.

Chiu, H. -Y., Lin, Z. -Y., Tu, H. -L., & Whang, C. -W. (2008). Analysis of glyphosate and aminomethylphosphonic acid by capillary electrophoresis with electrochemiluminescence detection. *J. Chromatogr. A*, 1177, 195-198.

Cho, M. S., Park, S. Y., Hwang, J. Y., & Choi, H. J. (2004). Synthesis and electrochemical properties of polymer composites with nanoparticles. *Mater. Sci. Eng., C*, 24, 15-18.

Cikalo, M., Goodall, D., & Mathews, W. (1996). Analysis of glyphosate using capillary electrophoresis with indirect detection. *J. Chromatogr. A*, 745, 189-200.

References

Clark, L. C., & Lyons, C. (1962). Electrode systems for continuous monitoring in cardiovascular surgery. *Ann. N.Y. Acad. Sci.*, *102*, 29-45.

Clark, L. C., Wolf, R., Granger, D., & Taylor, Z. (1953). Continuous recording of blood oxygen tensions by polarography. *J. Appl. Physiol.*, *6*, 189-193.

Clegg, B. S., Stephenson, G. R., & Hall, J. C. (1999). Development of an enzyme-linked immunosorbent assay for the detection of glyphosate. *J. Agric. Food Chem.*, *47*, 5031-5037.

Collings, A. F., & Caruso, F. (1997). Biosensors: Recent advances. *Rep. Prog. Phys.*, *60*, 1397-1445.

Collins, G. E., & Buckley, L. J. (1996). Conductive polymer-coated fabrics for chemical sensing. *Synth. Met.*, *78*, 93-101.

Cox, C. (1996). Herbicide Fact sheet: Glufosinate, Journal of pesticide reform, North West Coalition for alternatives to pesticides, Oregon, US.

Cruz, G. J., Morales, J., Castillo-Ortega, M. M., & Olayo, R. (1997). Synthesis of polyaniline films by plasma polymerization. *Synth. Met.*, *88*, 213-218.

Daniele, P. G., Stefano, C., Prenesti, E., & Sammartano, S. (1997). Copper (II) complexes of N-(phosphonomethyl)glycine in aqueous solution: a thermodynamic and spectrophotometric study. *Talanta*, *45*, 425-431.

Deepa, M., Ahmad, S., Sood, K. N., Alam, J., Ahmad, S., & Srivastava, A. K. (2007). Electrochromic properties of polyaniline thin film nanostructures derived from solutions of ionic liquid/polyethylene glycol. *Electrochim. Acta*, *7453-7463*.

References

Deepa, M., Srivastava, A. K., Sood, K. N., & Agnihotry, S. A. (2006). Nanostructured mesoporous tungsten oxide films with fast kinetics for electrochromic smart windows. *Nanotechnology*, *17*, 2625-2630.

Dellinger, T. M., & Braun, P. V. (2001). BiOCl nanoparticles synthesized in lyotropic liquid crystal nanoreactors. *Scr. Mater.*, *44*, 1893-1897.

Diaz, A. F., & Bargon, J. (1986). In: Skotheim, T. A. (Ed), *Electrochemical synthesis of conducting polymers. Handbook of conducting polymers* (Vol. 1, pp. 81-115). New York: Marcel Dekker.

Duke, C. B., & Schein, L. B. (1980). Organic solids: Is energy-based theory enough? *Phys. Today*, *33*, 42-48.

Dunford, H. B. (1999). *Heme Peroxidases*. New York: Wiley-VCH.

Dzantiev, B. B., Yazynina, E. V., Zherdez, A. V., Plekhanova, Y. V., Reshetilov, A. N., Chang, S. C., et al. (2004). Determination of the herbicide chlorsulfuron by amperometric sensor based on separation-free bienzyme immunoassay. *Sens. Actuators, B*, *98*, 254-261.

Environmental Protection Agency (EPA). (2006). Available from: <http://www.epa.gov/EPA-PEST/2006/June/Day-07/p8827.htm> [Accessed: 20 January 2008].

Ernst, A., Makowski, O., Kowalewska, B., Miecznikowski, K., & Kulesza, P. J. (2007). Hybrid bioelectrocatalyst for hydrogen peroxide reduction: Immobilization of enzyme within organic-inorganic film of structured Prussian blue and PEDOT. *Bioelectrochemistry*, *71*, 23-28.

References

Evtugyn, G. A., Budnikov, H. C., & Nikolskaya, E. B. (1998). Sensitivity and selectivity of electrochemical enzyme sensors for inhibitor determination. *Talanta*, *46*, 465–484.

FAO. Food and Agriculture Organization. Food Standards Programme. (2006). Available from: http://www.codexalimentarius.net/download/report/655/al29_24e.pdf [Accessed: 20 January 2008].

FAO/WHO. (1996). *Glyphosate Data Sheet 91. WHO/PCS/DS/96.91*. Geneva: WHO.

Feng, W., Bai, X., Lian, Y., Liang, J., Wang, X., & Yoshino, K. (2003). Well-aligned polyaniline/carbon-nanotube composite films grown by in-situ aniline polymerization. *Carbon*, *41*, 1551-1557.

Ferapontova, E., Schmengle, K., Borchers, T., Ruzgas, T., & Gorton, L. (2002). Effect of cysteine mutations on direct electron transfer of horseradish peroxidase on gold. *Biosens. Bioelectron.*, *17*, 953-963.

Fernandes, M. R., Garcia, J. R., Schultz, M. S., & Nart, F. C. (2005). Polaron and bipolaron transitions in doped poly(p-phenylene vinylene films). *Thin Solid Films*, *474*, 279-284.

Forster, S., & Konrad, M. (2003). From self-organizing polymers to nano and biomaterials. *J. Mater. Chem.*, *13*, 2671–2688.

Fraser, D. (1997). *An introduction to in vivo biosensing: Progress and Problems*. In: Fraser, D. (Ed.), *Biosensors in the Body, Continuous in vivo monitoring*. London: Wiley.

References

Freire, R. S., Pessoa, C. A., Mello, L. D., & Kubota, L. T. (2003). Direct electron transfer: An approach for electrochemical biosensors with higher selectivity and sensitivity. *J. Braz. Chem. Soc.*, *14*, 230-243.

Fukushima, T., Kosaka, A., Ishimura, Y., Yamamoto, T., Takigawa, T., Ishii, N., et al. (2003). Molecular ordering of organic molten salts triggered by single-walled carbon nanotubes. *Science*, *300*, 2072-2074.

Garcia de Llasera, M. P., Gomez-Almaraz, L., Vera-Avila, L. E., & Pena-Alvarez, A. (2005). Matrix solid-phase dispersion extraction and determination by high-performance liquid chromatography with fluorescence detection of residues of glyphosate and aminomethylphosphonic acid in tomato fruit. *J. Chromatogr. A*, *1093*, 139-146.

Geng, Y. H., Sun, Z. C., Li, J., Jing, X. B., Wang, X. H., & Wang, F. S. (1999). Water soluble polyaniline and its blend films prepared by aqueous solution casting. *Polymer*, *40*, 5723-5727.

George, P., & Hanania, G. (1953). Spectrophotometric study of ionizations in methemoglobin. *J. Biochem.*, *55*, 236-243.

Gerard, M., Chaubey, A., & Malhotra, B. D. (2002). Application of conducting polymers to biosensors. *Biosens. Bioelectron.*, *17*, 345-359.

Giesy, J. P., Dobson, S. & Solomon, K. R. (2000). Ecotoxicological risk assessment for roundup herbicide. *Rev. Environ. Contam. Toxicol.*, *167*, 35-120.

Gong, J., Cui, X. J., Xie, Z. W., Wang, S. G., & Qu, L.Y. (2002). The solid-state synthesis of polyaniline/H₄SiW₁₂O₄₀ materials. *Synth. Met.*, *129*, 187-192.

References

Goodwin, L., Startin, J. R., Keely, B. J., & Goodall, D. M. (2003). A nalysis of glyphosate and glufosinate by capillary electrophoresis– mass spectrometry utilising a sheathless microelectrospray interface. *J. Chromatogr. A* , 1004, 107-119.

Göpel, W., & Schierbaum, K. D. (1991). *Definitions and typical examples*. In: *Gopel, W., Jones, T. A., Kleitz, M., Lundsstrom, J., Seiyama, T. (Eds), Sensors-A comprehensive Survey. Chemical and Biochemical Sensors* (Vol. 2). New York: VCH.

Greef, R., Peat, R., Peter, L. M., & Pletcher, D. (1990). *Instrumental Methods in electrochemistry*. England: Ellis Horwood Limited.

Grennan, K., Killard, A. J., Hanson, C. J., Cafolla, A. A., & Smyth, M. R. (2006). Optimisation and characterisation of biosensors based on polyaniline. *Talanta*, 68, 1591–1600.

Guimard, N. K., Gomez, N., & Schmidt, C. E. (2007). Conducting polymers in biomedical engineering. *Prog. Polym. Sci.*, 32, 876-921.

Guisseppi-Elie, A., Wallace, G.G., & Matsue, T. (1997). In: Skotheim, T., Elsenbaumer, R., Reynolds, J.R. (Eds), *Chemical and biological sensors based on electrically conducting polymers. Handbook of Conducting Polymers* (pp. 963–991, 2nd ed.). New York: Marcel Dekker.

Guo, S., Zhou, Q., Lu, T., Ding, X., & Huang, X. (2008). Spectroscopic studies of interactions involving horseradish peroxidase and Tb^{3+} . *Spectrochim. Acta, Part A*, 70, 818–823.

References

- Han, M. G., Cho, S. K., Oh, S. G., & Im, S. S. (2002). Preparation and characterization of polyaniline nanoparticles synthesized from DBSA micellar solution. *Synth. Met.*, *126*, 53-60.
- He, P., Hu, N., & Rusling, J. F. (2004). Driving Forces for Layer-by-Layer Self-Assembly of Films of SiO₂ Nanoparticles and Heme Proteins. *Langmuir*, *20*, 722-729.
- Hingorani, S., Shah, D. O., & Multani, M. S. (1995). Effect of process variables on the grain growth and microstructure of ZnO-Bi₂O₃ varistors and their nanosize ZnO recursors. *J. Mater. Res.*, *10*, 461-467.
- Hock, B. (1997). Antibodies for immunosensors. *Anal. Chim. Acta*, *347*, 177-186.
- Holdcroft, S. (2001). Patterning π -conjugated polymers. *Adv. Mater.*, *13*, 1753-1765.
- Hong, J., Moosavi-Movahedi, A. A., Ghourchian, H., Rad, A. M., & Rezaei-Zarchi, S. (2007). Direct electron transfer of horseradish peroxidase on Nafion-cystein modified gold electrode. *Electrochim. Acta*, *52*, 6261-6267.
- Hong, S. Y., & Marnick, D. S. (1992). Understanding the conformational stability and electronic structures of modified polymers based on polythiophene. *Macromolecules*, 4652-4657.
- Hong, S. Y., Jung, Y. M., Bin Kim, S., & Park, S. M. (2005). Electrochemistry of conductive polymers. 34. Two-dimensional correlation analysis of real-time spectroelectrochemical data for aniline polymerization. *J. Phys. Chem. B*, *109*, 3844.
- Hori, Y., Tanaka, T., Fujisawa, M. & Shimada K. (2003). Toxicokinetics of DL-glufosinate enantiomer in human BASTA poisoning. *Biol. Pharm. Bull*, *26*, 540-543.

References

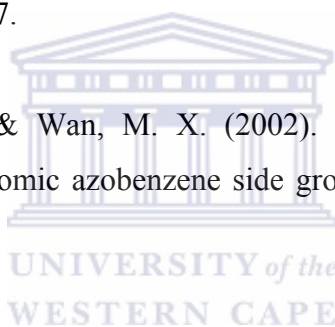
Huang, J. X., & Kaner, R. B. (2004). A general chemical route to polyaniline nanofibers. *J. Am. Chem. Soc.*, *126*, 851-855.

Huang, J. X., Virji, S., Weiller, B. H., & Kaner, R. B. (2004). Nanostructured polyaniline sensors. *Chem. Eur. J.*, *10*, 1314-1319.

Huang, J., & Kaner, R. B. (2006). The intrinsic nanofibrillar morphology of polyaniline. *Chem. Commun.*, 367-376.

Huang, J., & Wan, M. X. (1999). In situ doping polymerization of polyaniline microtubes in the presence of β -naphthalenesulfonic acid. *J. Polym. Sci., Part A: Polym. Chem.*, *37*, 151-157.

Huang, K., Qiu, H. J., & Wan, M. X. (2002). Synthesis of highly conducting polyaniline with photochromic azobenzene side groups. *Macromolecules*, *35*, 8653-8655.



Hyperlink: <http://nobelprize.org/chemistry/laureates/2000>.

Ibanez, M., Pozo, O. J., Sancho, J. V., Lopez, F. V., & Hernandez, F. (2005). Residue determination of glyphosate, glufosinate and aminomethylphosphonic acid in water and soil samples by liquid chromatography coupled to electrospray tandem mass spectrometry. *J. Chromatogr. A*, *1081*, 145-155.

Iijima, S. (1991). Helical microtubules of graphitic carbon. *Nature*, *354*, 56-58.

Ingrt, D., & Pileni, M. P. (2001). Limitations in producing nanocrystals using reverse micelles as nanoreactors. *Adv. Funct. Mater.*, *11*, 136-139.

References

Inzelt, G., & Horányi, G. (1990). Some problems connected with the study and evaluation of the effect of pH and electrolyte concentration on the behaviour of polyaniline film electrodes. *Electrochim. Acta*, 35, 27-34.

Iwuoha, E. I., & Smyth, M. (1996). Polymer-based amperometric biosensors. In: Michael E. G. Lyons (Eds), *Electroactive polymer electrochemistry, Part 2, Methods and Applications* (pp. 297-328). New York, USA: Plenum Press.

Iwuoha, E. I., Leister, I., Miland, E., Smyth, M. R., & Fágáin, C. O. (1997). Reactivities of organic-phase biosensors. 1. Enhancement of the sensitivity and stability of amperometric peroxidase biosensors using chemically modified enzymes. *Anal. Chem.*, 69, 1674-1681.

Iwuoha, E. I., Saenz de Villaverde, D., Garcia, N. P., Smyth, M. R., & Pingarront, J. M. (1997). Reactivities of organic phase biosensors. 2. The amperometric behaviour of horseradish peroxidase immobilized on a platinum electrode modified with an electrosynthetic polyaniline film. *Biosens. Bioelectron.*, 12, 749-761.

Iwuoha, E. I., Smyth, M. R., & Lyons, M. E. (1995). Solvent effects on the reactivities of an amperometric glucose sensor. *J. Electroanal. Chem.*, 390, 35-45.

Janata, J., & Josowicz, M. (2003). Conducting polymers in electronic chemical sensors. *Nat. Mater.*, 2, 19-24.

Jang, J., Bae, J., & Lee, K. (2005). Synthesis and characterization of polyaniline nanorods as curing agent and nanofiller for epoxy matrix composite. *Polymer*, 46, 3677-3684.

References

Jewell, T. & Buffin, D. (2001). Report for the Pesticide Action Network UK. From: <http://www.foe.co.uk/resource/reports/impacts_glufosinate_ammon.pdf> [Accessed: 20 September 2008].

Kalaji, M., Nyholm, L., & Peter, L. M. (1991). A microelectrode study of the influence of pH and solution composition on the electrochemical behaviour of polyaniline films. *J. Electroanal. Chem.*, 313, 271-289.

Kang, E. T., Neoh, K. G., & Tan, K. L. (1998). Polyaniline: A polymer with many interesting intrinsic redox states. *Prog. Polym. Sci.*, 23, 277-324.

Kang, E. T., Neoh, K. G., Tan, T. C., Khor, S. H., & Tan, K. L. (1990). Structural studies of poly(p-phenyleneamine) and its oxidation. *Macromolecules*, 23, 2918-2926.

Karube, I., Nomura, Y., & Arikawa, Y. (1995). Biosensors for environmental control. *Trends Anal. Chem.*, 14, 295-299.

Kataoka, H., Ryu, S., Sakiyama, N., & Makita, M. (1996). Simple and rapid determination of the herbicides glyphosate and glufosinate in river water, soil and carrot samples by gas chromatography with flame photometric detection. *J. Chromatogr. A*, 726, 253-258.

Kim, S. -C., Huh, P., Kumar, J., Kim, B., Lee, J. -O., Bruno, F. F., et al. (2007). Synthesis of polyaniline derivatives via biocatalysis. *Green Chem.*, 9, 44-48.

Kintzios, S., Pistola, E., Panagiotopoulos, P., Bonsel, M., Alexandropoulos, N., Bem, F., et al. (2001). Bioelectric recognition assay (BERA). *Biosens. Bioelectron.*, 16, 325-336.

References

- Kobayashi, T., Yoneyama, H., & Tamura, H. (1984). Polyaniline film coated electrodes as electrochromic display devices. *J. Electroanal. Chem.*, *161*, 419-423.
- Kohrausch, F. (1885). 2-Electrode cell with platinized platinum electrodes. *Wied Ann*, *26*, 161–165.
- Kolpin, D. W., Thurman, E. M., Lee, E. A., Meyer, M. T., Furlong, E. T., & Glassmeyer, S. T. (2006). Urban contributions of glyphosate and its degradate AMPA to streams in the United States. *Sci. Total Environ.*, *354*, 191–197.
- Konash, A., & Magner, E. (2005). Electrochemically mediated reduction of horseradish peroxidase by 1,10-ferrocene dimethanol in non-aqueous solvents. *Anal. Chem.*, *77*, 1647–1654
- Kong, Y. T., Boopathi, M., & Shim, Y. B. (2003). Direct electrochemistry of horseradish peroxidase bonded on a conducting polymer modified glassy carbon electrode. *Biosens. Bioelectron.*, *19*, 227–232.
- Kumar, C. V., & McLendon, G. L. (1997). Nanoencapsulation of cytochrome c and horseradish peroxidase at the galleries of α -zirconium phosphate. *Chem. Mater.*, *9*, 863-870.
- Kundu, K., & Giri, D. (1996). Evolution of the electronic structure of cyclic polythiophene upon bipolaron doping. *Am. Inst. Phys.*, *105*, 11075–11080.
- Lange, U., Roznyatovskaya, N. V., & Mirsky, V. M. (2008). Conducting polymers in chemical sensors and arrays. *Anal. Chim. Acta.*, *614*, 1-26.
- Langer, J. J., Framski, G., & Golczak, S. (2001). Polyaniline micro- and nanofibrils. *Synth. Met.*, *121*, 1319–1320.

References

- Langer, J. J., Framski, G., & Joachimiak, R. (2001). Polyaniline nano-wires and nano-networks. *Synth. Met.*, *121*, 1281-1282.
- Li, G. F., Martinez, C., Semancik, S., Smith, J. A., Josowicz, M., & Janata, J. (2004). The Effect of Morphology on the Response of Polyaniline-Based Conductometric Gas Sensors: Nanofibers vs. Thin Films. *Electrochem. Solid-State Lett.*, *7*, H44-H47.
- Li, H. -Q., Chen, A., Roscoe, S. G., & Lipkowski, J. (2001). Electrochemical and FTIR studies of L-phenylalanine adsorption at the Au(III) electrode. *J. Electroanal. Chem.*, *500*, 299-310.
- Li, J., Liu, L., Xiao, F., Gui, Z., Yan, R., Zhao, F., et al. (2008). Direct electron transfer and electrocatalysis of horseradish peroxidase immobilized in gemini surfactant – Ionic liquid composite film on glassy carbon electrode. *J. Electroanal. Chem.*, *613*, 51–57.
- Li, J., Wei, X., & Peng, T. (2005). Fabrication of herbicide biosensors based on the inhibition of enzyme activity that catalyzes the scavenging of hydrogen peroxide in a thylakoid membrane. *Anal. Sci.*, *21*, 1217-1222.
- Li, W., James, A., Bailey, & Wang, H. -L. (2006). Toward optimizing synthesis of nanostructured chiral polyaniline. *Polymer*, *47*, 3112-3118.
- Li, Z., & Hu, N. (2003). Direct electrochemistry of heme proteins in their layer-by-layer films with clay nanoparticles. *J. Electroanal. Chem.*, *558*, 155-165.
- Liang, L., Liu, J., Windisch, C. F., Exarhos, G. J., & Lin, Y. H. (2002). Direct assembly of large arrays of oriented conducting polymer nanowires. *Angew. Chem. Int. Ed.*, *41*, 3665–3668.

References

- Liao, C., & Gu, M. (2002). Electroless deposition of polyaniline film via autocatalytic polymerization of aniline. *Thin Solid Films*, 408, 37–42.
- Lieber, C. M. (2001). The incredible shrinking circuit. *Sci. Am.*, 285, 58–64.
- Liu, Y., Liu, H., & Hu, N. (2005). Core-shell nanocluster films of hemoglobin and clay nanoparticle: direct electrochemistry and electrocatalysis. *Biophys. Chem.*, 117, 27-37.
- Liu, J., & Wan, M. X. (2001). Studies on formation mechanism of polypyrrole microtube synthesized by template-free method. *J. Polym. Sci., Part A: Polym. Chem.*, 39, 997-1004.
- Liu, J., & Wan, M. X. (2001). Synthesis, characterization and electrical properties of microtubules of polypyrrole synthesized by a template-free method. *J. Mater. Chem.*, 11, 404-407.
- Liu, J., Lin, Y., Liang, L., Voigt, J. A., Huber, D. L., Tian, Z. R., et al. (2003). Templateless assembly of molecularly aligned conductive polymers nanowires: A new approach for oriented nanostructures. *Chem. Eur. J.*, 9, 604–611.
- Liu, J., Tian, S., & Knoll, W. (2005). Properties of polyaniline/carbon nanotube multilayer films in neutral solution and their application for stable low-potential detection of reduced beta-nicotinamide adenine dinucleotide. *Langmuir*, 21, 5596-5599.
- Liu, S. Q., & Ju, H. X. (2002). Renewable reagentless hydrogen peroxide sensor based on direct electron transfer of horseradish peroxidase immobilized on colloidal gold-modified electrode. *Anal. Biochem.*, 307, 110–116.

References

- Liu, W., Kumar, J., Tripathy, S., Senecal, K. J., & Samuelson, L. (1999). Enzymatically synthesized conducting polyaniline. *J. Am. Chem. Soc.*, *121*, 71-78.
- Liu, Y., Lei, J. P., & Ju, H. X. (2008). Amperometric sensor for hydrogen peroxide based on electric wire composed of horseradish peroxidase and toluidine blue-multiwalled carbon nanotubes nanocomposite. *Talanta*, *74*, 965-970.
- Liu, Y., Liu, H., & Hu, N. (2005). Core-shell nanocluster films of hemoglobin and clay nanoparticle: direct electrochemistry and electrocatalysis. *Biophys. Chem.*, *117*, 27-37.
- Long, Y., Chen, Z., Wang, N., Zhang, Z., & Wan, M. (2003). Resistivity study of polyaniline doped with protonic acids. *Physica B*, *325*, 208-213.
- Luo, X., Killard, A. J., Morrin, A., & Smyth, M. R. (2007). In situ electropolymerized silica-polyaniline core-shell structures: Electrode modification and enzyme biosensor enhancement. *Electrochim. Acta*, *52*, 1865-1870.
- Ma, G.-X., Lu, T.-H., & Xia, Y.-Y. (2007). Direct electrochemistry and bioelectrocatalysis of hemoglobin immobilized on carbon black, *Bioelectrochemistry*, *71*, 180-185.
- MacDiarmid, A. G. (1997). Polyaniline and polypyrrole: Where are we headed? *Synth. Met.*, *84*, 27-34.
- MacDiarmid, A. G., Chiang, J. C., Halpern, M., Huang, W. S., Mu, S. I., Somasiri, N. L., Wu, W., & Yaniger, S. I. (1985). Polyaniline interconversion of metallic and insulating forms. *Mol. Cryst. Liq. Cryst.*, *121*, 173-180.

References

MacDiarmid, A. G., Manohar, S. K., Masters, J. G., Sun, Y., Weiss, H., & Epstein, A. J. (1991). *Synth. Met.*, *41*, 621-626.

Maceij, M., Magdalen, T., Barbara, P., & Krystyna, J. (2003). Template synthesis of polyaniline and poly(2-methoxyaniline) nanotubes: comparison of the formation mechanisms. *Electrochem. Commun.*, *5*, 403-407.

Malinauskas, A., Malinauskeiene, J., & Ramanavicius, A. (2005). Conducting polymer-based nanostructured materials: electrochemical aspects. *Nanotechnology*, *16*, R51-R62.

Marty, J. L., Sode, K., & Karube, I. (1992). Biosensor for detection of organophosphate and carbamate insecticides. *Electroanalysis*, *4*, 249-252.

Mathebe, N. G., Morrin, A., & Iwuoha, E. I. (2004). Electrochemistry and scanning electron microscopy of polyaniline/peroxidase-based biosensor. *Talanta*, *64*, 115-120.

Michira, I. N. (2007). *Synthesis, electrodynamics and biosensor applications of novel sulphonated polyaniline nanocomposites*. Unpublished Ph.D Thesis, University of the Western Cape, South Africa.

Michira, I., Akinyeye, R., Somerset, V., Klink, M. J., Sekota, M., Al-Ahmed, A., et al. (2007). Synthesis, characterisation of novel polyaniline nanomaterials and application in amperometric biosensors. *Macromol. symp.*, *255*, 57-69.

Monk, P. M. (2001). *Fundamentals of electroanalytical chemistry*. New York, USA: John Wiley & Sons.

References

Morillo, E., Undabeytia, T., Maqueda, C., Madrid, L., & Bejarano, M. (1994). Cu(II)-Glyphosate system: A study by anodic stripping voltammetry and the influence on Cu adsorption by montmorillonite. *Chemosphere*, 28, 2185-2196.

Morrin, A., Ngamna, O., Killard, A. J., Moulton, S. E., Smyth, M. L., & Wallace, G. G. (2005). An amperometric enzyme biosensor fabricated from polyaniline nanoparticles. *Electroanalysis*, 17, 423-430.

Murray, R. W. (1984). In A. J. Bard (Ed.), *Electroanalytical Chemistry* (vol. 13, pp. 191). Dekker, New York: Dekker.

Nakamura, C., Hasegawa, M., Nakamura, N., & Miyake, J. (2003). Rapid and specific detection of herbicides using a self-assembled photosynthetic reaction center from purple bacterium on an SPR chip. *Biosens. Bioelectron.*, 18, 599.

Nandi, M., Gangopadhyay, R., & Bhaumik, A. (2008). Mesoporous polyaniline having high conductivity at room temperature. *Microporous Mesoporous Mater.*, 109, 239-247.

Norris, I. D., Kane-Maguire, L. A., & Wallace, G. G. (2000). Electrochemical synthesis and chiroptical properties of optically active poly-*o*-methoxyaniline. *Macromolecules*, 33, 3237-3243.

Okamoto, H., Okamoto, M., & Kotaka, T. (1998). Structure development in polyaniline films during electrochemical polymerization. II. Structure and properties of polyaniline films prepared via electrochemical polymerization. *Polymer*, 39, 4359-4367.

References

Oyama, N., Tatsuma, T., Sato, T., & Sotamura, T. (1995). Dimercaptan-Polyaniline Composite Electrodes for Lithium Batteries with High Energy Density. *Nature*, *373*, 598.-600.

Palys, B., Kudelski, A., Stankiewicz, & Jackowska, K. (2000). Influence of anions on formation and electroactivity of poly(2,5-dimethoxyaniline). *Synth. Met.*, *108*, 111-119.

Pan, Z. W., Dai, Z. R., & Wang, Z. L. (2001). Nanobelts of semiconducting oxides. *Science*, *291*, 1947-1949.

Park, T. -M., Iwuoha, E. I., & Smyth, M. R. (1997). Development of a sol-gel enzyme inhibition-based on amperometric biosensor for cyanide. *Electroanalysis*, 1120-1123.

Paterno, L. G., Manolache, S., & Denes, F. (2002). Synthesis of polyaniline-type thin layer structures under low-pressure RF-plasma conditions. *Synth. Met.*, *130*, 85–97.

Patil, V., Sainkar, S. R., & Patil, P. P. (2004). Growth of poly(2,5-dimethoxyaniline) coatings on low carbon steel. *Synth. Met.*, *140*, 57-63.

Penalva, J., Puchades, R., & Maquieira, A. (1999). Analytical properties of immunosensors working in organic media. *Anal. Chem.* *71*, 3862–3872.

Petit, C., Murakami, K., Erdem, A., Kilinc, E., Borondo, G. O., Liegeois, J. F., & Kauffmann, J. M. (1998). Horseradish Peroxidase immobilized electrode for phenothiazine analysis *Electroanalysis*, *10*, 1-8.

Piriyapittaya, M., Jayanta, S., Mitra, S., & Leepipatpiboon, N. (2008). Micro-scale membrane extraction of glyphosate and aminomethylphosphonic acid in water

References

followed by high-performance liquid chromatography and post-column derivatization with fluorescence detector. *J. Chromatogr. A*, 1189, 483–492.

Plesu, N., Iliu, G., Pascariu, A., & Vlase, G. (2006). Preparation, degradation of polyaniline doped with organic phosphorus acids and corrosion essays of polyaniline–acrylic blends. *Synth. Met.*, 156, 230–238.

Pud, A., Ogurstov, N., Korzhenko, A., & Shapoval, G. (2003). Some aspects of preparation methods and properties of polyaniline blends and composites with organic polymers. *Prog. Polym. Sci.*, 28, 1701-1753.

Qiu, H. J., & Wan, M. X. (2001). Synthesis, characterization, and electrical properties of nanostructural polyaniline doped with novel sulfonic acids (4-{n-[4-(4-Nitrophenylazo)phenoxy]alkyl}aminobenzene sulfonic acid). *J. Polym. Sci., Part A: Polym. Chem.*, 39, 3485-3497.

Qiu, H. J., Wan, M., Mathews, B., & Dai, L. (2001). Conducting polyaniline nanotubes by template-free polymerization. *Macromolecules*, 34, 675-677.

Rahman, M. A., Kumar, P., Park, D.-S., & Shim, Y.-B. (2008). Electrochemical Sensors based on organic conjugated polymers. *Sensors*, 8, 118-141.

Redshaw, N., Dickson, J. S., Ambrose, V., & Horswell, J. (2007). A preliminary investigation into the use of biosensors to screen stomach contents for selected poisons and drugs. *Forensic Sci. Int.*, 172, 106-111.

Rodriguez-Mozaz, S., Lopez de Alda, M. J., Marco, M. -P., & Barcelo, D. (2005). Biosensors for environmental applications: Future development trends. *Pure Appl. Chem.*, 76, 723-752.

References

- Saad, B., Ariffin, M., & Saleh., M. I. (1998). Flow injection potentiometric determination of paraquat in formulation and biological samples. *Talanta*, *47*, 1231-1236.
- Sadik, O., & Wallace, G. G. (1993). Pulsed amperometric detection of proteins using antibody containing conducting polymers. *Anal. Chim. Acta*, *279*, 209-212.
- Salomi, B. S., & Mitra, C. K. (2007). Electrochemical studies on horseradish peroxidase covalently coupled with redox dyes. *Biosens. Bioelectron.*, *22*, 1825–1829.
- Samuelson, L., Liu, W., Nagarajan, R., Kumar, J., Bruno, F. F., Cholli, A., et al. (2001). Nanoreactors for the enzymatic synthesis of conducting polyaniline. *Synth. Met.*, *119*, 271–272.
- Sangregorio, C., Wiemann, J. K., O'Connor, C. J., & Rosenzweig, Z. (1999). A new method for the synthesis of magnetoliposomes. *J. Appl. Phys.*, *85*, 5699–5701.
- Sariri, R., Sajedi, R. H., & Jafarian, V. (2006). Inhibition of horseradish peroxidase by thiol type inhibitors. *J. Mol. Liq.*, *123*, 20-23.
- Schuhmann, W. (1995). Conducting polymers and their application in amperometric biosensors. *Mikrochim. Acta*, *121*, 1–29.
- Shan, D., Wang, S., Zhu, D., & Xue, H. (2007). Studies on direct electron transfer and biocatalytic properties of hemoglobin in polyacrylonitrile matrix. *Bioelectrochemistry*, *71*, 198-203.

References

- Shi, J., Wang, Z., & Li, H. (2007). Electrochemical fabrication of polyaniline/multiwalled carbon nanotube composite films for electrooxidation of methanol. *J. Mater. Sci.*, *42*, 539-544.
- Shi, X., Shen, M., & Mo'hwald, H. (2004). Polyelectrolyte multilayer nanoreactors toward the synthesis. *Prog. Polym. Sci.*, *29*, 987-1019.
- Shinohara, T., Chiba, T., & Aizawa, M. (1988). Enzyme microsensor for glucose with an electrochemically synthesized enzyme-polyaniline film. *Sens. Actuators, B*, *13*, 79-86.
- Shirakawa, H., Louis, E. J., MacDiarmid, A. G., Chiang, C. K., & Heeger, A. J. (1977). Synthesis of electrically conducting organic polymers: halogen derivatives of polyacetylene, CH_x. *J. Chem. Soc. Chem. Commun.*, *16*, 578-580.
- Situmorang, M., Gooding, J. J., Hibbert, D. B., & Barnett, D. (1998). Electrodeposited polytyramine as an immobilization matrix for enzyme biosensors. *Biosens. Bioelectron.*, *13*, 953-962.
- Somerset, V. S., Klink, M. J., Baker, P. G. L., & Iwuoha, E. I. (2007). Acetylcholinesterase-polyaniline biosensor investigation of organophosphate pesticides in selected organic solvents. *J. Environ. Sci. Health., Part B*, *42*, 297-304.
- Song, Y. H., Wang, L., Ren, C. B., Zhu, G. Y., & Li, Z. (2006). A novel hydrogen peroxide sensor based on horseradish peroxidase immobilized in DNA films on a gold electrode. *Sens. Actuators, B*, *114*, 1001-1006.
- Songa, E. A., Somerset, V. S., Waryo, T., Baker, P. G. L., & Iwuoha, E. I. (2009). Amperometric nanobiosensor for quantitative determination of glyphosate and glufosinate residues in corn samples. *Pure Appl. Chem.*, *81*, 123-139.

References

Songa, E. A., Waryo, T., Jahed, N., Baker, P. G. L., Kgarebe, B. V., & Iwuoha, E. I. (2009). Electrochemical Nanobiosensor for Glyphosate Herbicide and its Metabolite. *Electroanalysis*, DOI: 10.1002/elan.200804452 [In Press].

Stalikas, C. D., & Konidari, C. N. (2001). Analytical methods to determine phosphonic and amino acid group-containing pesticides. *J. Chromatogr. A*, 907, 1-19.

Storrier, G. D., Colbran, S. B., & Hibbert, D. B. (1994). Chemical and electrochemical syntheses, and characterization of poly(2,5-dimethoxyaniline) (PDMA): a novel, soluble, conducting polymer. *Synth. Met.*, 62, 179-186.

Street, G. B. Polypyrrole: from powders to plastics. (1986). In: T. A. Skotheim, editor. *Handbook of conducting polymers* (vol. I, pp. 265-91). New York: Marcel Dekker.

Sun, D., Cai, C., Li, X., Xing, W., & Lu, T. (2004). Direct electrochemistry and bioelectrocatalysis of horseradish peroxidase immobilized on active carbon. *J. Electroanal. Chem.*, 566, 415-421.

Tadeo, J. L., Sanchez-Brunete, C., Perez, R. A., & Fernandez, M. D. (2000). Analysis of herbicide residues in cereals, fruits and vegetables. *J. Chromatogr. A*, 882, 175-191.

Tang, H., Kitani, A., & Shiotani, M. (1996). Effects of anions on electrochemical formation and overoxidation of polyaniline *Electrochim. Acta*, 41, 1561-1567.

Tang, J. L., Wang, B. Q., Wu, Z. Y., Han, X. J., Dong, S. J., & Wang, E. K. (2003). Lipid membrane immobilized horseradish peroxidase biosensor for amperometric determination of hydrogen peroxide. *Biosens. Bioelectron.* 18, 867-872.

References

- Tang, J., Jing, X., Wang, B., & Wang, F. (1988). Infrared spectra of soluble polyaniline. *Synth. Met.*, 24, 231-238.
- Tran-Minh, C. (1993). *Biosensors*. London: Chapman & Hall.
- Trojanowicz, M., & Krawczyk, T. K. (1995). Electrochemical biosensors based on enzymes immobilized in electropolymerized films. *Microchim. Acta*, 121, 167–181.
- Tsui, M. T. K., & Chu, L.M. (2003). Aquatic toxicity of glyphosate-based formulations: comparison between different organisms and the effects of environmental factors. *Chemosphere*, 52, 1189-1197.
- Tsui, M. T. K., & Chu, L. M. (2004). Comparative toxicity of glyphosate-based herbicides: aqueous and sediment porewater exposures. *Arch. Environ. Contam. Toxicol.*, 46, 316-323.
- US Environmental Protection Agency, N. P. (1990). *Phase I Report PB-91-125765*. Springfield, VA: National Technical Information Service.
- US EPA, P. P. (1992). *Pesticides in Groundwater database. A compilation of monitoring studies: 1971-1991. National Summary*. Washington: US EPA, Cited in Cox, C. 1995b op cit 12.
- Veitch, N. C. (2004). Horseradish peroxidase: a modern view of a classic enzyme. *Phytochemistry*, 65, 249–259.
- Virji, S., Huang, J., Kaner, R. B., & Weiller, B. H. (2004). Polyaniline nanofiber gas sensors: Examination of response mechanisms. *Nano Lett.*, 4, 491-496.

References

Wallace, G. G., Spinks, G. M., Kane-Maguire, L. A., & Teasdale, P. R. (2003). *Conductive electroactive polymers: Intelligent materials systems* (2nd ed.). United States of America: Taylor & Francis Group.

Wan, M. X., & Huang, J. (1999). Microtubules of conducting polymers. *Synth. Met.*, *101*, 708-7111.

Wan, M. X., & Li, J. (2000). Formation mechanism of polyaniline microtubules synthesized by a template-free method. *J. Polym. Sci., Part A: Polym. Chem.*, *38*, 2359-2364.

Wan, M. X., & Li, J. C. (1999). Microtubules of polyaniline doped with HCl and HBF₄. *J. Polym. Sci. Part A: Polym. Chem.*, *37*, 4605-4609.

Wan, M. X., Liu, J., Qiu, H. J., & Li, J. C. (2001). Template-free synthesized microtubules of conducting polymers. *Synth. Met.*, *119*, 71-72.

Wang, Y., & Jing, X. (2005). Effect of solution concentration on the UV-Vis spectroscopy measured oxidation state of polyaniline base. *Polym. Test.*, *24*, 153-156.

Watanabe, A., Mori, K., Misono, M., Nakamura, Y., & Matsuda, M. (1989). Comparative study of redox reactions of polyaniline films in aqueous and nonaqueous solutions. *Macromolecules*, *22*, 3323-3327.

Wei, Z. X., & Wan, M. X. (2003). Synthesis and characterization of self-doped poly(aniline-co-aminonaphthalene sulfonic acid) nanotubes. *J. Appl. Polym. Sci.*, *87*, 1297-1301.

Wei, Z., Zhang, Z., & Wan, N. (2002). Formation mechanism of self-assembled polyaniline micro/nanotubes. *Langmuir*, *18*, 917-921.

References

Welch, C. M., & Compton, R. G. (2006). The use of nanoparticles in electroanalysis: a review. *Anal. Bioanal. Chem.*, 384, 601-619.

Wen, T. -C., Huang, L. -M., & Gopalan, A. (2001). An in situ spectroelectrochemical investigation of the copolymerization of diaminobenzenesulfonic acid with aniline and its derivatives. *Electrochim. Acta*, 46, 2463-2475.

Whitesides, G. M., & Love, J. C. (2001). The art of building small. *Sci. Am.*, 285, 39–47.

WHO. (1994). *Glyphosate. Environmental Health Criteria 159. The International Programme on Chemical Safety (IPCS)*. Geneva: WHO.

WHO. (1996). *Guidelines for Drinking Water Quality*. Geneva: WHO.

World Health Organization/Food and Agriculture Organization (WHO/FAO). (2006). Food Standards Programme. Available from: http://www.codexalimentarius.net/download/report/655/al29_24e.pdf [Accessed: 20 January 2008].

Wring, S. A., & Hart, J. P. (1992). Chemically modified carbon-based electrodes and their application as electrochemical sensors for the analysis of biologically important compounds. *Analyst*, 117, 1215–1229.

Wu, C. G., & Bein, T. (1994). Conducting polyaniline filaments in a mesoporous channel host. *Science*, 264, 1757–1759.

Wu, Y., Shen, Q., & Hu, S. (2006). Direct electrochemistry and electrocatalysis of heme-proteins in regenerated silk fibroin film. *Anal. Chim. Acta*, 558, 179–186.

References

- Xia, Y., Wiesinger, J. M., & MacDiarmid, A. G. (1995). Camphor sulphonic acid fully doped polyaniline emeraldine salt: Conformations in different solvents studied by an ultraviolet/visible/near-infrared spectroscopic method. *Chwm. Mater.*, 7, 443-445.
- Xu, Q., Mao, C., Liu, N. -N., Zhu, J. J., & Sheng, J. (2006). Direct electrochemistry of horseradish peroxidase based on biocompatible carboxymethyl chitosan-gold nanoparticle nanocomposite. *Biosens. Bioelectron.*, 22, 768-773.
- Yan, R., Zhao, F. Q., Li, J. W., Xiao, F., Fan, S. S., & Zeng, B. Z. (2007). Direct electrochemistry of horseradish peroxidase in gelatin-hydrophobic ionic liquid gel films. *Electrochim. Acta*, 52, 7425-7431.
- Yang, Y. S., & Wan, M. X. (2002). Chiral nanotubes of polyaniline synthesized by a template-free method. *J. Mater. Chem.*, 12, 897-903.
- Yang, Y., & Heeger, A. J. (1994). A new architecture for polymer transistors. *Nature*, 372, 344-346.
- Yang, Y., Yang, M., Wang, H., Jiang, J., Shen, G., & Yu, R. (2004). An amperometric horseradish peroxidase inhibition biosensor based on a cysteamine self-assembled monolayer for the determination of sulfides. *Sens. Actuators, B*, 102, 162-168.
- Yulaev, M. F., Sitdikov, R. A., Dmitrieva, N. M., Yazynina, E. V., Zherdev, A. V., & Dzantiev, B. B. (2001). Development of a potentiometric immunosensor for herbicide simazine and its application for food testing. *Sens. Actuators, B*, 75, 129-135.
- Zhang, D., & Wang, Y. (2006). Synthesis and applications of one-dimensional nano-structured polyaniline: An overview. *Mater. Sci. Eng., B*, 134, 9-19.

References

Zhang, L., Zhang, Q., Lu, X. B., & Li, J. H. (2007). Direct electrochemistry and electrocatalysis based on film of horseradish peroxidase intercalated into layered titanate nano-sheets. *Biosens. Bioelectron.*, *23*, 102–106.

Zhang, S., Wright, G., & Yang, Y. (2000). Materials and techniques for electrochemical biosensor design and construction. *Biosens. Bioelectron.*, *15*, 273–282.

Zhang, X., & Manohar, S. K. (2004). Polyaniline nanofibers: chemical synthesis using surfactants. *Chem. Commun.*, *20*, 2360-2368.

Zhang, Z., & Wan, M. (2002). Composite films of nanostructured polyaniline with poly(vinyl alcohol). *Synth. Met.*, *128*, 83-89.

Zhang, Z., & Wan, M. (2003). Nanostructures of polyaniline composites containing nano-magnet. *Synth. Met.*, *132*, 205-212.

Zhang, Z., Wei, Z., Zhang, L., & Wan, M. (2005). Polyaniline nanotubes and their dendrites doped with different naphthalene sulfonic acids. *Acta Mater.*, *53*, 1373-1379.

Zhao, J. G., Henkens, R. W., & Crumbliss, A. L. (1996). Mediator-free amperometric determination of toxic substances based on their inhibition of immobilized horseradish peroxidases. *Biotechnol. Progr.*, *12*, 703–708.

Zhao, M., Sun, L., & Crooks, R. M. (1998). Preparation of Cu nanoclusters within dendrimer templates. *J. Am. Chem. Soc.*, *120*, 4877–4878.

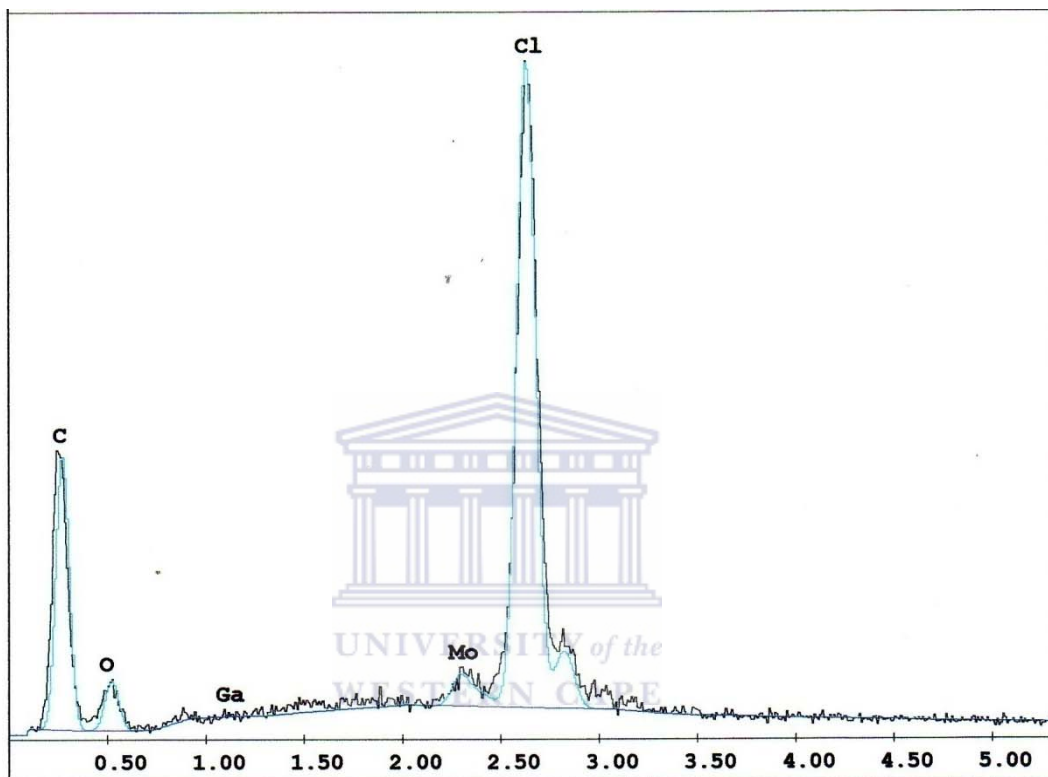
Zollner, H. (1993). *Handbook of enzyme inhibitors Part A, second revised and enlarged ed.*, Germany: VCH Verlagsgesellschaft GmbH.

References

Zotti, G., Cattarin, S., & Commisso, N. (1998). Microdimensional polyaniline: Fabrication and characterization of dynamics of charge propagation at microdisk electrodes. *J. Electroanal. Chem.*, 239, 387-396.



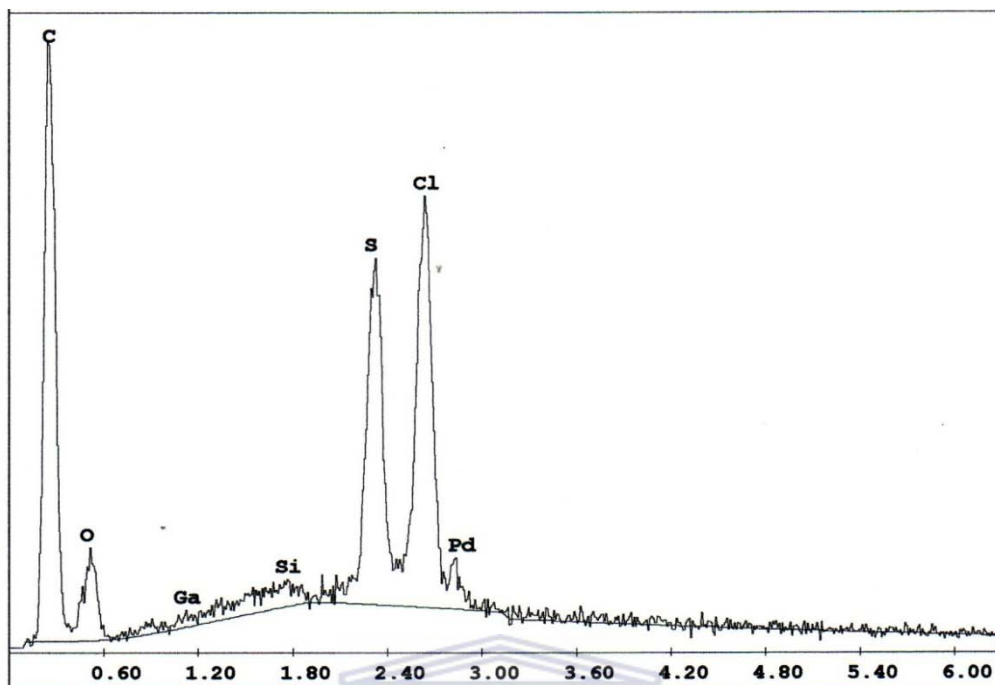
Appendices



Element	Wt %	At %	K-Ratio	Z	A	F
C K	62.16	76.45	0.1022	1.0248	0.1604	1.0001
O K	16.39	15.14	0.0220	1.0093	0.1331	1.0001
GaL	0.00	0.00	0.0000	0.8296	0.6697	1.0018
MoL	1.96	0.30	0.0202	0.8044	1.2532	1.0226
ClK	19.48	8.12	0.1780	0.9134	1.0002	1.0000
Total	100.00	100.00				

Element	Net Inte.	Bkgd Inte.	Inte. Error	P/B
C K	71.28	1.62	1.71	44.00
O K	13.88	1.60	4.21	8.67
GaL	0.00	7.40	0.00	0.00
MoL	11.24	11.68	7.40	0.96
ClK	229.78	12.08	0.98	19.02

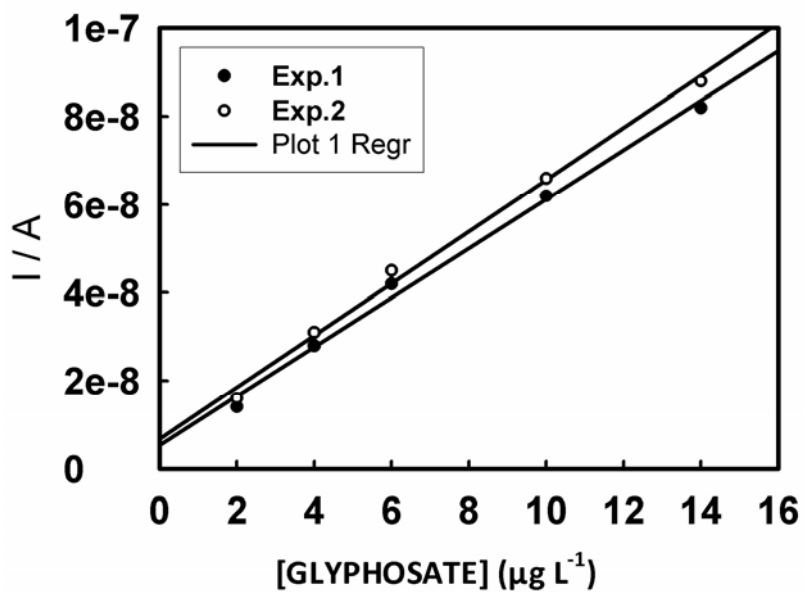
Appendix A1. EDX spectrum for undoped poly(2,5-dimethoxyaniline)(PDMA).



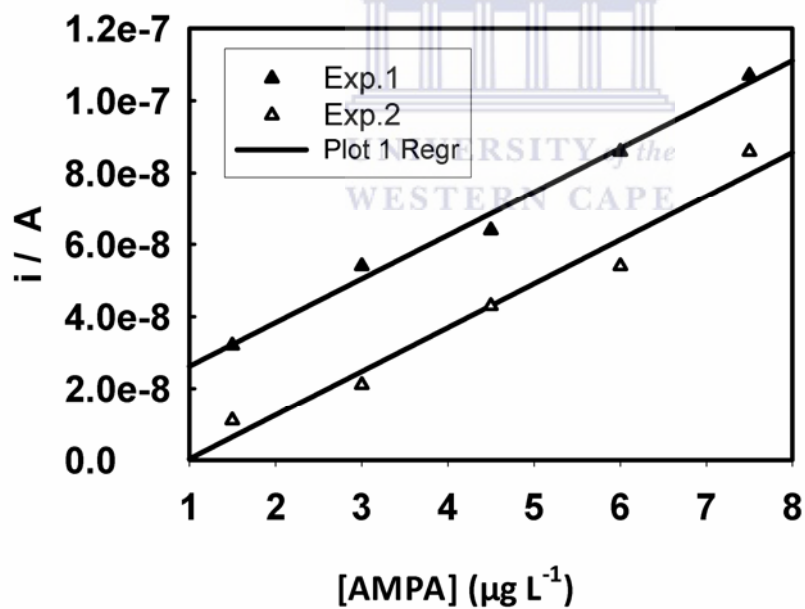
Element	Wt %	At %	K-Ratio	Z	A	F
C K	63.95	77.48	0.1264	1.0221	0.1934	1.0001
O K	16.87	15.34	0.0237	1.0066	0.1396	1.0001
GaL	0.73	0.15	0.0042	0.8274	0.6903	1.0019
SiK	0.46	0.24	0.0035	0.9689	0.7748	1.0074
S K	6.09	2.76	0.0550	0.9623	0.9298	1.0108
ClK	8.20	3.37	0.0679	0.9110	0.9084	1.0003
PdL	0.27	0.04	0.0022	0.7589	1.0513	1.0000
BrK	3.43	0.62	0.0268	0.7740	1.0109	1.0000
Total	100.00	100.00				

Element	Net Inte.	Bkgd Inte.	Inte. Error	P/B
C K	107.28	1.62	1.39	66.22
O K	18.18	2.00	3.66	9.09
GaL	3.02	6.20	18.39	0.49
SiK	6.36	12.56	12.48	0.51
S K	90.62	14.56	1.71	6.22
ClK	106.70	13.64	1.53	7.82
PdL	1.28	12.98	57.66	0.10
BrK	3.74	1.20	9.37	3.12

Appendix A2. EDX spectrum for doped poly(2,5-dimethoxyaniline)(PDMA-PSS).



(a)



(b)

Appendix A3. Calibration curves for biosensor response to (a) glyphosate and (b) AMPA standard solutions.